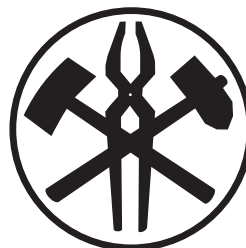


ISSN 1408-7073



**RMZ**

**MATERIALS AND  
GEOENVIRONMENT**

**MATERIALI IN GEOOKOLJE**

Volume  
Letnik 53

Ljubljana, Oktober 2006

No.  
Št. 2

## **RMZ - Materials and Geoenvironment**

RMZ - Materiali in geokolje

Old title: Rudarsko-metalurški zbornik (Mining and Metallurgy Quarterly),  
ISSN 0035-9645, 1952-1997.

Is issued quarterly by the *Faculty of Natural Science and Engineering, Ljubljana*, the *Institute for Mining, Geotechnology and Environment Ljubljana* and *Premogovnik Velenje, Velenje*.

Izdaja *Naravoslovnotehniška fakulteta Univerze v Ljubljani, Inštitut za rudarstvo, geotehnologijo in okolje Ljubljana* in *Premogovnik Velenje*, štirikrat letno.

Financially supported also by Ministry of Education, Science and Sport of Republic of Slovenia.  
Pri financiranju revije sodeluje *Ministrstvo za šolstvo, znanost in šport Republike Slovenije*.

Editor-in-Chief (Glavni urednik)

Editorial Management

Advisory Board

Uredniški odbor

Jože Pezdič

Jakob Likar

Evgen Dervarič, Premogovnik Velenje

Tadej Dolenc, Univerza v Ljubljani

Stevo Dozet, GeoZS, Ljubljana

Jadran Faganelli, Univerza v Ljubljani

Vasilij Gontarev, Univerza v Ljubljani

Mariusz Orion Jedrysek, University of Wroclaw

František Kavička, Technical University of Brno

Klaus Koch, Technische Universität Clausthal

Tomaž Kolenko, Univerza v Ljubljani

Jakob Lamut, Univerza v Ljubljani

Jakob Likar, Univerza v Ljubljani

David John Lowe, British Geological Survey

Jernej Pavšič, Univerza v Ljubljani

Andrej Paulin, Univerza v Ljubljani

Jože Pezdič, Univerza v Ljubljani

Simon Pirc, Univerza v Ljubljani

Esad Prohić, Sveučilište, Zagreb

Anton Smolej, Univerza v Ljubljani

Janez Stražišar, Univerza v Ljubljani

Andrej Šubelj, IRGO Ljubljana

France Šusteršič, Univerza v Ljubljani

Rado Turk, Univerza v Ljubljani

Milivoj Vulić, Univerza v Ljubljani

Editorial Office (Uredništvo):

Barbara Bohar Bobnar

Iztok Anželj

Nives Vukič

Digital Layout (Priprava za tisk):

Tomaž Sterniša s.p., Ljubljana

Print (Tisk): R-TISK d.o.o., Ljubljana

RMZ - Materials and Geoenvironment

Aškerčeva cesta 12, p.p. 312

1001 Ljubljana, R. Slovenija

Telefon: +386 (0)1 470 45 00

Telefaks: +386 (0)1 470 45 60

*Indexation bases of RMZ-M&G: CA SEARCH-Chemical Abstracts, METADEX, GeoRef,*

*Energy Science and Technology, PASCAL. Main of 23 bases registered*

*Baze v katerih je RMZ-M&G indeksiran: CA SEARCH-Chemical Abstracts, METADEX,*

*GeoRef, Energy Science and Technology, PASCAL. Najpomembnejši med 23 registriranimi*

*The authors themselves are liable for the contents of the papers.*

*Za mnenja in podatke v posameznih sestavkih so odgovorni avtorji.*

**Copyright © 2001 RMZ - MATERIALS AND GEOENVIRONMENT**

Naklada 300 izvodov. Printed in 300 copies.

**Online Journal/Elektronska revija:** <http://www.rmz-mg.com>

Letna naroč za posameznike: 4.000,00 SIT, za inštitucije: 8.000,00 SIT

Yearly subscription 20 EUR, institutions 40 EUR

Tekoči račun pri Novi Ljubljanski banki, d.d. Ljubljana:

UJP 01100-6030708186

Davčna številka: 24405388

ISSN 1408-7073

# **RMZ - MATERIALS AND GEOENVIRONMENT**

PERIODICAL FOR MINING, METALLURGY AND GEOLOGY

**RMZ - MATERIALI IN GEOKOLJE**  
REVIJA ZA RUDARSTVO, METALURGIJO IN GEOLOGIJO

## *Historical Review*

More than 80 years have passed since in 1919 the University Ljubljana in Slovenia was founded. Technical fields were joint in the School of Engineering that included the Geologic and Mining Division while the Metallurgy Division was established in 1939 only. Today the Departments of Geology, Mining and Geotechnology, Materials and Metallurgy are part of the Faculty of Natural Sciences and Engineering, University of Ljubljana.

Before War II the members of the Mining Section together with the Association of Yugoslav Mining and Metallurgy Engineers began to publish the summaries of their research and studies in their technical periodical Rudarski zbornik (Mining Proceedings). Three volumes of Rudarski zbornik (1937, 1938 and 1939) were published. The War interrupted the publication and not until 1952 the first number of the new journal Rudarsko-metalurški zbornik - RMZ (Mining and Metallurgy Quarterly) has been published by the Division of Mining and Metallurgy, University of Ljubljana. Later the journal has been regularly published quarterly by the Departments of Geology, Mining and Geotechnology, Materials and Metallurgy, and the Institute for Mining, Geotechnology and Environment.

On the meeting of the Advisory and the Editorial Board on May 22<sup>nd</sup> 1998 Rudarsko-metalurški zbornik has been renamed into "RMZ - Materials and Geoenvironment (RMZ - Materiali in Geokolje)" or shortly RMZ - M&G.

RMZ - M&G is managed by an international advisory and editorial board and is exchanged with other world-known periodicals. All the papers are reviewed by the corresponding professionals and experts.

RMZ - M&G is the only scientific and professional periodical in Slovenia, which is published in the same form nearly 50 years. It incorporates the scientific and professional topics in geology, mining, and geotechnology, in materials and in metallurgy.

The wide range of topics inside the geosciences are welcome to be published in the RMZ - Materials and Geoenvironment. Research results in geology, hydrogeology, mining, geotechnology, materials, metallurgy, natural and anthropogenic pollution of environment, biogeochemistry are proposed fields of work which the journal will handle. RMZ - M&G is co-issued and co-financed by the Faculty of Natural Sciences and Engineering Ljubljana, and the Institute for Mining, Geotechnology and Environment Ljubljana. In addition it is financially supported also by the Ministry of Education Science and Sport of Slovenian Government.

Editor in chief

## Table of Contents - Kazalo

### **Investigation of the Thermodynamic Model and Ternary Interaction Parameter Influence for Sn-Ag-Bi Liquid Alloys**

ŽIVKOVIĆ, D., KATAYAMA, I., YAMASHITA, H., MANASJEVIĆ, D., ŽIVKOVIĆ, Ž. .... 155

### **Measured temperatures on die bearing surface in aluminium hot extrusion**

TERČELJ, M., TURK, R., KUGLER, G., FAJFAR, P., CVAHTE, P..... 163

### **Characterization of solidification and hot workability of MgAl<sub>6</sub>Mn foundry alloy**

MRVAR, P., TERČELJ, M., KUGLER, G., FAZARINC, M., MEDVED, J. .... 175

### **Sinteza in analiza hitro strjenih trakov iz bakrovih zlitin**

Synthesis and analysis of rapidly solidified copper alloys ribbons

ŠULER, M., BIZJAK, M., KOSEC, L., KOSEC, B., KNESSL, A. C., ANŽEL, I. .... 193

### **Some methods of analysing caving processes in sublevel coal mining**

Nekateri načini analiziranja rušnih procesov pri podetažnem odkopavanju premoga

LIKAR, J., DERVARIČ, E., MEDVED, M., ČADEŽ, J., JEROMEL, G. .... 203

### **Calculation of volume with the use of “NTF” method**

Izračun volumnov z uporabo “NTF” metode

VULIĆ, M., DURGUTOVIĆ, A. .... 221

### **Permsko-triasna meja ter zgornjepermski in spodnjeskitski skladi na jugovzhodnem obrobju Ljubljanskega Barja, osrednja Slovenija**

Permo-Triassic boundary and Upper Permian as well as Lower Scythian Beds  
in the Southeastern Borderland of the Ljubljana Marsh, Central Slovenia

DOLENEC, M., DOZET, S., LOJEN, S. .... 229

**Some Considerations on the Series Solution of Differential Equations  
and its Engineering Applications**

YILMAZ, L. .... 247

**Zbirka ulitkov profesorja Milana Trbižana**

Castings collection of professor Milan Trbižan

TRBIŽAN, K., TURK, R., JUTERŠEK, M., DÖPP, R., ŽEKŠ, B., TRBIŽAN, M. .... 261

**Autor's Index, Vol. 53, No. 2** ..... 275**Instructions to Authors** ..... 276**Template** ..... 278**Number of paper indexing in different bases** ..... 283

Število indeksiranih člankov v posameznih bazah

# Investigation of the Thermodynamic Model and Ternary Interaction Parameter Influence for Sn-Ag-Bi Liquid Alloys

DRAGANA ŽIVKOVIĆ<sup>1\*</sup>, IWAO KATAYAMA<sup>2</sup>, HIROMI YAMASHITA<sup>2</sup>,  
DRAGAN MANASIEVIĆ<sup>1</sup>, ŽIVAN ŽIVKOVIĆ<sup>1</sup>

<sup>1</sup>University of Belgrade, Technical Faculty, VJ12, 19210 Bor, Serbia

E-mail: dzivkovic@tf.bor.ac.yu

<sup>2</sup>Osaka University, Graduate School of Engineering, Osaka, Japan

Received: October 11, 2006

Accepted: October 20, 2006

**Abstract:** The results of thermodynamic model and ternary interaction parameter influence investigation for the Sn-Ag-Bi system are presented in this paper. The calculation of thermodynamic properties was done using general solution model, Hillert and Toop model for the liquid alloys at 900K in the following sections: Sn-AgxBi<sub>y</sub> Ag-BixSny, and Bi-AgxSny (where x:y is equal to molar ratio of 1:1, 1:3 and 3:1). Based on the calculation results, the most accurate thermodynamic data for the Sn-Ag-Bi system was obtained using asymmetric Hillert model including ternary interaction parameter.

**Keywords:** thermodynamics, phase diagrams, ternary alloys, Ag-Bi-Sn system, lead-free solders

\* Corresponding author: Dr Dragana Živković, Phone/Fax: +381 30 424 547,

## INTRODUCTION

Due to the importance of the ternary Sn-Ag-Bi system as potential lead-free solder material<sup>[1,2]</sup>, different investigations have been done in order to determine its phase equilibria and thermodynamic properties. KATTNER ET AL.<sup>[3]</sup> calculated the phase diagram from the referent thermodynamic data of binary systems, which are numerous<sup>[4-9]</sup>. HASSAM ET AL.<sup>[10]</sup> experimentally investigated liquidus surface of this ternary system, while the more complete analysis of the Sn-Ag-Bi ternary phase diagram and optimization of the ternary thermodynamic Redlich-Kister parameters, based on available binary thermodynamic data, was done by

OHTANI ET AL.<sup>[11]</sup>. The data on calculated liquidus projection and invariant equilibria in the Sn-Ag-Bi system can also be found in<sup>[12]</sup>.

In the frame of experimental thermodynamic investigations of the liquid Sn-Ag-Bi alloys, HASSAM ET AL.<sup>[13]</sup> determined enthalpies of formation and KATAYAMA ET AL.<sup>[14]</sup> measured tin activities using fused salt EMF method.

The aim of this work was identification of the most accurate thermodynamic model to describe thermodynamic behavior of liquid Sn-Ag-Bi alloys and also, investigation of the ternary interaction influence in the example of Sn-Ag-Bi system.

## THEORETICAL FUNDAMENTALS

The calculations in this work have been done using general solution model<sup>[15]</sup>, Hillert model<sup>[16]</sup> and Toop model<sup>[17]</sup>. Such obtained data were compared with the results of application of Redlich-Kister-Muggianu model<sup>[18]</sup>, using the data on evaluated ternary thermodynamic parameters by OHTANI ET AL.<sup>[11]</sup>.

The basic theoretical interpretations of these models are given:

- General solution model<sup>[15]</sup>

$$G^E = x_1 x_2 (A_{12}^o + A_{12}^1 (x_1 - x_2) + A_{12}^2 (x_1 - x_2)^2) + x_2 x_3 (A_{23}^o + A_{23}^1 (x_2 - x_3) + A_{23}^2 (x_2 - x_3)^2) + x_3 x_1 (A_{31}^o + A_{31}^1 (x_3 - x_1) + A_{31}^2 (x_3 - x_1)^2) + f x_1 x_2 x_3 \quad (1)$$

where  $A_{ij}^o$ ,  $A_{ij}^1$ ,  $A_{ij}^2$  are parameters for binary system "ij" independent of composition, corresponding to the Redlich-Kister parameters only relying on temperature, which have been used in the regular type equation:

$$\Delta G_{ij}^E = X_i X_j (A_{ij}^o + A_{ij}^1 (X_i - X_j) + A_{ij}^2 (X_i - X_j)^2 + \dots + A_{ij}^n (X_i - X_j)^n) \quad (2)$$

where  $X_i$  and  $X_j$  indicate the mole fraction of component "i" and "j" in "ij" binary system. The function f is the ternary interaction coefficient expressed by

$$f = (2\xi_{12} - 1)\{A_{12}^2 ((2\xi_{12} - 1)x_3 + 2(x_1 - x_2)) + A_{12}^1\} + (2\xi_{23} - 1)\{A_{23}^2 ((2\xi_{23} - 1)x_1 + 2(x_2 - x_3)) + A_{23}^1\} + (2\xi_{31} - 1)\{A_{31}^2 ((2\xi_{31} - 1)x_2 + 2(x_3 - x_1)) + A_{31}^1\}, \quad (3)$$

where  $\xi_{ij}$  are the similarity coefficients defined by hi called the deviation sum of squares:

$$\xi_{ij} = h_i / (h_i + h_j) \quad (4)$$

where are

$$\begin{aligned} \eta_I &= \int_{X_i=0}^{X_i=1} (\Delta G_{12}^E - \Delta G_{13}^E)^2 dX_1 \\ \eta_{II} &= \int_{X_i=0}^{X_i=1} (\Delta G_{21}^E - \Delta G_{23}^E)^2 dX_2 \\ \eta_{III} &= \int_{X_i=0}^{X_i=1} (\Delta G_{31}^E - \Delta G_{32}^E)^2 dX_3 \end{aligned} \quad (5)$$

and

$$\begin{aligned} X_{1(12)} &= x_1 + x_3 \xi_{12} \\ X_{2(23)} &= x_2 + x_1 \xi_{23} \\ X_{3(31)} &= x_3 + x_2 \xi_{31} \end{aligned} \quad (6)$$

- Hillert model<sup>[16]</sup>

$$G^E = \frac{x_2}{1-x_1} \Delta G^E_{12}(x_1; 1-x_1) + \frac{x_3}{1-x_1} \Delta G^E_{13}(x_1; 1-x_1) + \frac{x_2 x_3}{v_{23} v_{32}} \Delta G^E_{23}(v_{23}; v_{32}) \quad (7)$$

where is:  $v_{ij} = 1/2 (1+x_i-x_j)$

- Toop model<sup>[17]</sup>

$$\begin{aligned} G^E &= \frac{x_2}{1-x_1} \Delta G^E_{12}(x_1; 1-x_1) + \frac{x_3}{1-x_1} \Delta G^E_{13}(x_1; 1-x_1) + \\ &(x_2 + x_3)^2 \Delta G^E_{23} \left( \frac{x_2}{x_2 + x_3}; \frac{x_3}{x_2 + x_3} \right) \end{aligned} \quad (8)$$

In all given equations,  $G^E$  and  $\Delta G^E_{ij}$  correspond to the integral molar quantity for ternary and binary systems, respectively, while  $x_1, x_2, x_3$  correspond to the mole fraction of components in investigated ternary system.

## RESULTS AND DISCUSSION

Basic data for the calculation were thermodynamic data for the constitutive subsystems

in the ternary Sn-Ag-Bi system. The values of integral molar Gibbs excess energies,  $\Delta G^E_{ij}$ , for the binary systems Ag-Bi, Bi-Sn and Sn-Ag were taken from the Version 1.1 of the COST 531 Database for Lead Free Solders<sup>[9]</sup>, according to the references<sup>[3,5,7,8]</sup>. The Redlich-Kister parameters for the liquid phase of the constitutive binaries are given in Table 1.

**Table 1.** Redlich-Kister parameters for the liquid phase of the constitutive binary systems

System	$L^0(T)$	$L^1(T)$	$L^2(T)$
Ag-Sn	-5146.7-5.0103T	-15799.3+3.3208T	-6687.5
Ag-Bi	3340.81+39.16749T-5.969876TlnT	-5485.45-1.07133T	-3055.34+1.77449T
Bi-Sn	490+0.966T	-30-0.235T	0

Related similarity coefficients were determined according to Equations.(4-6) at investigated temperature of 900K and their values are:  $\xi_{\text{Bi-Sn}} = 0.033$ ;  $\xi_{\text{Sn-Ag}} = 0.447$  and  $\xi_{\text{Ag-Bi}} = 0.973$ . They are also shown graphically in Figure 1.

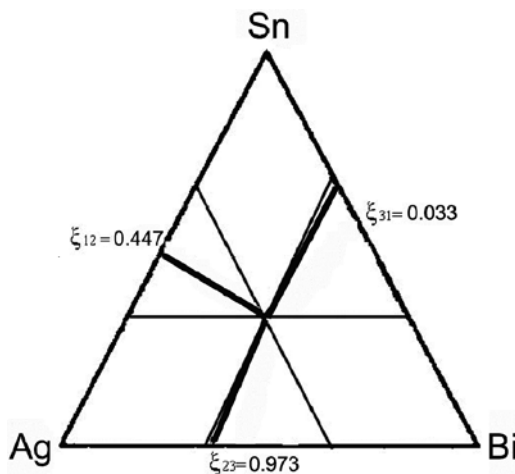


**Figure 1.** The selected binary compositions for three binaries in the investigated ternary system according to general solution model at 900K (shown as bold solid lines)

The similarity coefficient concept, given in Figure 1, pointed out to the asymmetric behavior of the investigated system Sn-Ag-Bi, which was the main reason for choosing asymmetric models - Hillert and Toop, as the additional predicting methods used in this paper.

Furthermore, the comparison with available literature data - the results of Redlich-Kister-Muggianu model (using the data on evaluated ternary thermodynamic parameters by OHTANI ET AL.<sup>[11]</sup>) and the experimental EMF

results of KATAYAMA ET AL.<sup>[14]</sup>, was done. The illustration of the comparison between calculated and experimentally determined tin activities<sup>[14]</sup>, in the form of  $\ln g_{\text{Sn}}$  vs. composition, is shown in Figure 2 for the sections Sn-AgxBi<sub>y</sub> (x:y equal to 3:1, 1:1 and 1:3) at 900K.

The comparison shows that calculated results differ slightly comparing to each other. Although not uniform for all sections, the agreement with experimental points<sup>[14]</sup> is fairly well comparing to the RKM literature data<sup>[11]</sup> including optimized ternary interaction parameter.

In order to accurately examine the deviation between used models at one side and experimental data<sup>[14]</sup> at the other side, the root mean square deviation analysis was applied to tin activities data:

$$\text{RMS} = 1/N \times [\sum (a_{\text{Sn exp}} - a_{\text{Sn calc}})^2]^{1/2} \quad (10)$$

where are: RMS - root mean square deviation, N – the number of counting points,  $a_{\text{Sn exp}}$  – experimental, literature results<sup>[14]</sup> and  $a_{\text{Sn calc}}$  – calculated values for tin activity. The results of this analysis, done for the investigated three sections with molar ratio Ag:Bi=3:1, 1:1 and 1:3, are presented in Table 2, pointing out that Hillert model is the most adequate model for thermodynamic description of ternary Sn-Ag-Bi system, which was expected (Figure 1.) since investigated Sn-Ag-Bi system behaves asymmetrically.

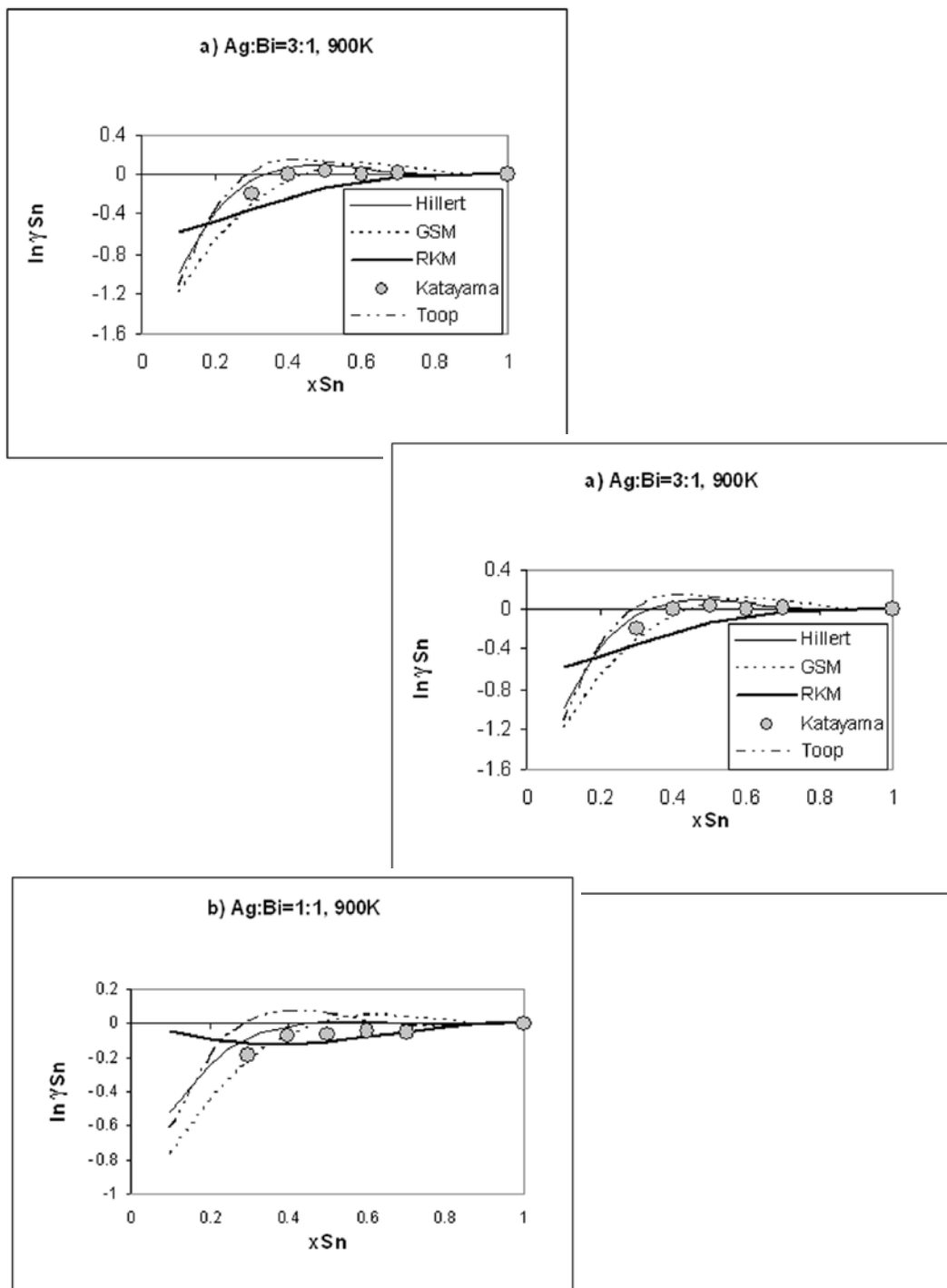


**Figure 2.** The comparison between calculated and derived  $\ln\gamma_{\text{Sn}}$  from experimental data<sup>[14]</sup> for the sections  $\text{Sn}-\text{Ag}_x\text{Bi}_y$  ( $x:y$  equal to 3:1 – a, 1:1 – b and 1:3 -c) at 900K

**Table 2.** The results of the root mean square deviation analysis

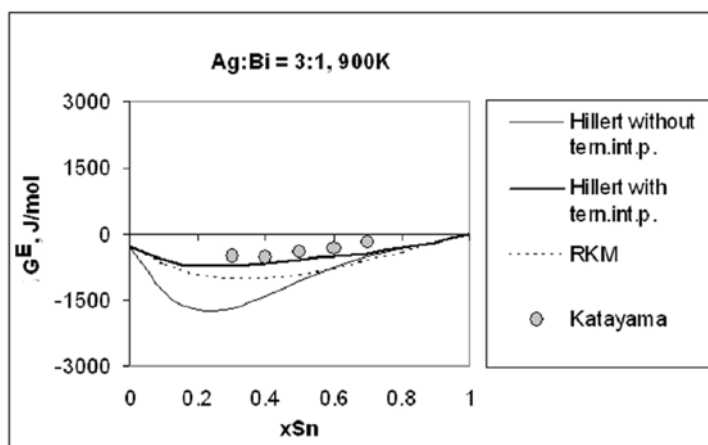
Model	RKM	GSM	Toop	Hillert
St	0.008035	0.007063	0.089173	0.005085

Therefore, thermodynamic calculations in the investigated ternary system Bi-Sn-Ag (taken as 1-2-3 in order) were carried out at 900K according to Hillert model, Equation 7, in the following sections: Sn-Ag<sub>x</sub>Bi<sub>y</sub>, Ag-Bi<sub>x</sub>Sn<sub>y</sub>, and Bi-Ag<sub>x</sub>Sn<sub>y</sub>, where x:y is

molar ratio equal to 1:1, 1:3 and 3:1. The values of calculated integral molar Gibbs excess energies for liquid alloys, in chosen sections, are given in the form of polynomial expressions in Table 3.

**Table 3.** Integral molar excess Gibbs energies, (given as  $G^E = A + Bx_i + Cx_i^2 + Dx_i^3 + Ex_i^4$ ) for liquid alloys in different sections in the Sn-Ag-Bi system at 900K

Section (i:j)	A	B	C	D	E
Ag:Bi=1:1	510.89	-7596.5	19853	-19927	7159
Ag:Bi=3:1	-293.04	-14586	46831	-51199	19250
Ag:Bi=1:3	915.81	-5778.7	13480	-13120	4505.4
Bi:Sn=1:1	335.15	-2640	7953.8	-30020	24375
Bi:Sn =3:1	279.97	-3594.7	10606	-39114	31821
Bi:Sn =1:3	216.67	-230.49	4623	-23223	18625
Sn:Ag=1:1	-2159.9	6480.1	-4121.4	-200.13	/
Sn:Ag=3:1	-690.93	2359.4	-1438.3	-227.99	/
Sn:Ag=1:3	-3542.2	10111	-4288	-3351.4	1070.8

**Figure 3.** Investigation of the ternary interaction parameter influence on GE values

The influence of the ternary interaction parameter for the liquid phase, given in<sup>[11]</sup> as:  $L_{\text{Ag},\text{Bi},\text{Sn}}^l = x_{\text{Ag}}(1700+76.2T) + x_{\text{Bi}}(11000+4T) + x_{\text{Sn}}(20000-38.95T)$ , was also investigated. The comparison between the values for the integral molar Gibbs excess energies for the section Ag:Bi=3:1 at 900K, calculated using Hillert model with and without ternary interaction parameter and literature data – obtained by Redlich-Kister-Muggianu model using the data on evaluated ternary thermodynamic parameters<sup>[11]</sup> and experimental ones<sup>[14]</sup>, are shown in Figure 3.

The best agreement with experimental values<sup>[14]</sup> was observed for the calculated Hillert results including ternary interaction parameter. Therefore, it may be concluded that the most accurate thermodynamic data on the Sn-Ag-Bi system could be obtained using asymmetric Hillert model including ternary interaction parameter.

## CONCLUSIONS

The results of thermodynamic properties and phase diagram prediction in the Sn-Ag-Bi system are presented in this paper. The calculation of thermodynamic properties was done using general solution model, Hillert and Toop model for the liquid alloys at 900K in sections  $\text{Sn}-\text{Ag}_x\text{Bi}_y\text{Ag}-\text{Bi}_x\text{Sn}_y$ , and  $\text{Bi}-\text{Ag}_x\text{Sn}_y$ , where x:y is equal to 1:1, 1:3 and 3:1. The calculated results were compared with available referent data and the results of the root mean square deviation analysis pointed out to the Hillert model, including ternary interaction parameter, as the most adequate model for thermodynamic description of ternary Sn-Ag-Bi system.

## REFERENCES

- [1] [http://www.pb-free.com/ica authored\\_papers/low\\_alpha\\_solders.pdf](http://www.pb-free.com/ica authored_papers/low_alpha_solders.pdf)
- [2] N.C. LEE: Advancing Microelectronics, 26 (5) (1999) 29.
- [3] U. KATTNER, W.J. BOETTHINGER,: J.Electron.Mater., 23 (7) (1994) 603.
- [4] R. HULTGREN ET AL.: Selected values of the Thermodynamic Properties of Binary Alloys, Metals Park, OH, ASM, 1973.
- [5] C.S. OH, J.H. SHIM, B.J. LEE, D.N. LEE: J.Alloys Comp., 238 (1996) 155.
- [6] B.J. LEE, C.S. OH, J.H. SHIM: J.Electron.Mater., 25 (1996) 983.
- [7] H. OHTANI, K. ISHIDA: J.Electron.Mater., 23 (8) (1994) 747.
- [8] D. MALAKHOV ET AL.: Mater. Trans., 43 (2002) 1879.
- [9] Version 1.1 of the COST 531 Database for Lead Free Solders
- [10] S. HASSAM, E. DICHI, B. LEGENDRE: J.Alloys Comp., 268 (1998) 199.
- [11] H. OHTANI, I. SATOH, M. MIYASHITA, K. ISHIDA: Mater. Trans. JIM, 42 (5) (2001) 722.
- [12] [www.metallurgy.nist.gov/phase/solder/agbisn.html](http://www.metallurgy.nist.gov/phase/solder/agbisn.html)
- [13] S. HASSAM, M. GAMBINO, J. P.BROS, Z. METALLKND.: 85 (7) (1994) 460.
- [14] I. KATAYAMA, T. TANAKA, S. AKAI, K. YAMAZAKI, T. IIDA: Materials Science Forum (in print)
- [15] K.C. CHOU: Calphad, 19(3) (1995) 315.
- [16] M. HILLERT: Calphad, 4 (1980) 1.
- [17] G.W. TOOP: Trans.Met.Soc. AIME, 233 (1965) 850.
- [18] O. REDLICH, A.T. KISTER: Ind.Eng.Chem., 24 (1948) 345.



# Measured temperatures on die bearing surface in aluminium hot extrusion

MILAN TERČELJ<sup>1</sup>, RADOMIR TURK<sup>1</sup>, GORAN KUGLER<sup>1</sup>, PETER FAJFAR<sup>1</sup>, P. CVAHTE

<sup>1</sup>Faculty of Natural Sciences and Engineering, University of Ljubljana,  
Aškerčeva 12, 1000 Ljubljana, Slovenia;

E-mail: milan.tercelj@ntf.uni-lj.si, rado.turk@ntf.uni-lj.si,  
goran.kugler@ntf.uni-lj.si, peter.fajfar@ntf.uni-lj.si, peter.cvahte@impol.si

Received: October 05, 2006 Accepted: October 20, 2006

**Abstract:** The paper presents an improved technique of temperature measurement on the bearing surface of industrial die during hot extrusion of aluminium. The measurement was carried out by using a method of split die and three thermocouples (incorporation of the K type and welded at distances from 0.18 to 1.32 mm from the bearing surface) with high measuring accuracy. Extrusion exit speeds were increased to the extent that Mg<sub>2</sub>Si, with a known melting point, started to melt on the extruded profile. This state was determined by the phenomenon of oscillations of the measured temperature of the nearest two thermocouples and by the phenomenon of visually remarked deterioration of surface finish of the extruded profile. The applied method of temperature measurements is good either from the point of economic effect of industrial technologies, i.e. for increased productivity and for looking for technological solutions to cool industrial dies locally (close to the bearing surface of die) more intensively, or from the point of more accurate numerical modelling and optimizing the process of hot extrusion.

**Keywords:** AA 6063, aluminium hot extrusion, die bearing surface, temperature measurement

## INTRODUCTION

Aluminium hot extrusion (Figure 1a) is a forming process, whereby a billet material is forced by compression to flow through a suitably shaped opening in a die to obtain a profile of smaller, but of uniform cross section. In this way produced various profile shapes due to their small weight and good mechanical properties have found their application in electrical and automotive industries, aeronautics, household goods, etc. The process of hot extrusion occurs at a billet temperature between 450 °C to or slightly above 500 °C, and at a profile exit speed

between 5 to 100 m/min. The die opening through which the extrudates pass gives the profile the desired shape and dimensions, and the tribological conditions on the bearing surface (beside its quality) in the opening influence the quality of the extrudate surface. The contact pressure on the bearing surface (on it occur the sticking-, the transition- and the slipping zone, Figure 1b) reaches values above 100 MPa, while locally the temperatures increase even above 600 °C, since much heat is generated as a result of friction with the extruding profile. The temperature on

the bearing surface of the die (and/or of the extrudate surface) is of crucial importance, as it determines the maximum extrusion speed; should the temperature on the profile surface reach the melting temperature of the phase (particles) with the lowest melting point, it results in an increased surface roughness thus diminishing the aesthetic and utility value of the product<sup>[1-3]</sup>.

Temperature is generally measured<sup>[4-7]</sup> by inserting a thermocouple on the bearing surface of the die using the principle of the so-called grounded thermocouples of chromel-alumel type, in which the wires are connected to the front top of the thermocouple making the "hot point" ( $\phi=1\text{ mm}$ ) of the measurement system (Figure 2). Such a measurement system requires very accurate placing of the thermocouples with regard to the bearing surface of the die and very precise calibration before extrusion (usually at the melting point of Si

particles ( $577^\circ\text{C}$ ) in extruding Al-1.2%Si alloy, Figure 2). Furthermore on, there exists a danger of changing the thermocouple position with regard to the calibration state due to the presence of highly normal contact pressures between the die bearing surface and the extrudate. This factors together with the use of dimensionally over-massive thermocouples (hot point  $\Phi=1\text{ mm}$ ) with an excessively long reaction time (longer than 0.6 s) essentially decrease the accuracy of the results obtained. Some authors<sup>[5,7]</sup> report that it is not entirely clear what the thermocouple inserted in this way actually measures: whether the temperature on the bearing surface or the temperature on the surface layer of the extruded profile and/or the temperature under the profile surface.

For a more precise measurement of temperature on the tribologically loaded parts of a die during hot forming such as laboratory

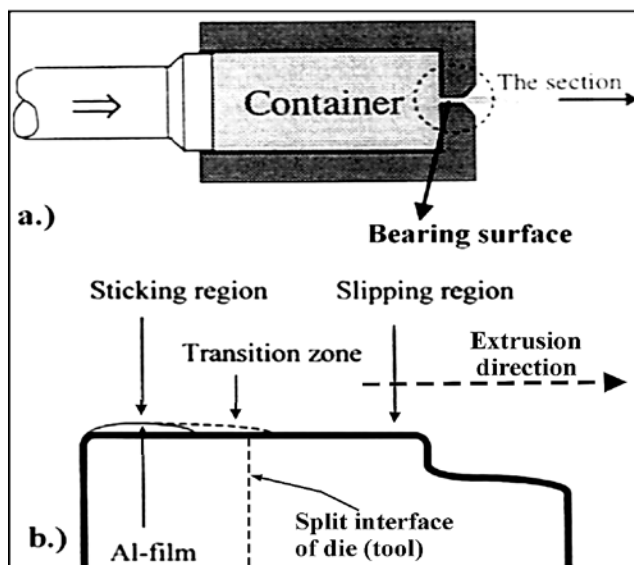


**Figure 1.** The principle of aluminium hot extrusion (a.) and a schematic depiction of occurring zones on the bearing surface of die with the marked division of die (b.).

hot rolling<sup>[8]</sup> and/or forging<sup>[9]</sup>, investigators used thermocouples of type K. In the case of hot rolling YONEYAMA ET AL.<sup>[8]</sup> welded and embedded the relatively thin wires of thermocouples (making channels) directly under the tribologically loaded surface by means of a special arbour  $\phi=5$  mm, which was then inserted in a roll, while TERČELJ ET AL.<sup>[9]</sup> welded and embedded thin thermocouples close to the tribologically loaded surface by means of split die for hot forging in channels manufactured on the interface of the die. This kind of arrangement opens the option of more precise temperature measurements on the bearing surface of an industrial die applied for hot aluminium extrusion, a need expressed by several authors for some time<sup>[7, 10-11]</sup>.

A knowledge of and control over the temperature on the bearing surface of the die and/or on the surface of the extruded profile is important from the viewpoint of the economy of the process (we want to work at as high speeds as possible), from the tribological

aspect (higher temperature accelerates the wear of the bearing surface, the use of PVD coating), and from the point of view of the mechanical properties, structure and quality of the extrudate surface. Further, a precise knowledge of temperature is important for the improvement of the precision of FEM simulations (as a tool for the optimisation of the extruding process) and, along with it, a knowledge of the extrudate temperature on the basis of which the optimal extrusion speeds, etc. will be better determined (assessed)<sup>[6, 10-13]</sup>.

The paper presents an improved method of temperature measurement on the bearing surface and/or at different distances from the bearing surface of an industrial die by means of the method of a split die and a thermocouple of type K with very short reaction time. This and a precise knowledge of the distance of the thermocouples from the tribologically loaded surface assured a more accurate assessment of the heat transfer coefficient.

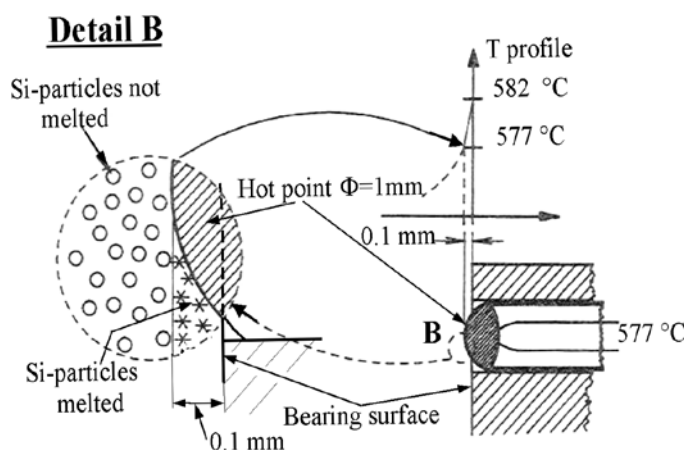


**Figure 2.** The basic principle of the previously way of temperature measurement on the bearing surface of die in aluminium hot extrusion<sup>[5]</sup>.

## Characteristics of applied measurement and materials

Temperature assessment of the contact of the extrudate with the die was carried out by measurement of the temperature close to the bearing surface (Table 1) of an industrial die made from AISI H11 during the hot extrusion of billets of AA 6063 with dimensions  $\phi=210$  mm x 800 mm in round rod  $\phi=30$  mm. The diameter of the container was  $\phi=236$  mm, which means that the extrusion ratio was ER=61.9. Figure 3 gives a schematic picture of the process of hot extrusion of aluminium, the assembly of die and backer with the spot of nitrogen cooling marked in the  $\phi=60$  mm circularly formed channel and 132.2 mm from the die bearing surface. Applied press equipment can extrude at the maximum extruding force 28 MN, and the maximum ram speed 15 mm/s. The applied initial temperatures of the front (this part entered the container first) and back part of individual billets are given in Table 2. The back parts of the billets had a deliberately lower temperature since during extrusion

this part was additionally heated due to heat generation during extruding. Table 2 also presents the ram speed, profile exit speed and die cooling.

On the sectioned surface (contact interface) of the first part of the split die (Figure 1b, Figure 4 - Detail A) electroerosion was used to make very narrow channels (1 mm wide and 2 mm deep), which ended in the shape of a sectioned wedge at different distances directly below the die bearing surface (Figure 4, Detail A). Four thermocouples of NiCr-Ni type K with 0.2 mm wire diameter and up to 10.000 °C/s response time were applied to assure a precise measurement even in cases of rapid temperature changes, i.e. in cases of a change of friction on the bearing surface. The thermocouples mentioned above were welded at a distance of 0.18 to 1.32 mm (Table 1) from the bearing surface. The method used allowed a very precise reading of the distance of the welded thermocouple from the bearing surface using lower magnification of an optical microscope (Figure 4, Detail A). The small distance of

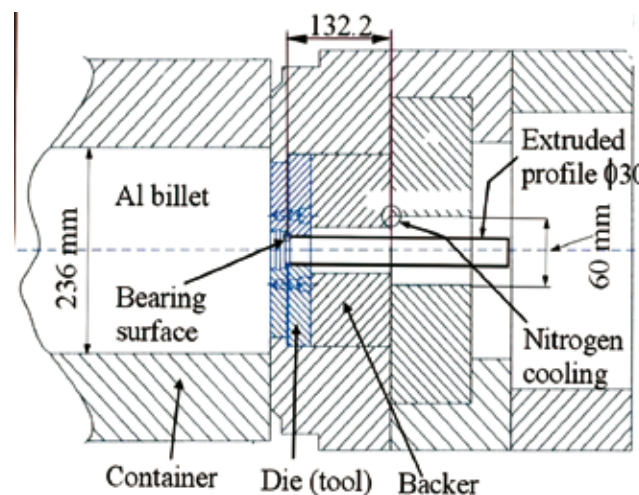


**Figure 3.** Schematic depiction of die assembly with the main dimensions and cooling spot

**Table 1.** Measured thermocouple (TC) distance from die bearing surface.

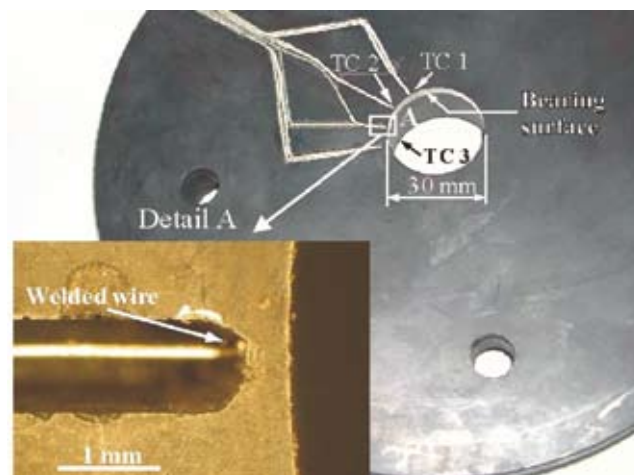
TC no.	1	2	3	4
Distance [mm]	0.18	0.30	0.55	1.32

**Table 2.** Cooling, temperature of billets (back/front), ram and profile exit speed.

Billet No.		1	2	3	4
Die cooling, N 2		No	Yes	No	Yes
Temp. [°C]	Back	470	459	461	457
	Front	459	466	459	458
Ram speed [mm/s]		5.7 8.8	8.8	13.6	13.6
Profil exit speed [m/ min]		21.2 32.7	32.7	50.5	50.5

the welded thermocouples from the bearing surface provided an additional guarantee of the possibility of an even more precise measurement of the least change of temperature on its surface or observation of when the surface of the extruded profile began to melt (e.g. of an Mg<sub>2</sub>Si (Figure 5) particles (eutectic phase) with a known melting point

(591 °C)<sup>[14-15]</sup>), resulting in a temperature oscillation at mixed friction (slipping and hydrodynamic). The wires were welded in the middle of the 6 mm long bearing surface, and the distance between the welded wires (NiCr-Ni) was 0.8 mm. For comparison the temperature measurement on the roll surface during hot aluminium rolling carried out by

**Figure 4.** Dividing surface of split die used with channels made for embedding and welding

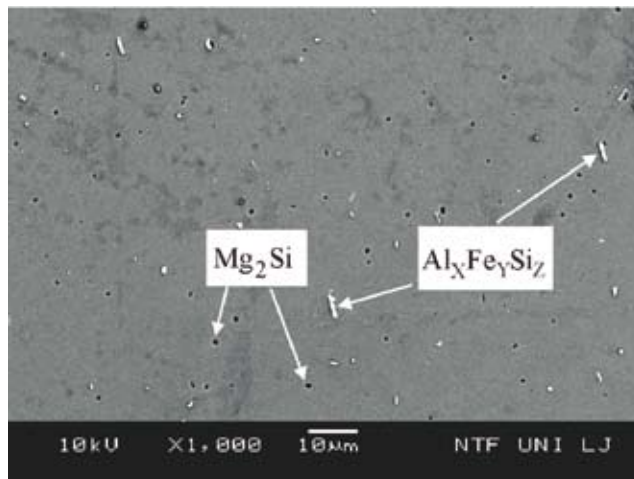


**Figure 5.** BEC image of homogenized initial billet microstructure; distribution of  $Mg_2Si$  and  $AlFeSi$  particles across the cross-section of the billet visible.

YONEYAMA AT AL.<sup>[8]</sup> should be mentioned; namely they welded the thermocouples (type K) at a distance of 0.15 and 0.25 mm from the surface, and on the basis of results obtained in this way, determined the heat transfer coefficient in the hot rolling of aluminium. On the first die already mentioned above only one industrial measurement was carried out due to damage to the wires of thermocouple at the end of the extrusion process, but on the second die the remaining six measurements were carried out without any difficulties. During measurement of temperature the speed of the ram was varied both in the case of nitrogen cooling of die and in the case of non-cooling of the die (Table 2).

## RESULTS OF MEASUREMENTS

The response of measured temperatures to the modified speed was selective enough and recorded both non-cooling and additional

nitrogen cooling of the die. Each observation of an individually extrusion recorded the temperature resulting to all technological phases (billet bearing contact with the die bearing surface) of extrusion process (Figure 6), i.e. insertion and filling of container with extrudate, backward movement of the ram, extrusion phase and its completion. After entering the container and the movement of the ram forward, the billet filled the space (Stage 1) since its diameter (210 mm) was by 26 mm smaller than that of the container (236 mm). The temperatures measured of all three thermocouples increased distinctively, but the contact between the extrudate and the extrusion surface was still unstable so that it came to strong oscillations of the temperatures measured. This was followed by the drop of temperature (Stage 2) due to a temporary recurrent moving away of the ram in order to remove the air (burbcycle). During the extrusion process the temperature increased (Stage 3), towards the end of the extrusion a steady state was established when

the supplied heat (slipping and aluminium forming generated heat) equalled the removal of heat in the interior of the die. Temperature (ca. 328 °C) on the bearing surface of the die before the beginning of extrusion process was a great deal lower than the expected temperature of the die at the placing in the extrusion equipment (450 °C) according to the criteria of industrial technology. During the extrusion of the billet No. 1 (no cooling, ram speed 5.7 mm/s) the temperature measured on the bearing surface increased all the time but it increased distinctively at the change of ram speed to 8.8 mm/s. Maximum temperature measured on TC 1 was 550 °C, on the second thermocouple (TC 2) it was ca. 543 °C and on the third thermocouple (TC 3) it was ca. 531 °C (Table 3). Towards the end of the extrusion phase a steady state was established in which the equation

for heat transfer and conduction are easier to solve (Chapter 4). A slight temperature oscillation was noticed on the thermocouple TC 1, which may be the result of less stable friction conditions, especially in the transition zone (Figure 1b)<sup>[3]</sup> on the bearing surface of the die. By the end of the process (Stage 4) the temperatures measured displayed a distinctive drop.

FEM simulations of the temperature on the surface of a profile (CHANDA<sup>[16]</sup>) on modification of the extrusion speed do not display such an expressed growth (or fall) of temperature, which implies that the heat transfer coefficient adopted in FEM simulations was not correct (probably too low). The same conclusion can be drawn on the basis of the rapid growth of temperature immediately below the bearing surface of the die at the beginning of compression of the billet.

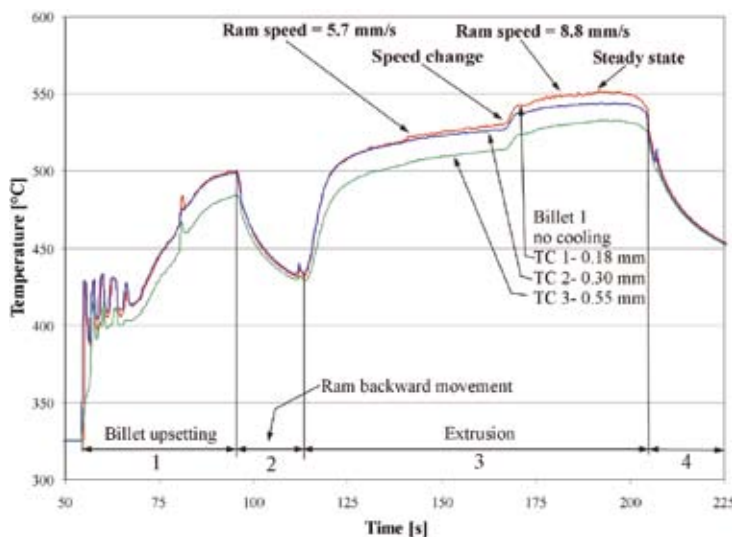


**Figure 6.** Time course of measured values of temperature in the die for different distances from the bearing surface, billet No. 1, ram speed=5.7 and 8.8 mm/s, no cooling.

During the extrusion of the second billet (Figure 7) the die was intensively nitrogen cooled, and the ram speed was kept constant all the extrusion time at 8.8 mm/s (the same as the maximum speed of billet No. 1). The final temperature measured on TC 1 was ca. 1 °C higher than for billet 1.

At billet 3 (no cooling of die, Figure 8) the ram speed was increased to 13.6 mm/s, which resulted in an additional temperature oscillation in the first two thirds of billet extrusion due to unstable friction conditions in the transition zone (Figure 1b). Towards the end of billet extrusion (in the last quarter – establishment of steady state) the already visible beginning of melting of the present eutectic particle Mg<sub>2</sub>Si occurred on the surface of the extruded profile. This was also reflected as an accentuated oscillation of temperatures measured and can be noticed at TC 1 and TC 2, which are welded the closest to the bearing surface, and to a lesser extent at TC 3. An

accentuated oscillation of surface temperatures mentioned above can be attributed to the interchanging occurrence of slipping and hydrodynamic friction, which resulted in the oscillation of temperature on the surface of extruded profile due to their different friction coefficients and the heat consequently produced. The maximum temperature of thermocouple TC 1 measured was ca. 580 °C. The fact that TC 2 on the reaching of melting point of Mg<sub>2</sub>Si showed approximately the same values as TC 1 (it is welded closer to the bearing surface) may be similarly explained by differently produced frictional heat due to uneven distribution of particles of the phase of the eutectic Mg<sub>2</sub>Si phase across the cross-section of the billet, and consequently, on the surface of the extruded round profile. In the case of a lesser concentration of particles in Mg<sub>2</sub>Si phase on the spot under TC 2, slipping friction was present to a greater extent, thus increasing the temperature on this part of bearing surface (before reaching the melting

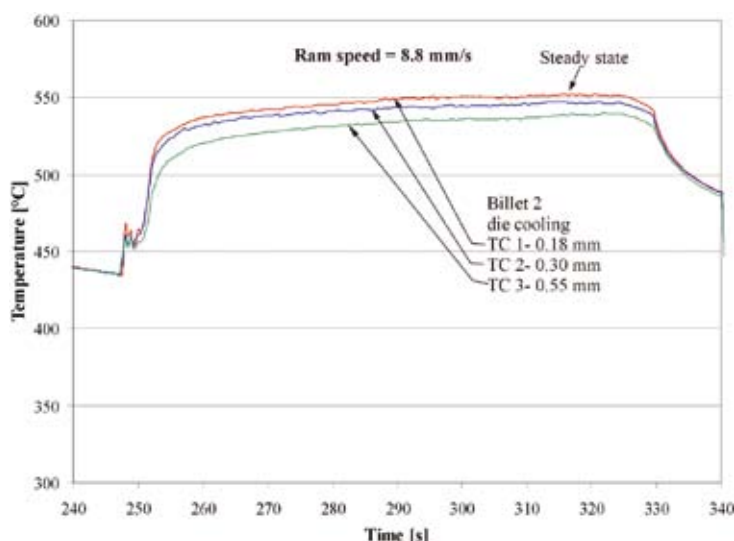


**Figure 7.** Time course of measured values of temperature in the die for different distances from the bearing surface, billet No. 2, ram speed=8.8 mm/s, die cooling (N<sub>2</sub>).

point of the  $Mg_2Si$  phase in billet 3 and in the extrusion of all previously applied billets TC 2 always showed lower values than TC 1). The third thermocouple (TC 3) at a distance of 0.55 mm from the bearing surface scarcely recorded the attainment of melting point temperature of the  $Mg_2Si$  phase, which means that thermocouples at greater distances from the bearing surface are not suitable for a more precise measurement of its temperature changes. As already known, when the melting point temperature of the phase ( $Mg_2Si$ ) reaches  $591\text{ }^{\circ}\text{C}$ <sup>[14-15]</sup>, this causes a deterioration of extruded profile surface quality.

After casting the billets were slowly cooled and later they were reheated (2.1 hours) to the temperature of homogenisation ( $575\text{ }^{\circ}\text{C}$ ) for 2.5 hours, followed by a renewed slow cooling ( $350\text{ }^{\circ}\text{C/h}$ ), thus assuring the formation of eutectic  $Mg_2Si$  (Fig. 5) with a known melting

point temperature. The eutectic thus serves as a calibrating value of the temperature on the extruding profile surface (oscillation of temperature on the bearing surface of the nearest thermocouples) in the determination of the heat transfer coefficient between the bearing surface of the die and the surface of the extruded profile.

In our opinion, measurement of temperature on the surface of the extruded profile using a pyrometer, especially due to difficulties in determination of the emission coefficient which depends on many factors such as, for example roughness of the surface, measurement angle, etc.<sup>[17]</sup>, would not be more precise than our approach since we were able to perceive the change of friction using a sensitive thermocouple. We could observe very sensitively the local occurrence of hydrodynamic friction when the melting point of  $Mg_2Si$  was reached.

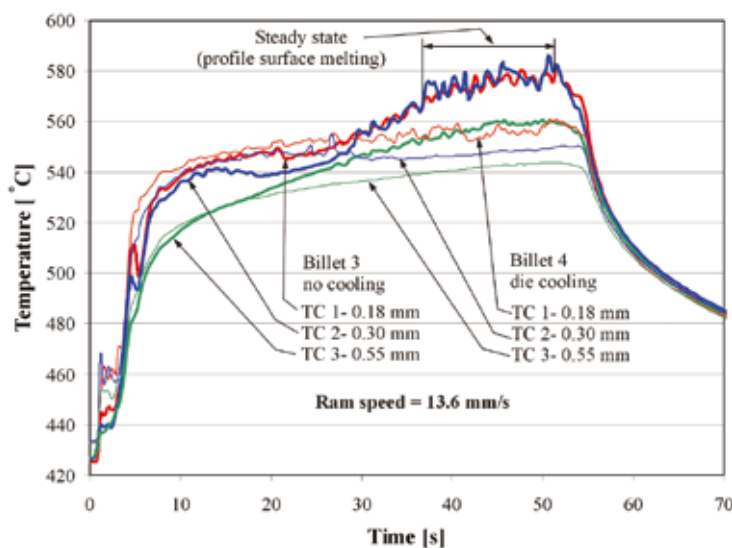


**Figure 8.** Comparison between the measured temperatures on the die bearing surface during extruding of the billet No. 3 and of the billet No. 4.

**Table 3.** Average temperatures and their relative errors in thermocouples obtained in measurements after the stationary state was established.

	TC 1 (r=15.18)	TC 2 (r=15.30)	TC 3 (r=15.55)
Billet 1	550.0 (1± 0.002) °C	543.3 (1± 0.002) °C	530.6 (1± 0.002) °C
Billet 2	550.8 (1± 0.002) °C	545.7 (1± 0.002) °C	535.3 (1± 0.003) °C
Billet 3	575.6 (1± 0.010) °C	574.7 (1± 0.010) °C	557.6 (1± 0.005) °C
Billet 4	556.5 (1± 0.004) °C	548.0 (1± 0.002) °C	542.0 (1± 0.002) °C

LEFSTAD AND REISO<sup>[15]</sup> reported two limiting temperatures (591 °C and 612 °C) on the surface of an extruded profile in extrusion of AA 6063. Which of those two temperatures would be limiting depends above all on the preliminary (previous) billet heat treatment (speed, cooling after casting, temperature of homogenisation, etc.) or the presence or absence of eutectic Mg<sub>2</sub>Si<sup>[18-19]</sup>.

Billet No. 4 was extruded at the same speed as billet No. 3; however, the die was nitrogen cooled. On the surface of the extruded round profile the beginning of melting was not observed since the maximum temperatures of the thermocouple at TC 1 were approximately 19 °C lower than for billet No. 3 (Figure 8). A slight temperature oscillation was noticed only in TC 1 and TC 2, which is connected with the already mentioned unstable friction conditions in the transition zone of the bearing surface.

All the measured values (Figures 6-8) the and their relative errors after the stationary state was established are given in Table 3.

## CONCLUSIONS

In industrial hot extrusion of aluminium we used the improved method of temperature measurement on the bearing surface of die. The applied split die allows the making of channels for embedding of thermocouples on split interface of the first part of die and their welding on the top (end) of the channel just below the die bearing surface. The measurements of temperature field were carried out using four thermocouples, which were welded at different distances from bearing surface. The ram speed at the extrusion of each further billet was increased until the melting point temperature of Mg<sub>2</sub>Si eutectic phase on the profile was reached.

The temperature was measured in the conditions of cooling of die (132 mm from bearing surface) as well as in cases of non-cooling of die. In spite of a relatively great distance of cooling from bearing surface it had an impact on its considerable decrease. This fact have lead us to the possibility of applying of a more locally cooled die (as near to the bearing surface as possible), which would help to remove the heat generated as a result of friction (slipping) between the extruded profile and die bearing surface, billet

plastic deformations, etc. more intensively. Consequently, the extrusion speed could be increased even more relevantly and consequently the economy of this process.

## REFERENCES

- [1] T. SHEPPARD: Extrusion of aluminium Alloys, Kluwer Academic Publishers, 1999, ISBN 0-412-59070-0.
- [2] T. BJÖRK, R. WESTERGÅRD, S. HOGMARK: Wear of surface treated dies for aluminium extrusion- a case study, Wear, 249 (2001) 316-323.
- [3] M.P. CLODE, T. SHEPPARD: Formation of die lines during extrusion of AA 6063, Materials Science and Technology, 6 (1990) 755-763.
- [4] G. GRASMO, K. HOLTHE, S. STÖREN, H. VALBERG, R. FLATVAL, L. HANSEN, M. LEFSTAD, O. LOHNE, T. WELO, J. HERBERG: Modelling of two dimensional extrusion, Procc. of 5<sup>th</sup> Int. Alum. Extr. Techn. Seminar, (1992) 367-376.
- [5] M. LEFSTAD, O. REISO: Temperature measurements in extrusion dies, Materials Science Forum, 217-222 (1996) 409-414.
- [6] R.J. DASHWOOD, H.B. MCSHANE, A. JAKSO: Computer prediction of Extrusion Limit Diagram, Procc. of 6<sup>th</sup> Int. Alum. Extr. Techn. Seminar, (1996) 331-339.
- [7] A.W. HANSEN, H. VALBERG, T. WELO: Accurate Temperature Measurements Inside the Tool in Hot Working of Metals, Procc. of 6<sup>th</sup> Int. Alum. Extr. Techn. Seminar, (1996) 11-15.
- [8] T. YNEYAMA, H. ASAOKA, H. KIMURA, I. HOSHINO, M. KOKUBA: Heat Transfer and Roll Surface Temperature in the Hot Rolling of Aluminium Sheet, Journal of Tribology, 121 (1999) 753-760.
- [9] M. TERČELJ, R. TURK, M. KNAP: Assessment of temperature on die surface in laboratory hot forming, Applied Thermal Engineering, 23 (2003) 113-123.
- [10] P.K. SAHA: Thermodynamics and Tribology in Aluminium Extrusion, Wear, 218 (1998) 179-190.
- [11] X. DUAN, T. SHEPARD: Simulation and control of microstructure evolution during hot extrusion of hard aluminium alloys, Materials Science and Engineering A351(2003) 282-292.
- [12] M. SHIOMI, D. TAKANO, K. OSAKADA, M. OTSU: Forming of aluminium alloy at temperatures just beloww melting point, Int. Journal of Machine Tools & Manufacture, 43 (2003) 229-235.
- [13] A. PYZALLA, K.B. MÜLLER, J. WEGENER: Influence of the Extrusion Parameters on the Microstructure and Properties of an Al-Si Alloy, Z.Metallkd. 91 (2000) 831-837.
- [14] H.W.L. PHILLIPS: Annotated Equilibrium Diagrams of Some Aluminium Alloys System, The Institute of Metals, London, 1959.
- [15] M. LESTAND, O. REISO: Metallurgical Speed limitations During the Extrusion of AlMgSi-Alloys, Procc. of 6<sup>th</sup> Int. Alum. Extr. Techn. Seminar, (1996) 11-18.
- [16] T. CHANDA, J. ZHOU, J. DUSZCZYK: A comparative study on isi-speed extrusion and isothermal extrusion of 6061 Al alloy using 3D FEM simulation, Journal of Materials Processing Technology, 114(2001) 145-153.
- [17] P. WRIGHT, S.F. METCALFE, A.D. TUNE: Aluminium Extrusion, 5/3(2000) 21-30.
- [18] C. HSU, K.A.Q. OREILLY, B. CANTOR, R. HAMERTON: Non-equilibrium reactions in 6xxx series Al alloys, Mat. Sci. and Eng. A304-306 (2001) 119-124.
- [19] S.E. URRETA, F. LOUCHET, A. GHILARDUCCI: Fracture behaviour of an Al-Mg-Si industrial alloy, Materials Science and Engineering A302(2001) 300-307.
- [20] B. BOUROGA, V. GIZET, V. GATTO, J.P. BARDON: Thermal Aspects of Hot Forging: Measurement and Simulation, 2<sup>nd</sup> ESAFORM Conference, (1999) 105-108.
- [21] <http://www.sz-metal.si>



# Characterization of solidification and hot workability of MgAl6Mn foundry alloy

PRIMOŽ MRVAR, MILAN TERČELJ, GORAN KUGLER,  
MATEVŽ FAZARINC AND JOŽEF MEDVED

University of Ljubljana; Faculty of Natural Sciences and Engineering,  
Department of Materials and Metallurgy, Aškerčeva cesta 12, 1000 Ljubljana, Slovenia;

E-mail: primoz.mrvar@ntf.uni-lj.si, milan.tercelj@ntf.uni-lj.si,  
goran.kugler@ntf.uni-lj.si, jozef.medved@ntf.uni-lj.si

Received: September 11, 2006 Accepted: October 20, 2006

**Abstract:** Solidification at cooling rate 7 K/min and hot workability of MgAl6Mn (AM60) alloy have been studied. Metallographic examinations, simultaneous thermal analyses (STA) and thermodynamic calculations are also included in the contribution. The following characteristic temperatures of the solidification process have been established from the cooling curves and STA curves: the liquidus temperature  $T_L$ , solidus  $T_S$ , and eutectic temperature  $T_E$ , respectively. The  $Mg_{17}Al_{12}$  phase and eutectic ( $\alpha_{Mg} + Mg_{17}Al_{12}$ ), which precipitated on the boundaries of the primary  $\alpha_{Mg}$  grains, are observed in MgAl6Mn alloy. It is caused by the local Al – micro segregations in last solidified areas. In MgAl6Mn alloy also formation of the  $Al_4Mn$  inter-metallic compound occurred. The consequence of that is the decreased concentration of the dissolved Al in the Mg-Al liquid solution. Further, the deformation behavior of as-cast MgAl6Mn alloy in the temperature range 200–450 °C and in the strain rate range 0.001–10 s<sup>-1</sup> has been studied using processing maps. Upper (400–450 °C) and lower (200–250 °C) temperature regions and higher strain rates (5, 10 s<sup>-1</sup>) are not appropriate for hot forming due to cracking on grain boundaries. The main reason for cracking in lower temperature range (200–250 °C) cracking is presence of  $Mg_{17}Al_{12}$  inter-metallic phase and ( $\alpha_{Mg} + Al_{12}Mg_{17}$ ) un-equilibrium eutectic. In upper temperature range (400–450 °C) the melting of ( $\alpha_{Mg} + Al_{12}Mg_{17}$ ) eutectic at 426 °C is responsible for grain boundary cracking. Calculated activation energy Q for researched alloy amounts 160.5 kJ mol<sup>-1</sup>.

**Key words:** MgAl6Mn alloy, solidification process, inter-metallic compounds, as-cast state, hot forming

## INTRODUCTION

The use of the up-to date light alloys and their development are in the sharp ascent especially in transportation industry since in the last years the use of the magnesium alloys for the various purposes was strongly increased. The advantages of the magnesium alloys are in its little weight of the final products, good machinability, corrosion resistance and good

mechanical properties. Thus they can compete with aluminium alloys and even steels. Due to the high prices of the basic material and difficulties on the technological melting, on casting and on hot working processes of the magnesium alloys, the thermodynamically investigations of the solidification and of hot working are needed for better knowl-

edge and optimisation of all technological processes. Magnesium alloys are based upon the binary diagram of Mg-Al and it contain from 2 to 9 mass. % Al<sup>[1]</sup>. Decreased hot formability of Mg alloys originates from their hexagonal close-packed structure. MgAl6Mn (AM60) alloy is predominately used for casting and its product have found application in the aircraft parts, car parts, etc.; but its application could be increased if the mechanical properties (tensile strength, ductility, hardness, etc.) will be improved. It is well known that deformed microstructure posses higher mechanical properties in comparison to as-cast state and that the homogenisation process is needed before hot forming; mentioned homogenization process thus increases the production costs.

Thus the aim of this research was to study the solidification and the possibility of hot working of AM60 foundry alloy without prior homogenisation process. The solidification of gravity cast magnesium alloy AM60 has been investigated with the various methods of the thermal analysis: "in situ" simple thermal analysis and simultaneous thermal analysis. The experimental results were upgraded with the thermodynamic calculation and the results of the metallographic analysis. Further the deformation behavior of as-cast MgAl6Mn alloy in the temperature

range 200-450 °C and in the strain rate range 0.001-10 s<sup>-1</sup> using processing maps has been studied in order to reveal optimal hot working conditions.

## CASTING - EXPERIMENTAL PROCEDURE AND RESULTS

### Casting proceeding, specimens and material

The investigated alloy was prepared by the re-melting of the standard MgAl6Mn (AM60) alloy what was done in the graphite crucible of the inductive furnace. In Table 1 the chemical composition of the MgAl6Mn alloy and the fraction of the each element is presented. The melting was taking place under the protective atmosphere of argon. When the temperature of 720 °C was achieved the melt from the graphite crucible was cast into measuring cells Figure 1a, and the cooling curves were measured. Thermal analysis was taking place in simple thermal



a.)

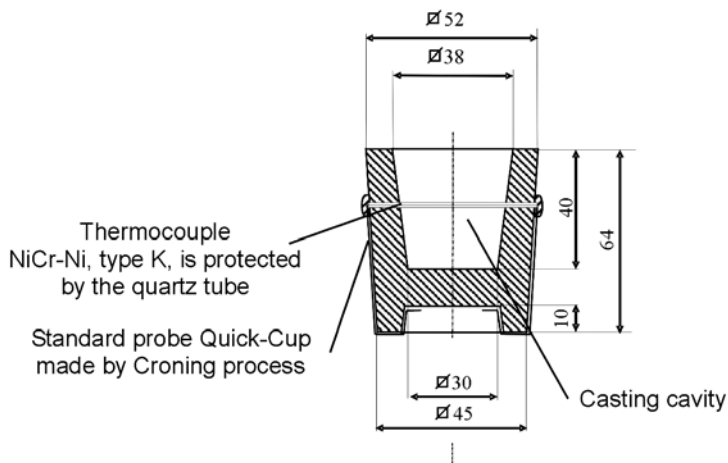


b.)

**Figure 1.** Equipment with the measuring cell for "in situ" thermal analyses.

**Table 1.** Chemical composition of MgAl6Mn alloy and according to the standard EN 1753

Element	AM60 [mass.-%]	Sample [mass.-%]
Al	5,8-6,40	6,28
Zn	<0,20	0,1267
Mn	>0,3	0,3056
Cu	<0,008	0,005
Si	<0,05	0,0294
Fe	<0,004	0,0032
Ni	<0,001	<0,0008
Mg	remain	93,2

**Figure 2.** Detailer presentation of the measuring cell for "in situ" simple thermal analyses and samples for further investigations.

analyses called ETA1.2<sup>[2-3]</sup> (Figures 1 and 2). In Figure 1a the measuring cell with holder and in Figure 1b the measuring system are presented, respectively.

The thermal analysis of MgAl6Mn alloy (dimensions  $\phi=5$  mm x 4 mm) has been investigated by the STA 449 Jupiter (Netzsch) apparatus (nitrogen protective atmosphere). The samples were heated to the temperature of 720 °C by the rate of 7 K/min, and then were cooled by the same rate to the room temperature.

## Thermodinamical calculation

Thermodynamical calculation (Figure 3) was made by the Thermo-Calc software according to the chemical composition given in Table 1. All the equilibrium phases and their temperature range of stability had been calculated. At 632 °C phase Al<sub>8</sub>Mn<sub>5</sub> precipitate from liquid and then at temperature 617 °C the primary crystals of aMg form and start to grow. The inter-metallic compound Mg<sub>2</sub>Si also precipitates at temperature 538 °C. Inter-metallic compound Al<sub>8</sub>Mn<sub>5</sub> transform into Al<sub>11</sub>Mn<sub>4</sub> and later it will be transformed into the inter-metallic compound Al Mn. In

coordinate with phase diagram presented on Figure 3 at temperature of crossing the solvus line ( $287^{\circ}\text{C}$ ) the  $\text{Mg}_{17}\text{Al}_{12}$  inter-metallic compound start to precipitate from  $\alpha_{\text{Mg}}$ . At room temperature microstructure is form from solid solution of  $\alpha_{\text{Mg}}$  and inter-metallic compounds  $\text{Al}_4\text{Mn}$  and  $\text{Mg}_{17}\text{Al}_{12}$ .

### Simultaneous thermal analyses

With apparatus for simultaneous thermal analyses (STA) the MgAl6Mn alloy was analysed. The results in form of heating and cooling curves are presented in Figure 4 and 5, respectively. At heating process (Figure 4)

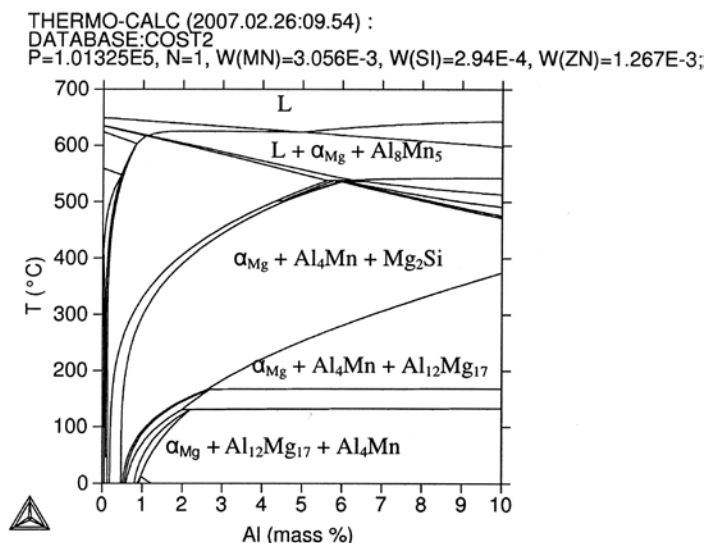


**Figure 3.** Isopleth phase diagram Mg - Al - Mn at 0.3056 mass. % manganese, THERMOCALC

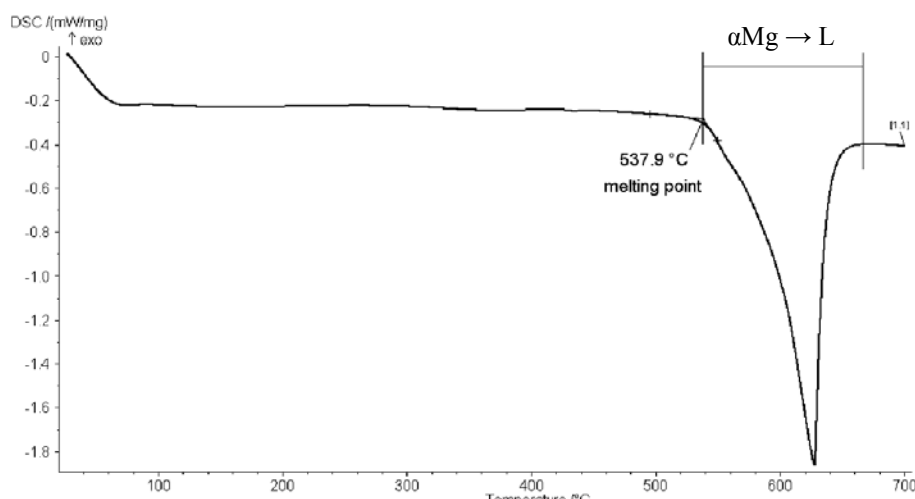


**Figure 4.** STA heating curve of the AM60 alloy in the as-cast state

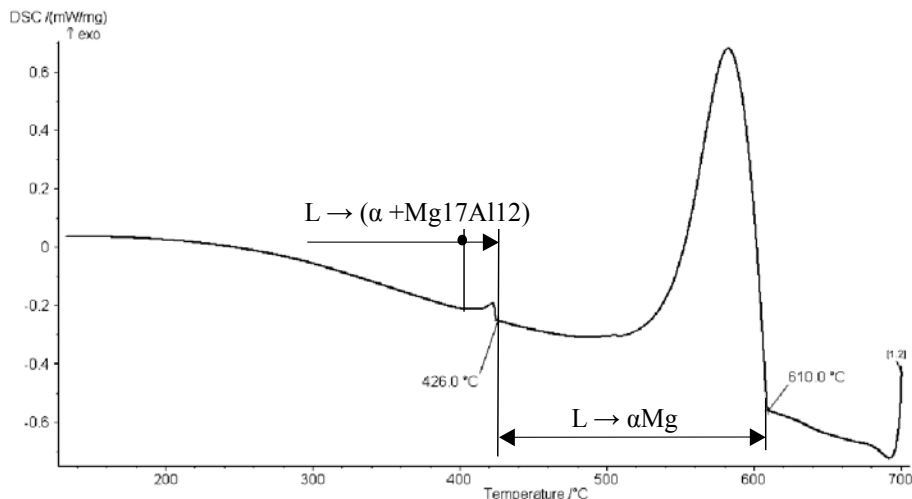


**Figure 5.** STA cooling curve of the AM60 alloy

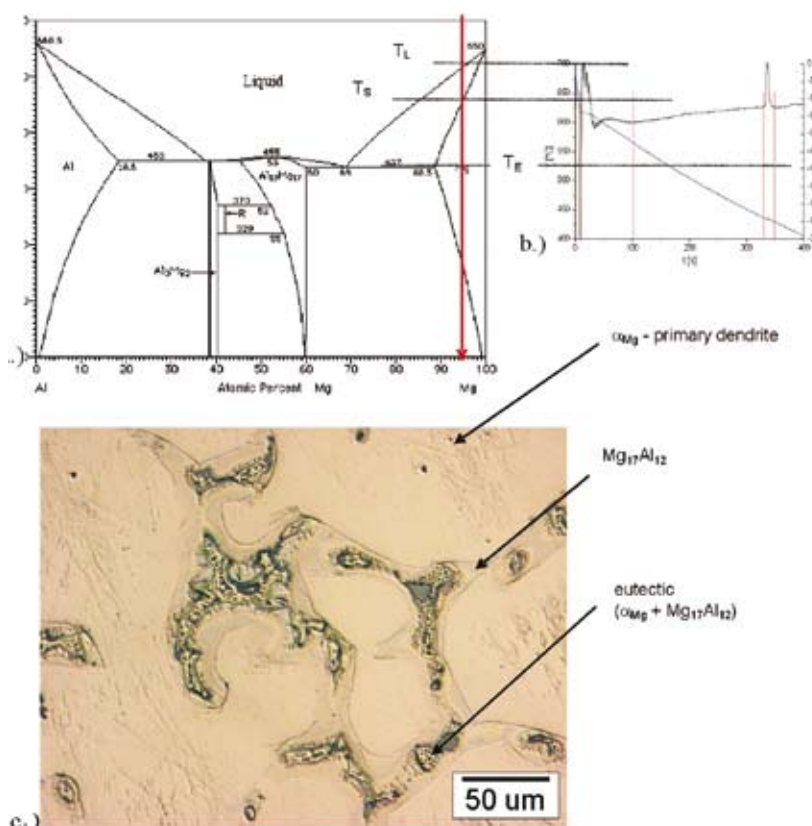


**Figure 6.** Solidification of AM60 alloy at low cooling rate, a.) binary phase diagram, b.) cooling curve, c.) microstructure of AM60 (as-casted state) at solidification rate 7 K/min

the melting start at solidus temperature ( $T_s$ ), which is detected at 537.9 °C. From STA liquidus temperature could be determined from cooling curve which is detected at 610 °C (Figure 5). Because the local micro segregation happened during the relatively slow solidification process (cooling rate = 7 K/s) in the last solidified areas which are rich on Al, the eutectic reaction occurred ( $L \rightarrow \alpha_{Mg} + Mg_{17}Al_{12}$ ) at 426 °C.

### **“In situ” simple thermal analyses and solidification process**

An “In situ” simple thermal analysis (ETA) was used in order to follow the solidification process of the alloy. This way the microstructure and properties could be determined indirectly<sup>[3]</sup>.

On a Figures 6a-c are clearly shown the connection between the cooling curve (Figure 6b) of the investigated sample (alloy MgAl6Mn), binary phase diagram (Figure 6a) and obtained microstructure (Figure 6c).

After the pouring of molten metal into measuring cell, the maximal temperature that was detected was cca. 700 °C (see Figure 6b). Then the cooling and contraction in liquid state follows as long as liquidus temperature ( $T_L$ ) is reached. Further the solidification process occurred and finished at solidus temperature ( $T_s$ ). Measured cooling rate in the centre of the measuring cell (Figure 2) was 7 K/s. Microstructure components were composed from the primary precipi-

tated crystals of  $\alpha_{Mg}$ . Along the boundaries of the crystal grains the eutectic ( $\alpha_{Mg} + Al_{12}Mg_{17}$ ) has been solidified, where the local increasing of the aluminium fraction was taking places in the melt due to the aluminium segregation and therefore the eutectic solidification occurred. The reason for that is in fact that the primary solidified crystals of  $\alpha_{Mg}$  doesn't have nominal composition of alloy X<sub>Al</sub> but the concentration of Al increased and shifted left towards eutectic point (Figures 6). Formed heterogeneous eutectic is characteristically for low cooling rates. On basis of typical parameters on a cooling curve it is possible to conclude and to estimate quality of alloys.

## **HOT WORKING – EXPERIMENTAL PROCEDURE AND RESULTS**

### **Equipment and experiments for hot deformation**

A computer controlled servo-hydraulic machine Gleeble 1500D was used for compression testing (Figure 7). For reduction of friction between the cylindrical specimen and the tool and to avoid their mutual welding, graphite lubricant was used. Cylindrical specimens of Rastegew type with dimensions  $\phi=10$  mm x 15 mm (for hot compression tests) were cut from gravity cast block of dimensions 30 mm x 40 mm x 40 mm (see Figure 2). During testing, a stress module in the Gleeble 1500D control system calculated the instantaneous cross-sectional area of the specimen from the L-strain measurement and computed the true stress.

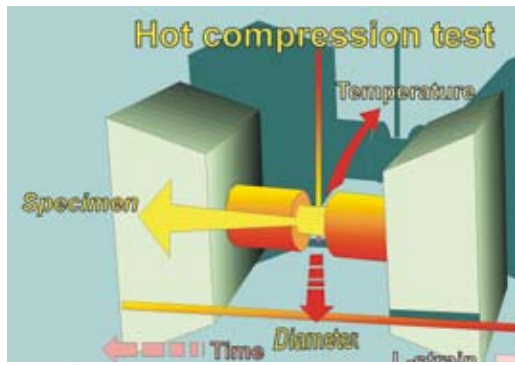


**Figure 7.** Schematic representation of the Gleeble compression testing arrangement

Testing was performed in the temperature range of 200 °C to 450 °C, at six different strain rates (0.001, 0.01, 0.1, 1, 5 and 10 s<sup>-1</sup>). The heating rate was 3 °C/s, soaking time on deformation temperature was 15 s. After deformation the specimens were rapidly quenched with water.

On Figure 8a the flow stresses for temperature area 200 - 450 °C and strain rate 5 s<sup>-1</sup> and on Figure 8b for the same temperature area but for strain rate 0.001 s<sup>-1</sup> are presented. From Figure 8a is

visible that hardening process occurs at samples compressed at 200 and 250 °C as a consequence of presence precipitates of Al<sub>12</sub>Mg<sub>17</sub> inter-metallic phase and ( $\alpha_{\text{Mg}} + \text{Al}_{12}\text{Mg}_{17}$ ) eutectic (see Figure 9a) on grain boundaries and due to decreased activity of dynamic recovery (DRV) and recrystallization (DRX). The consequence is occurrence of cracks in/on the deformed specimen (Figure 9b). Precipitation of eutectic ( $\alpha_{\text{Mg}} + \text{Al}_{12}\text{Mg}_{17}$ ) begins with regards to equilibrium diagram (see Figures 3 - 6) at cca 426 °C, on the other hand the precipitation of Al<sub>12</sub>Mg<sub>17</sub> inter-metallic compound that is more hard than  $\alpha_{\text{Mg}}$  and thus it is from plasticity point of view undesired (in fact its precipitation begin after finished solidification process); consequently at lower temperature its fraction is still higher that additionally decreased the hot deformability. Further by decreased intensity of dynamic recovery and recrystallization at lower temperature it results in occurrence of

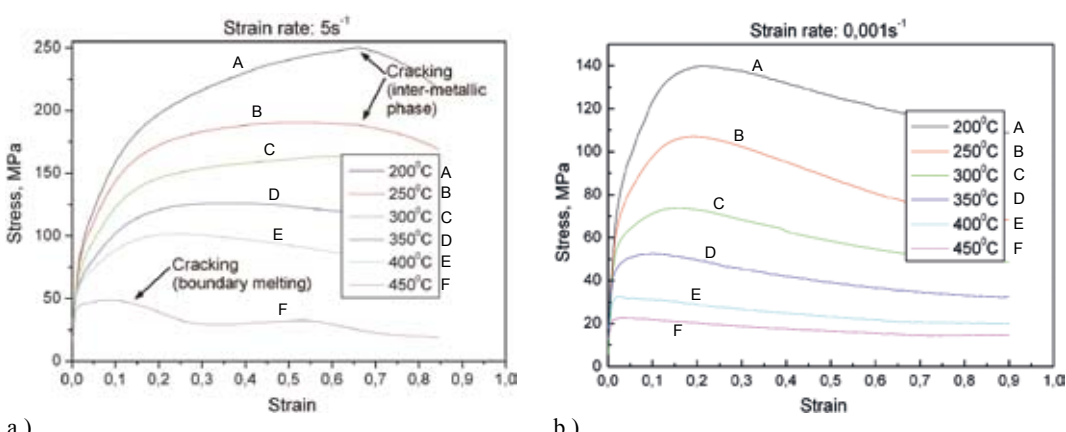


**Figure 8.** Flow curves, **a**-strain rate 5 s<sup>-1</sup>, **b**-strain rate 0.001 s<sup>-1</sup>

micro- and macro-cracks (see Figure 9b) on deformed specimen (on Figure 8a the occurrence of crack is expressed by rash change of course of flow stress). Less expressed change of flow stress course is visible at 250 °C (Figure 8a) but it also results in surface cracking of deformed specimen. The shape (course) of flow curves in temperature region 350 - 450 °C indicate the presence of dynamic recrystallization (Figure 9c); further the quick fall of flow curves occurs also at 450 °C (Figure 8a). This shape of

flow stress indicates melting of precipitated phases on grain boundaries that also results in micro- and macro-cracks of the deformed specimen (Figure 9d).

At lower strain rates ( $0.001 - 1\text{s}^{-1}$ ) and at all tested temperatures after achieving of maximum the fall of flow stress is visible (Figure 8b). The density of macro-cracks obtained at higher temperatures is higher from those obtained at lower temperatures (see Figures 9b and 9d).

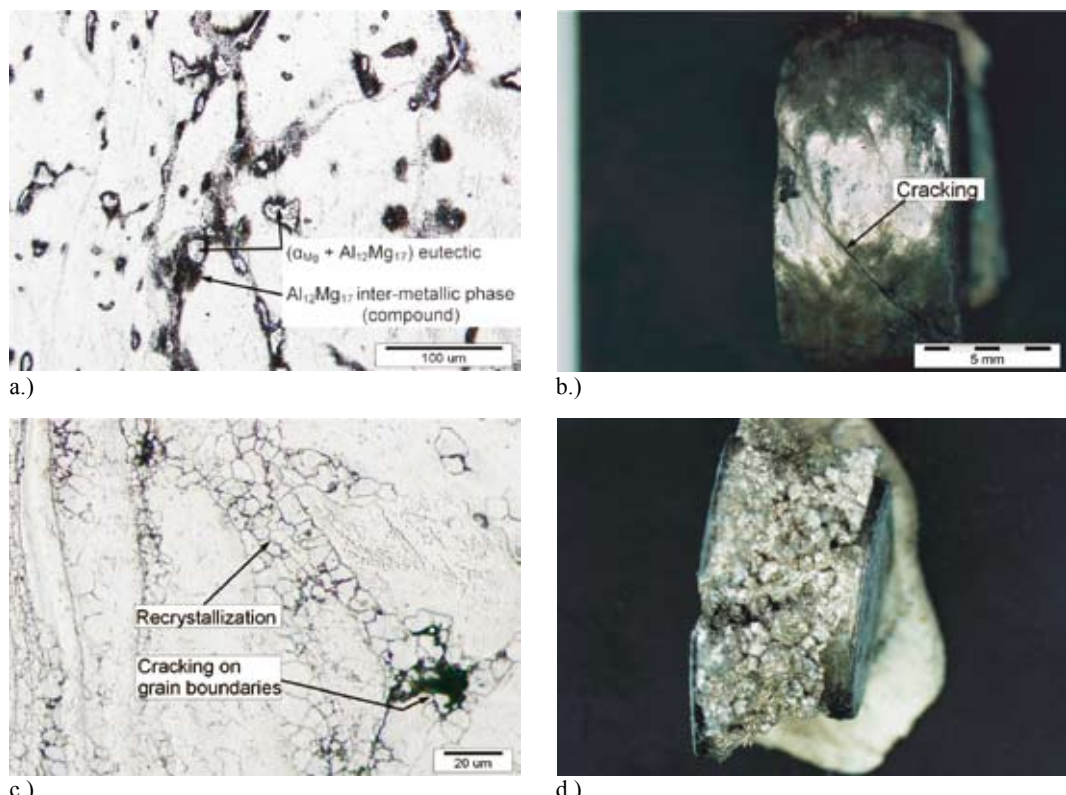


**Figure 9.** a-precipitation of  $\text{Al}_{12}\text{Mg}_{17}$  inter-metallic phase and  $(\alpha_{\text{Mg}} + \text{Al}_{12}\text{Mg}_{17})$  eutectic on grain boundaries, b-crack on deformed specimen at 200 °C and strain rate  $5\text{s}^{-1}$ , c-dynamic recrystallization and d-cracking on grain boundaries at 450 °C and strain rate  $5\text{s}^{-1}$

Figures 10 a-b prove the presence of dynamic recrystallization at higher temperatures (350 °C).

### Analytical description of flow curves

From the maximum flow stresses for different temperatures and strain rates, we calculated the constants of the hyperbolic sine equation<sup>[4-6]</sup>

$$Z = \dot{\varepsilon} \exp(Q/RT) = A(\sinh \alpha \sigma)^n \quad (1)$$

For this purpose we first defined the function  $\chi^2$ , which determines the difference between measured and calculated values of maximum flow stresses

$$\chi^2 = \sum_{i=1}^N \frac{(z_i - a_1 x_i - a_2 y_i - a_3)^2}{e_i^2} \quad (2)$$

where N is the number of measurements,  $z_i = \ln(\sinh \alpha \sigma_i)$ ,  $x_i = \ln \dot{\varepsilon}_i$  and  $y_i = 10^4 T^{-1}$ . Parameter  $a_1 = n^{-1}$ ,  $a_2 = 10^4 Q n^{-1} R^{-1}$  and  $a_3 = n^{-1} \ln A$ . For the error calculation we took into account only measurement errors of the parameter  $z_i$ , given by  $e_i = \alpha e_i^\sigma \ln(\coth \alpha \sigma_i)$ , where  $e_i^\sigma$  are the measurement errors of the flow stress. The details of the minimization procedure of the above expression (2) are given elsewhere<sup>[7]</sup>.  $\chi^2$  has a minimum for  $Q = 160.5 \text{ kJ mol}^{-1}$ ,  $\alpha = 0.0216 \text{ MPa}^{-1}$ ,  $n = 4.8$  and  $A = 7.73 \cdot 10^9 \text{ s}^{-1}$ . For these parameters a comparison between the calculated and measured dependence of peak stress on temperature for five different strain rates is shown on Figure 11. The value for the activation energy is approximately on the level as those for aluminium<sup>[7]</sup>.

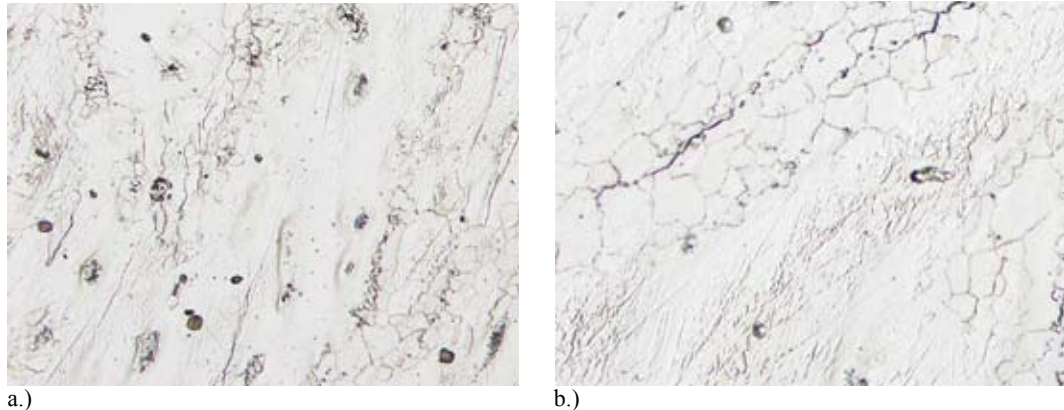


**Figure 10.** a-b-dynamic recrystallization in deformed specimen at 350 °C and strain rate 0.001 s<sup>-1</sup>, precipitation of Al<sub>12</sub>Mg<sub>17</sub> inter-metallic phase

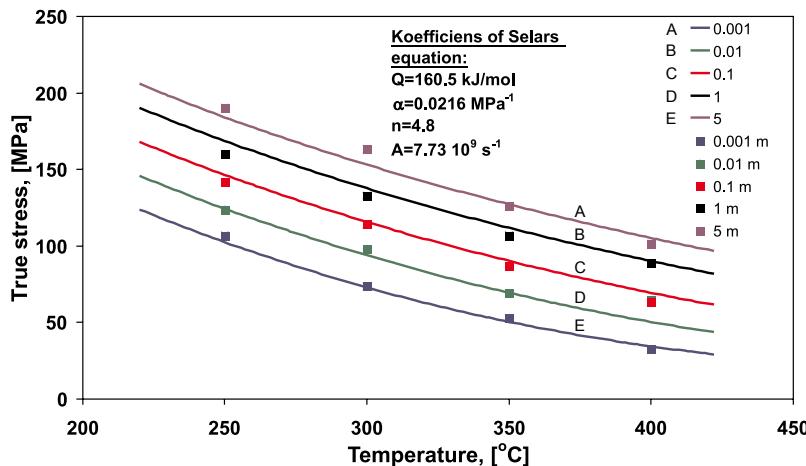


**Figure 11.** Comparison between measured (m) and calculated dependence of peak stress on temperature for five different strain rates of 0.001, 0.01, 0.1, 1 and 5 s<sup>-1</sup>

## PROCESSING MAP

Processing Map is developed on the basis of a dynamic material model (DMM) which has been developed and widely used by the group of Y. V. R. K. Prasad<sup>[8]</sup>. The Processing Map of material can be described as an explicit representation of its response to the imposed process parameters.

### Efficiency of power dissipation.

The workpiece under hot deformation conditions of this model works as an essential energy dissipater. The constituent equation describes the manner in which energy (P) is converted at any instant into two forms, thermal energy (G) making temperature increase and microstructural change caused by transform of metallurgical dynamics (J), which are not recoverable. In general, most of the dissipation is due to a temperature rise and only a small amount of energy dissipates through microstructural changes. The power

partitioning between G and J is controlled by the constitutive flow behavior of the material and is decided by the strain rate sensitivity (*m*) of flow stress as shown in the equation

$$\frac{dJ}{dG} = \frac{\dot{\varepsilon} \frac{d\sigma}{d\varepsilon}}{\sigma \frac{d\dot{\varepsilon}}{d\ln\sigma}} = \frac{\dot{\varepsilon} \sigma}{\sigma \dot{\varepsilon} d\ln\varepsilon} \approx \frac{\Delta \log\sigma}{\Delta \log\varepsilon} = m \quad (3)$$

For an ideal dissipator it can be shown that both quantities J and G are equal in their amount, which means that *m* = 1 and *J* = *J*<sub>max</sub> whereas the efficiency of power dissipation  $\eta$  is given by:

$$\eta = \frac{J}{J_{\max}} = \frac{2m}{m+1} \quad (4)$$

The variation of  $\eta$  with temperature and  $\dot{\varepsilon}$  represents the relative value of energy dissipation occurring through microstructural changes. Microstructural changes can be stable, which includes a dynamic recovery and dynamic recrystallization, and instable which

includes wedge cracking, void formation at hard particles, dynamic strain ageing and macrostructural cracking. As new surfaces will form during instable changes, more energy is required, while stable changes always take place by grain boundary migration.

## FLOW INSTABILITY

The instability map is defined by a stability criterion for a dynamic material, where the differential quotient of its dissipative function has to satisfy an inequality condition, given by equation 5, to allow a stable flow.

$$\xi \left( \frac{\dot{\varepsilon}}{\varepsilon} \right) = \frac{\partial \ln(m/(m+1))}{\partial \ln \dot{\varepsilon}} + m > 0 \quad (5)$$

A superimposition of the efficiency of power dissipation and an instability maps for each deformed material is desired. Figure 12 represents processing and instability contour map for temperature range from 200 °C to 450 °C and strain rates 0.001 s<sup>-1</sup> to 10 s<sup>-1</sup> at strain 0.4. The instable zone with  $\xi < 0$  appears in the temperature ranges between 200 °C - 250 °C and 400 - 450 °C at higher and lower strain rates. Also lower values for efficiency of power dissipation in above mentioned temperature regions (200 - 250 °C and 400 - 450 °C) and entire strain rates regions indicate the microstructural changes that can result in cracking. Areas with lower values of efficiency of power dissipation are on lower and upper temperature regions for all tested strain rates. Mentioned lower values for efficiency of power dissipation indicate that larger part of energy is transferred in heat and smaller part in microstructure changes; consequently it could indicate lower deformability.

On Figure 13a the macroscopic view of occurrence of cracks on the surface of the specimen deformed at strain rate of 10 s<sup>-1</sup> and temperature of 450 °C is presented. Mentioned cracks are consequence of precipitated ( $\alpha_{\text{Mg}} + \text{Al}_{12}\text{Mg}_{17}$ ) eutectic (melting point 426 °C, Figures 3 - 6) on grain boundaries (Figures 13b-d). Since the mentioned eutectic is at 450 °C in liquid state and due to relative motion on grain boundaries during hot forming process it results in micro-cracking. At compression on 450 °C the cracks occur at all strain rates with exception at lowest (0.001 s<sup>-1</sup>, Figures 14). On Figure 14a is thus macro view of surface of deformed specimen, on Figure 14b microstructure of larger area of deformed specimen and on Figures 14c-d the recrystallized grains are presented. The presence of dynamic recrystallization namely hinder the cracks growth as a consequence of ( $\alpha_{\text{Mg}} + \text{Al}_{12}\text{Mg}_{17}$ ) eutectic on grain boundaries.

The compression on temperature 400 °C and strain rates 5 in 10 s<sup>-1</sup> also results in macro-cracks (Figure 15a) and micro-cracks (Figure 15b). These are consequence of precipitation of mentioned ( $\alpha_{\text{Mg}} + \text{Al}_{12}\text{Mg}_{17}$ ) eutectic and  $\text{Al}_{12}\text{Mg}_{17}$  inter-metallic phase on grain boundaries (Figures 15c-d).

At lower strain rates the process of crack growth is hindered by the process of dynamic recrystallization; on Figure 16a the macro-view of deformed specimen at 400 °C and strain rate of 1 s<sup>-1</sup>, on Figure 16b the microstructure of larger area of deformed specimen and on Figure 16c-d the presence of dynamic recrystallization is presented.

In the lower temperature region (200 – 250 °C) the hot forming is not possible since at higher

(10 and 5 s<sup>-1</sup>) and also at lower strain rates (1, 0.01 and 0.001 s<sup>-1</sup>, Figure 17) macro-cracks occur (flow localisation bands, angle to compression axis is cca 45°). The mean reason was above mentioned ( $\alpha_{\text{Mg}} + \text{Al}_{12}\text{Mg}_{17}$ ) eutectic and  $\text{Al}_{12}\text{Mg}_{17}$  inter-metallic phase.

On Figure 18a macroscopic view of deformed specimen at 300 °C and strain rate of 1 s<sup>-1</sup> is shown. Its surface and its microstructure (Figure 18b) is error free. The same results at temperature 300 °C were also obtained for higher strain rates, i.e. 5 s<sup>-1</sup> and 10 s<sup>-1</sup>.

Areas with lower values of efficiency of power dissipation  $\eta < 0.2$  (see Figure 12) are in very good accordance with obtained behavior of the alloy during its hot compression, i.e. in this area (at lower temperatures) micro-cracking occurred due to absence of dynamic recovery and dynamic recrystallization.

On the Figure 12 is thus denoted the areas where during hot compression cracks occurred and also the area (hatched) for safe hot forming.

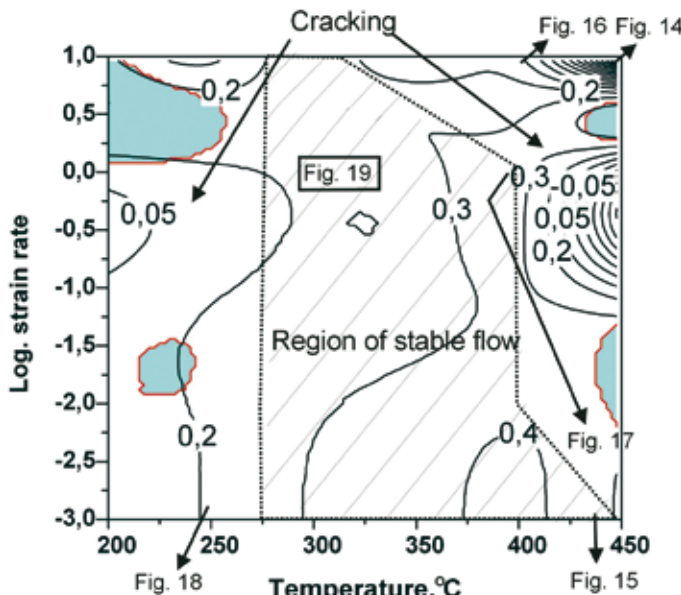


**Figure 12.** Superimposition of power dissipation map and instability map for temperature range from 200 °C to 450 °C, strain rates 0.001 s<sup>-1</sup> to 10 s<sup>-1</sup> and at strain 0.4

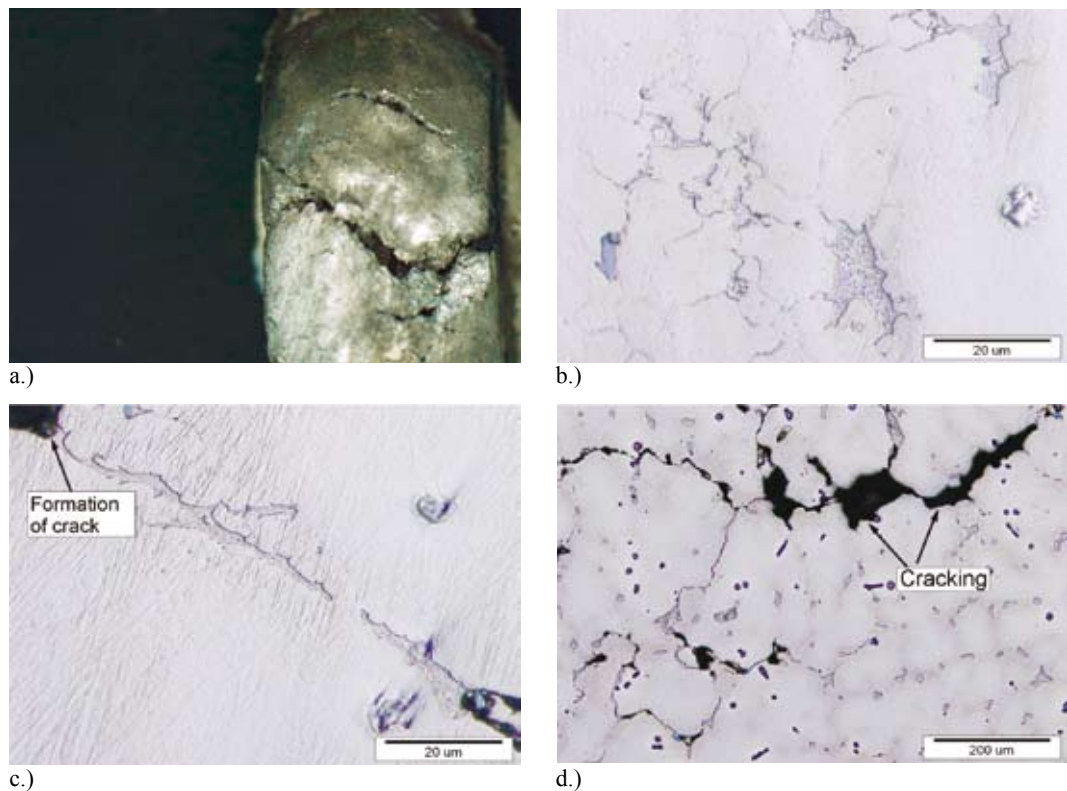


**Figure 13.** a-macroscopic view of deformed specimen, b-precipitations of  $(\alpha_{\text{Mg}} + \text{Al}_{12}\text{Mg}_{17})$  eutectic on grain boundaries, c-begin of crack formation on grain boundary with  $(\alpha_{\text{Mg}} + \text{Al}_{12}\text{Mg}_{17})$  eutectic, d-grain boundary cracking, deformation conditions: strain rate =  $10\text{s}^{-1}$ , temperature =  $450\text{ }^{\circ}\text{C}$

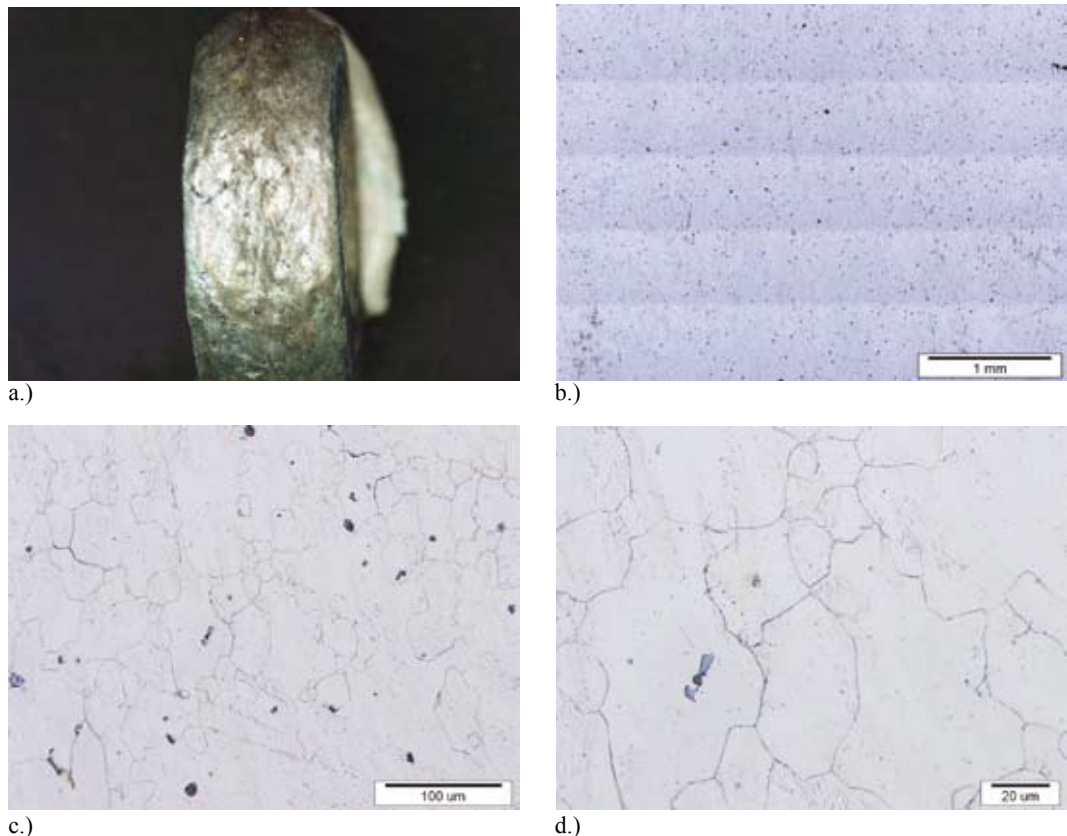


**Figure 14.** a-macroscopic view of deformed specimen, b-microstructure of larger deformed area, c-d-error free microstructure (recrystallization), deformation conditions: strain rate=0.001 s<sup>-1</sup>, temperature =450 °C

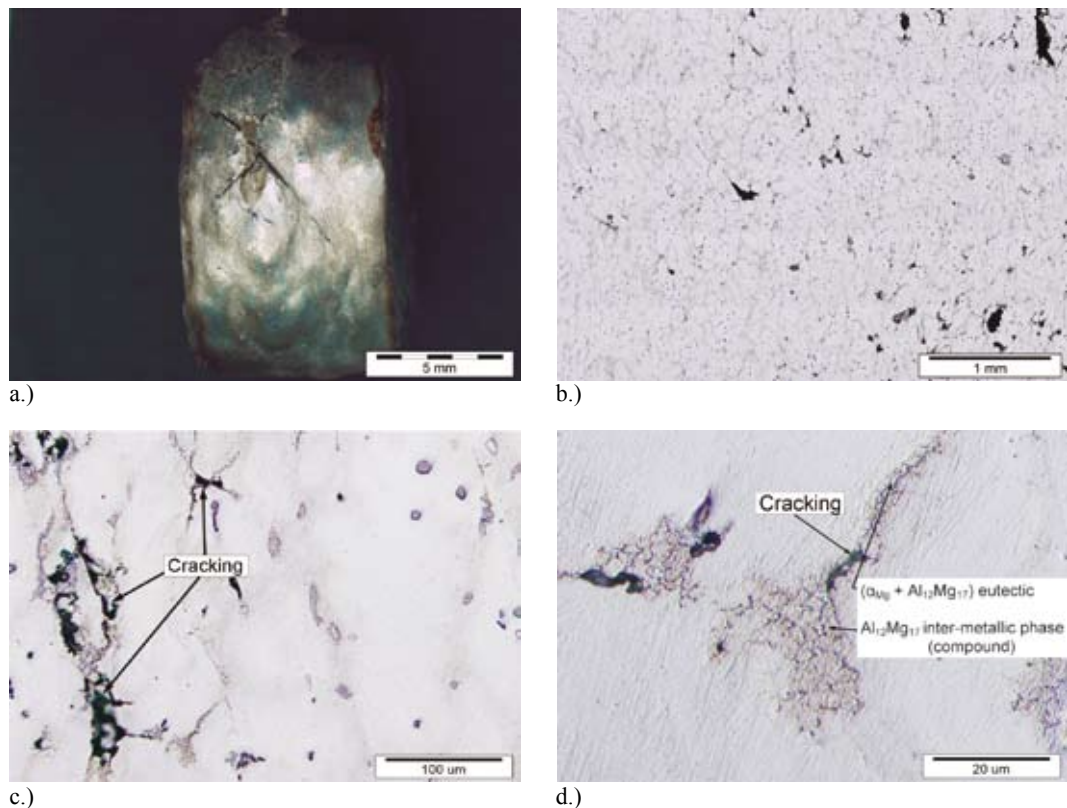


**Figure 15.** a-macroscopic view of deformed specimen, b-microstructure of larger deformed area, c-d-grain boundary cracking, and deformation conditions: strain rates = 5 - 10 s<sup>-1</sup>, temperature = 400 °C

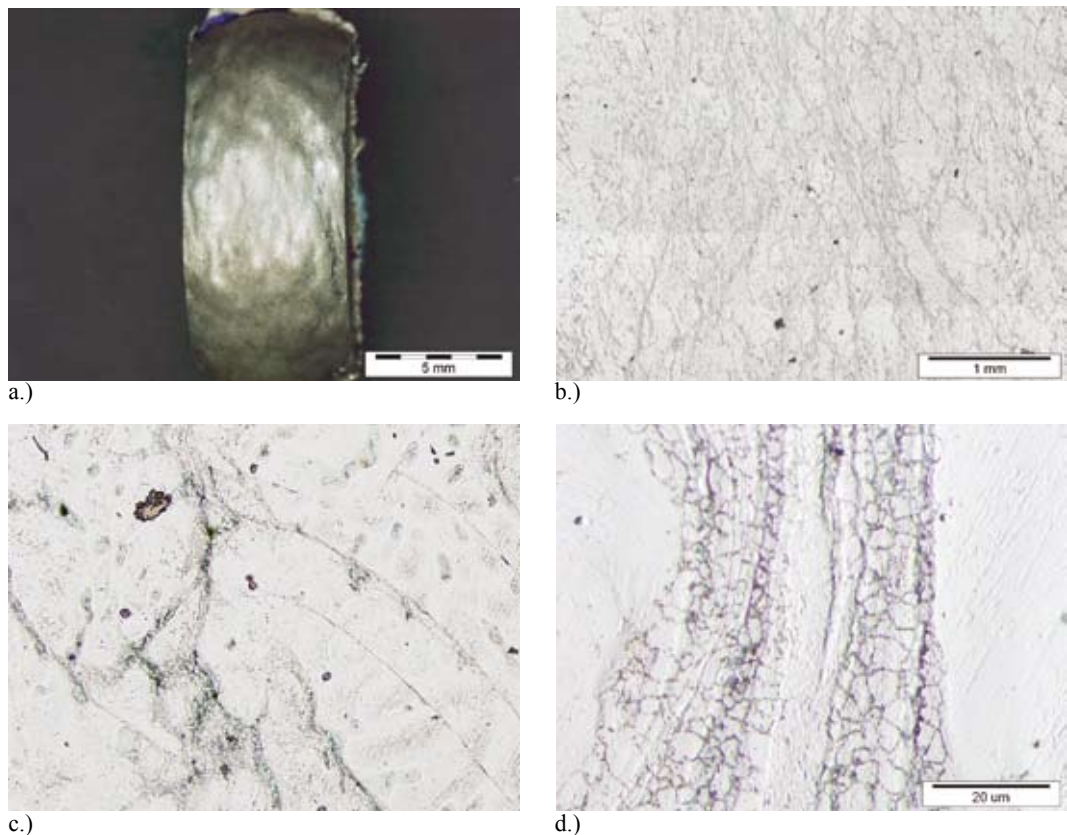


**Figure 16.** a-macroscopic view of deformed specimen, b-microstructure of large deformed area, c-d-error free microstructure (recrystallization on grain boundaries), deformation conditions: strain rate = $1\text{ s}^{-1}$ , temperature = $400\text{ }^{\circ}\text{C}$

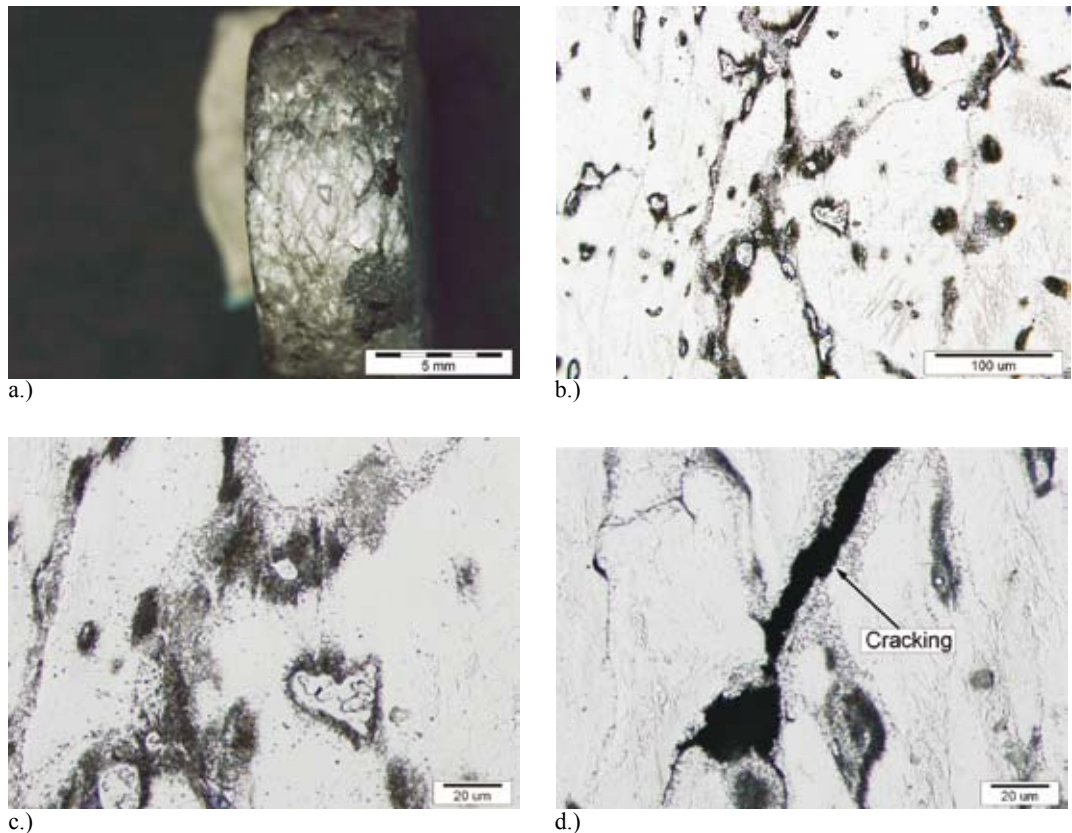


**Figure 17.** a-macroscopic view of deformed specimen, b-c-precipitation of ( $\alpha_{\text{Mg}} + \text{Al}_{12}\text{Mg}_{17}$ ) eutectic and  $\text{Al}_{12}\text{Mg}_{17}$  inter-metallic phase on grain boundaries, d-cracking on grain boundaries, deformation conditions: strain rate=0.001 s<sup>-1</sup>, temperature = 250 °C

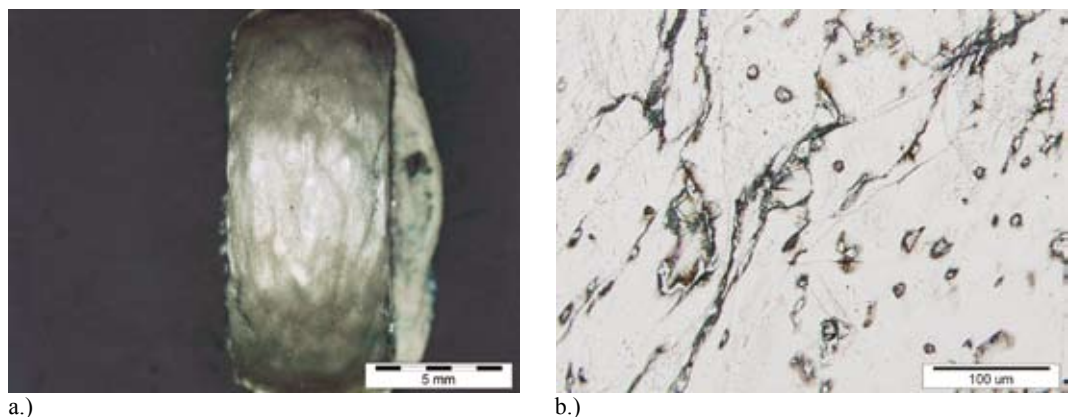


**Figure 18.** a-macroscopic view of deformed specimen, b-error free microstructure of deformed specimen, deformation conditions: strain rate =1s<sup>-1</sup>, temperature =300 °C

## CONCLUSIONS

From the cooling curves the solidification of the Mg-Al alloys was observed. The STA results show the accordance of the solidification course with the cooling curves. At the alloy AM60 the additional solidification peak was observed from the STA curves. That phenomena was connected by the eutectic crystallization, where the residual melt was transformed into the eutectic ( $\alpha_{\text{Mg}} + \text{Al}_{12}\text{Mg}_{17}$ ), which was established by the thermodynamic calculation and by the optical microscopy.

Due to the presence of manganese in the AM60 alloy the formation of the inter-metallic compound  $\text{Al}_4\text{Mn}$  is taking place with decreasing concentration of the dissolved aluminium in the molten metal, but the formation of eutectic ( $\alpha_{\text{Mg}} + \text{Al}_{12}\text{Mg}_{17}$ ) occurred at low cooling rate. The deformation characteristic of gravity

as-cast MgAl6Mn alloy in the temperature range 200-450 °C and in the strain rate range 0.001-10 s<sup>-1</sup> has been studied using processing maps. The following conclusions can be from mentioned investigation:

- [1] The alloy exhibit DRV and DRX in medium temperature range (300-400 °C) and at lower strain rates (0.001-1s<sup>-1</sup>). Thus hot deformation can be performed in mentioned temperature and strain rates regions.
- [2] At temperatures higher than 426 °C the material exhibit lower ductility due to melting of ( $\alpha_{\text{Mg}} + \text{Al}_{12}\text{Mg}_{17}$ ) eutectic which is located on a grain boundaries.
- [3] At temperatures 250 °C and lower than the grain boundary cracking on grain boundaries due to precipitates of  $\text{Al}_{12}\text{Mg}_{17}$  inter-metallic phase and ( $\alpha_{\text{Mg}} + \text{Al}_{12}\text{Mg}_{17}$ ) eutectic.
- [4] From technological (production) point of view the optimal temperature for hot forming is at 300 °C where the higher strain rates (5-10 s<sup>-1</sup>) could be applied.

## REFERENCES

- [1] T.B. MASSALSKI, H. OKAMOTO: Binary Alloys Phase Diagrams 2<sup>nd</sup> ed. L. Subramanian, Kaprzak eds., ASM, Metal Park, Ohio, (1990).
- [2] J. MEDVED, P. MRVAR: Thermal analysis of the Mg-Al alloys. Mater. sci. forum, 2006, let. 508, zv. 2, 603-608
- [3] P. MRVAR, J. MEDVED, M. TRBIZAN, A. PAPEŽ, J. RAMOVŽ: Nonmetallic inclusions and intermetallic compounds in alloy AM60. Livar. vestn., 2005, let. 52, zv. 4, 146-159
- [4] C.M. SELLARS, W.J. MCG. TEGART, La relation entre la resistance et la structure dans la deformation a chaud, Mem. Sci. Rev. Metal., 63 (1966), 731-746
- [5] C.M. SELLARS, W.J. MCG. TEGART, Int. Metall. Rev., 17 (1972), 1-24
- [6] J.J. JONAS, C.M. SELLARS, W.J. MCG. TEGART, Metall. Rev., 130 (1969), 1-24
- [7] G.KUGLER, M.KNAP, H.PALKOVSKI AND R.TURK, Estimation of activation energy for calculating the hot workability properties of metals, Metalurgia, 43/4 (2004) 267-272.
- [8] Y.V.R.K. PRASAD, S. SASIDHARA, Hot Working Guide, A Compendium of Processing Maps, ISBN: 0-87170-589-2, ASM International 1997.

# Sinteza in analiza hitro strjenih trakov iz bakrovih zlitin

## Synthesis and analysis of rapidly solidified copper alloys ribbons

M. ŠULER<sup>1</sup>, M. BIZJAK<sup>1</sup>, L. KOSEC<sup>1</sup>, B. KOSEC<sup>1</sup>, A. C. KNEISSL<sup>2</sup>, I. ANŽEL<sup>3</sup>

<sup>1</sup>Naravoslovnotehniška fakulteta, Univerza v Ljubljani, Aškerčeva 12, Ljubljana, Slovenija;

E-mail: marko.suler@gmail.com, milan.bizjak@ntf.uni-lj.si,  
ladislav.kosec@ntf.uni-lj.si, borut.kose@ntf.uni-lj.si

<sup>2</sup>Montanuniversität Leoben, Franz-Josef Straße 18, Leoben, Austria

E-mail: kneissl@unileoben.ac.at

<sup>3</sup>Fakulteta za strojništvo, Univerza v Mariboru, Smetanova 17, Maribor, Slovenija

E-mail: ivan.anzel@uni-mb.si

**Received:** October 11, 2006    **Accepted:** October 20, 2006

**Izvleček:** Po postopku hitrega strjevanja na vrtečem se kolatu smo izdelali binarne bakrove zlitine z do 4,41 mas% železa in ternerne zlitine, ki so poleg železa vsebovale še do 0,014 mas% ogljika. V vseh hitro strjenih zlitinah smo dosegli veliko prenasičenje trdne raztopine. Trakovе hitro strjenih zlitin smo analizirali z metodami optične in vrstične elektronske mikroskopije, s katerimi smo ugotovili mikrostrukturne značilnosti po debelini trakov po hitrem strjevanju in mikrostrukturne spremembe po toplotni obdelavi, ki so bile odvisne predvsem od koncentracije zlitinskih elementov in debeline trakov. Z rentgensko struktурno analizo in transmisijsko elektronsko mikroskopijo smo ugotovili spremembe mrežnih parametrov osnovnih celic kristalne mreže bakra po hitrem strjevanju v odvisnosti od koncentracije dodanih elementov. Razpad prenasičenih trdnih raztopin med toplotno obdelavo smo spremljali s sprotnimi meritvami električne upornosti. Ugotovili smo zelo velik vpliv ogljika na kinetiko razpada prenasičenih trdnih raztopin.

**Abstract:** In the present work, the synthesis of rapidly solidified ribbons of copper alloys is presented. Binary copper alloys, with a maximum iron content of 4.41 mass.% and similar alloys with a maximum copper content of 0.014 mass.% were produced by rapid-solidification on a rotating wheel (melt-spinning). In both groups of alloys, highly supersaturated solid solutions were achieved. Rapidly quenched ribbons were examined both prior to and after heat treatment using optical and scanning electron microscopy in order to determine microstructural characteristics along the thickness of the ribbons. Thickness of the ribbons and the concentration of alloyed elements had the highest effect on microstructural changes after heat treatment. Analysis by X-ray diffraction and transmission electron microscopy were carried out to evaluate the resulting crystallography and changes in the face centered cubic cell which were controlled by the concentration of the alloyed elements. To evaluate the decomposition of supersaturated solid solutions during heat treatment, which is controlled mostly by the concentration of copper in the alloy, in-situ electric resistivity measurements were also carried out.

**Ključne besede:** bakrove zlitine, hitro strjevanje, razpad prenasičenih trdnih raztopin, mrežni parameter

**Key words:** copper alloys, rapid solidification, decomposition of supersaturated solid solutions, lattice parameter

## Uvod

Hitro strjene zlitine je moč izdelati po različnih postopkih, med katerimi sta danes v industriji najbolj uveljavljena postopka izdelave prahov z razprševanjem taline in izdelave tankih trakov s hitrim strjevanjem na vrtečem se kolatu.

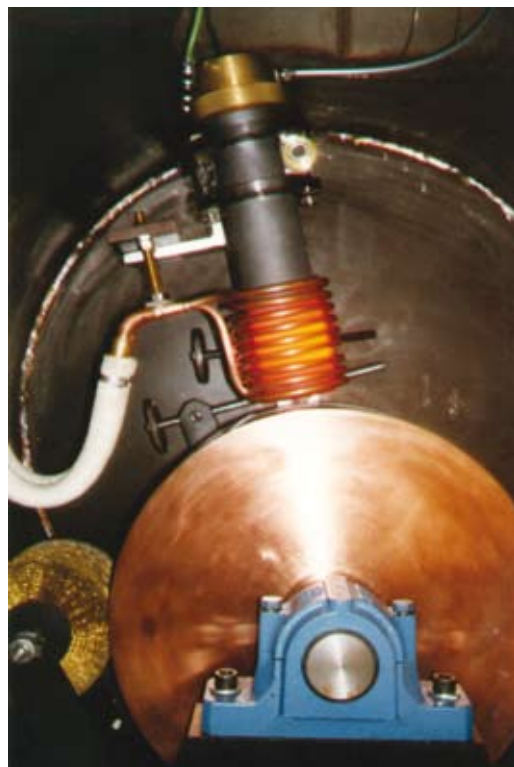
Postopki hitrega strjevanja so omogočili večjo topnost zlitinskih elementov v trdnih raztopinah, kar je še posebej pomembno pri izdelavi zlitin z elementi, ki imajo v ravnotežnem stanju majhno topnost v trdnem<sup>[1,2]</sup>. Po hitrem strjevanju nastala mikrostruktura je nestabilna in prehaja med toplotno obdelavo v bolj stabilno<sup>[3,4]</sup>. Na prečnem prerezu trakov hitro strjenih zlitin so področja značilne mikrostrukture, kar se kaže predvsem v velikosti in obliki kristalnih zrn<sup>[5,6]</sup>. Delo zajema sintezo in karakterizacijo hitro strjenih zlitin bakra in železa ter hitro strjenih zlitin bakra, železa in ogljika.

Maksimalna topnost železa v trdnem bakru je le 4,1 mas.% pri temperaturi 1096 °C, ki pa se s temperaturo hitro zmanjšuje in je zanemarljivo majhna oziroma blizu 0 že pri 600°C. Pri počasnem ohlajanju zlitin bakra z železom so v mikrostrukturi izločki faz bogatih z železom že pri zlitini z najmanj železa, s hitrim strjevanjem pa je možno doseči prenasičene trdne raztopine pri sobni temperaturi tudi pri zlitinah, v katerih vsebnost železa celo presega maksimalno topnost pri 1096 °C (4,1 mas.% Fe). Maksimalna topnost ogljika v bakru je le 0,008 mas.% pri 1100°C in se s temperaturo še hitreje zmanjšuje<sup>[7]</sup>.

Kljub zanemarljivo majhni topnosti železa in ogljika v trdnem bakru smo s hitrim

strjevanjem zadržali v bakrovi matici velik del obeh zlitinskih elementov.

Na sliki 1 je prikazana naprava (melt spinner), s katero smo odlili trakove hitro strjenih zlitin z bakrenim bobnom, tuljavo in talilnim loncem<sup>[8]</sup>. Pri karakterizaciji zlitin smo uporabili naslednje preiskovalne: svetlobna (OLYMPUS BX61) in vrstična elektronska mikroskopija (JEOL JSM – 5610), simultana termična analiza (NETZSCH STA 449), rentgenska struktturna analiza (Philips PW 3710, Cu<sub>Kα</sub>), transmisijnska elektronska mikroskopija (JEM 2000 FX) in sprotne meritve električne upornosti (IRT) med toplotno obdelavo.



**Slika 1.** Naprava za izdelavo hitro strjenih trakov na vrtečem se valju

**Figure 1.** Melt spinnig device

## EKSPERIMENTALNO DELO IN ANALIZA REZULTATOV

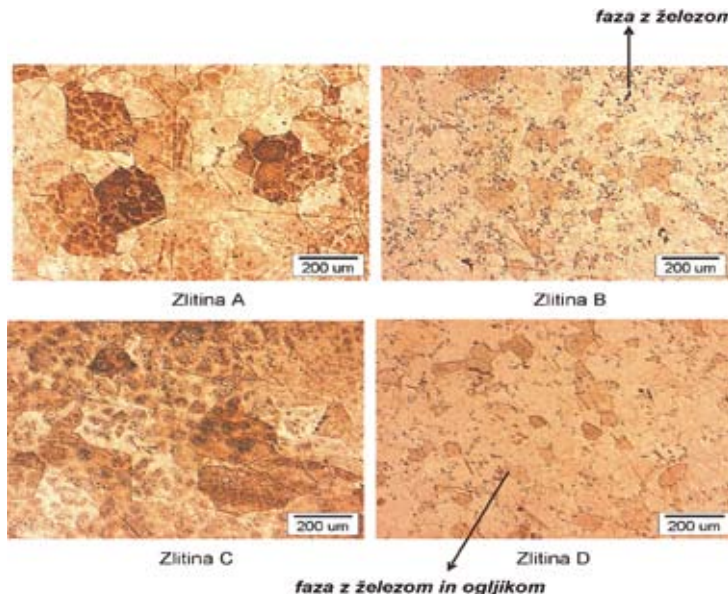
Kemične sestave ter oznake posameznih hitro strjenih zlitin so v tabeli 1.

Na sliki 2 so mikrostrukture počasi ohlajenih zlitin ozziroma vložkov, katere smo nato po postopku hitrega strjevanja odlili v trakove. Kristalna zrna so relativno velika in se manjšajo s koncentracijo zlitinskih elementov (pri zlitinah B in D s 4 ozziroma 4,5 mas. % dodatka so bistveno manjša kot pri zlitinah A in C s 3 mas. % dodatka).

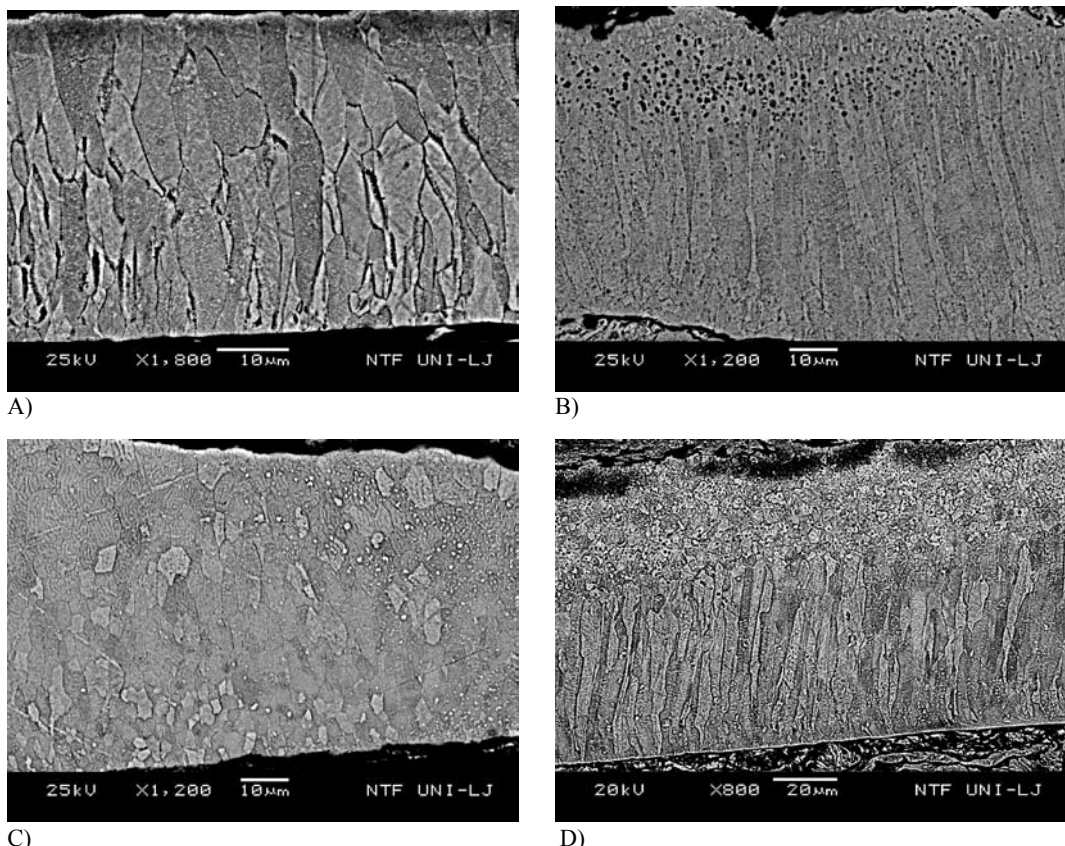
**Tabela 1.** Kemična sestava zlitin

**Table 1.** Chemical composition of the alloys

Zlิตina	Fe[mas.%]	Cu[mas.%]	C[mas.%]	S[mas.%]
A	3,00	96,986		0,014
B	4,41	95,576		0,014
C	2,99	96,984	0,012	0,014
D	3,92	96,052	0,014	0,014



**Slika 2.** Mikrostruktura klasično odlitih zlitin  
**Figure 2.** Microstructure of classically casted alloys



**Slika 3.** Mikrostruktura na prečnih prerezih trakov hitro strjenih zlitin  
**Figure 3.** Microstructure on crosssections of rapidly solidified ribbons

opazovanju mikrostrukture na prosti površini hitro strjenega traku lahko na posameznih zrnih opazimo tudi podstrukturo v obliki pasov oziroma trakov<sup>[9,10]</sup>.

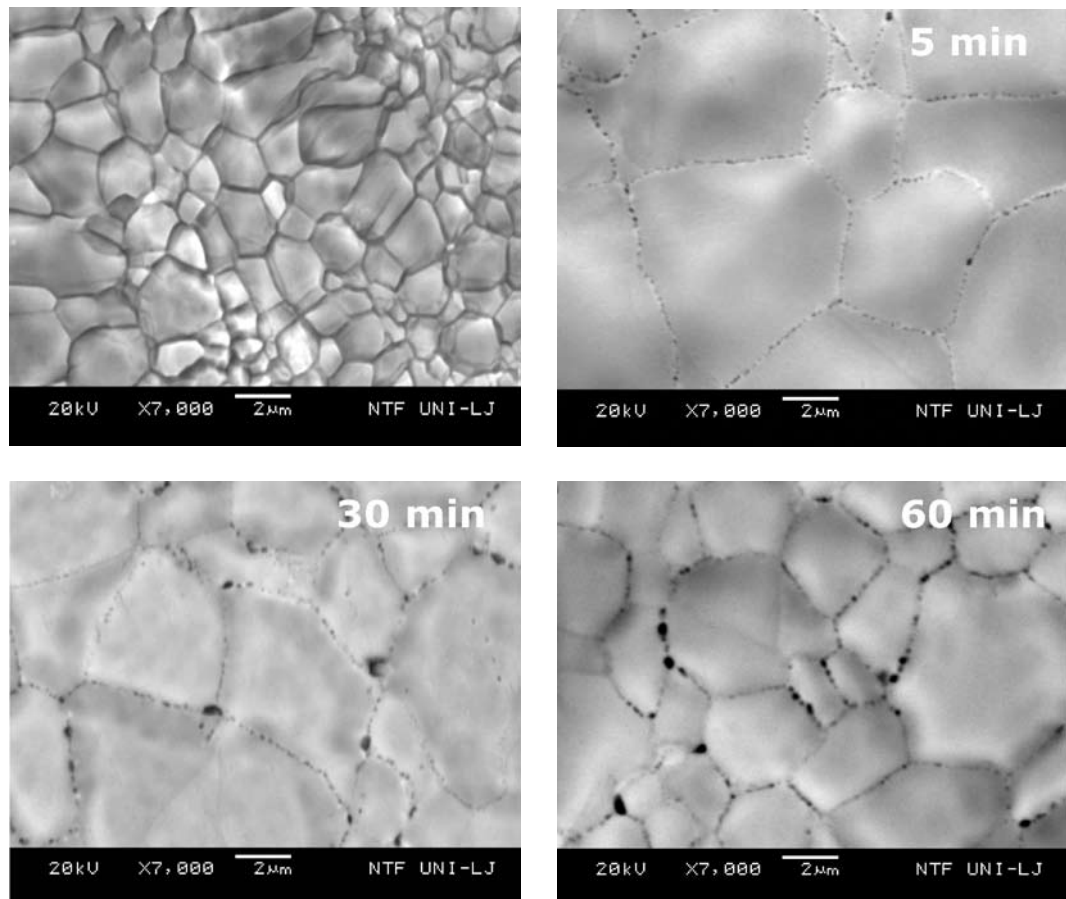
Na nivoju opazovanja pri povečavi približno 10000x z vrstičnim elektronskim mikroskopom je mikrostruktura homogena. Trakove vseh hitro strjenih zlitin smo žarili na temperaturi 715 °C po 5, 10, 15, 30 in 60 minut. Da bi videli, koliko železa se izloči iz trdne raztopine po eno urnem žarjenju smo pri vseh zlitinah s pomočjo EDS izmerili kvantitativno kemično sestavo v točkah v

sredini kristalnih zrn tako v hitro strjenih, kot eno uro žarjenih zlitinah. Spremembe koncentracije železa znotraj kristalnih zrn med izotermnim žarjenjem posameznih trakov hitro strjenih zlitin po eni uri so prikazane v tabeli 2, spremembe mikrostrukture po posameznih časih žarjenja pa na sliki 4.

Ker s pomočjo diferenčne scanning kalorimetrije (DSC) nismo zaznali razpada prenasičenih trdnih raztopin oziroma transformacij, ki bi se eventuelno pojavile že pri nižjih temperaturah, smo se odločili še za metodo sprotnega merjenja električne

**Tabela 2.** Sprememba koncentracije železa znotraj kristalnih zrn po enournem žarjenju na 715°C**Table 2.** Changes of iron concentration within the crystal grains after annealing for one hour at 715°C

ZLITINA	Sprememba koncentracije železa [mas. %]
A	0,16
B	1,17
C	0,27
D	1,08

**Slika 4.** Sprememba mikrostrukture med izotermnim žarjenjem na temperaturi 715°C**Figure 4.** Microstructural changes during isothermal annealing at 715°C

**Tabela 3.** Temperaturni in časovni intervali razpada prenasičenih trdnih raztopin v preiskovanih zlitinah  
**Table 3.** Temperature and time intervals of decomposition of supersaturated solid solutions in investigated alloys

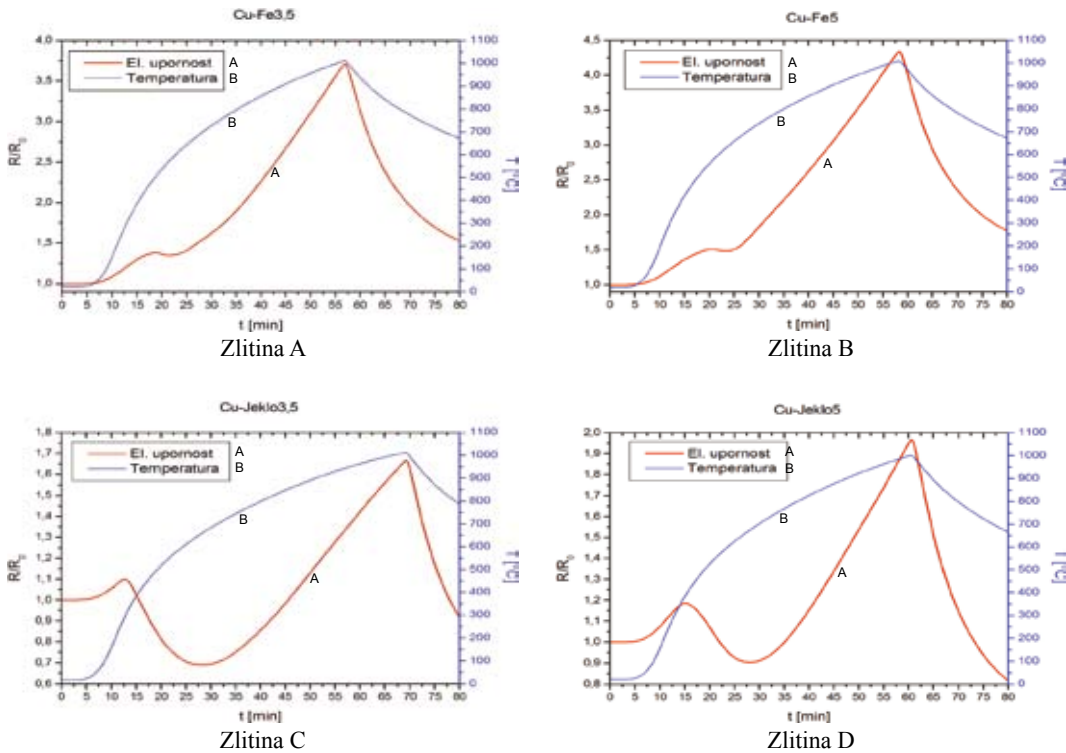
Zlิตina	A	B	C	D
Temperaturni interval transformacije [ °C]	500°C do 563°C ΔT=63°C	564°C do 629°C ΔT=65°C	388,5°C do 660°C ΔT=271,5°C	379°C do 675,5°C ΔT=296,5°C
Trajanje transformacije [min]	2,65	3,1	12,9	15,4
Relativna sprememba upornosti med transformacijo	-0,04	-0,05	-0,41	-0,28
Relativna sprememba upornosti med celotnim časom segrevanja (25-1020°C)	3,71	4,35	1,66	1,96

upornosti (IRT) med počasnim segrevanjem, kar se je izkazalo za bolj učinkovito metodo za ugotavljanja temperaturnih in časovnih intervalov razpada prenasičenih trdnih raztopin pri posameznih zlitinah<sup>[11,12,13]</sup>.

Na sliki 5 so rezultati sprotnih meritev spremembe električne upornosti med segrevanjem trakov hitro strjenih zlitin. Za vsako izmed v okviru prispevka analizirano zlitino lahko iz diagramov zveznih meritev električne upornosti direktno izmerimo čas poteka transformacij in določimo temperature, pri katerih se transformacije začnejo ozziroma končajo. Temperaturni in časovni intervali transformacij posameznih zlitin so v tabeli 3<sup>[10,13]</sup>.

Transformacije se pri zlitinah bakra z železom in ogljikom (C in D) začnejo pri nižjih temperaturah in tudi temperatura konca transformacije je pri teh zlitinah

opazno višja. Temperaturni intervali in časi trajanj transformacij pri zlitinah z ogljikom so opazno daljši kot pri binarnih zlitinah bakra in železa. V temperaturnem intervalu transformacij se električna upornost trakov hitro strjenih zlitin s temperaturo zmanjšuje. Ta pojav je veliko bolj izrazit pri zlitinah z ogljikom, saj je med samo transformacijo, kljub povečevanju temperature relativni padec upornosti kar 0,41 pri zlitini C ozziroma 0,28 pri zlitini D. Relativna sprememba upornosti ozziroma njeno zmanjšanje med samo transformacijo pri zlitinah brez ogljika ni tako velika. Ker je bila relativna sprememba upornosti med samimi transformacijami pri zlitinah z železom in ogljikom tako izrazita, smo sprva pričakovali tudi izrazito odstopanje pri koncu segrevanja, to je pri temperaturi 1020 °C. Vendar je tu prišlo do velike spremembe relativne upornosti ravno pri zlitinah brez ogljika. Tabela 3 pove, da je končni porast relativne spremembe upornosti



**Slika 5.** Rezultati zveznih meritev električne upornosti posameznih hitro strjenih zlitin  
**Figure 5.** In-situ electric resistivity measurements results

pri zlitinah brez ogljika za več kot dvakrat večji kot pri zlitinah z ogljikom.

Z rentgensko strukturno analizo nismo zaznali precipitatov v zlitinah CuFe (B) in CuFe (D), saj dobljeni spektri ustrezajo čistemu bakru, kar je posledica premajhnega volumskega deleža precipitatov v trakovih hitro strjenih zlitin B in D. Opazili pa smo zamik vrhov k manjšim kotom z večjim prenasičenjem (slika 6). S tem se spremeni tudi velikost kristalne rešetke bakra, kar je prikazano v tabeli 4. Opazili smo tudi, da hitrost strjevanja nima bistvenega vpliva na mrežni parameter rešetke, saj je razlika v velikosti osnovne celice hitro strjenega čistega bakra in žarjenega čistega bakra neznatna.

Pri 20000-kratni povečavi smo s pomočjo TEM znotraj kristalnih zrn v zlitini B na mestih, kjer smo doslej govorili še o homogeni trdni raztopini, že zasledili precipitate velikosti nekaj deset nanometrov, kjer so le-ti vidni kot drobno dispergirane temne pikice.

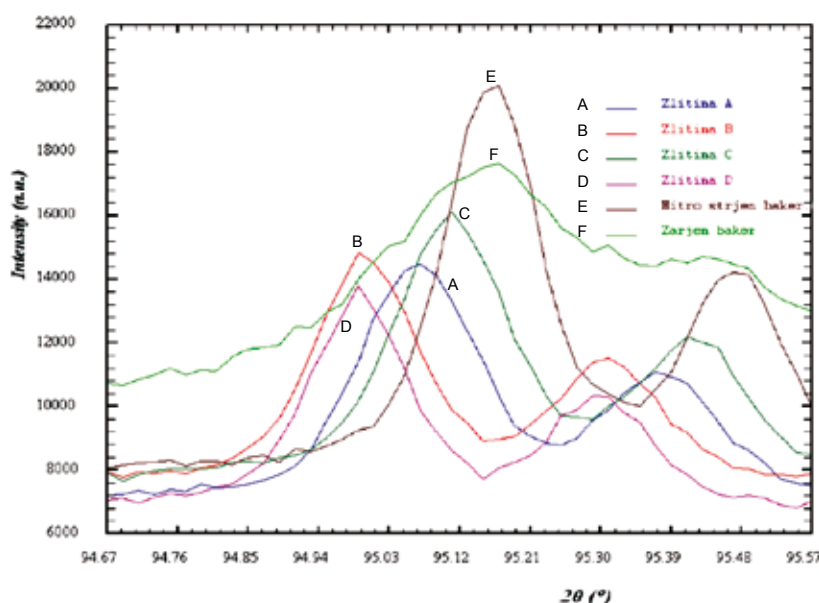
Pri še večjih povečavah smo opazili, da se znotraj bakrene matice pojavljajo v bistvu precipitati dveh velikostnih redov; večji so veliki 20-30 nm, med tem ko merijo manjši v premeru le nekaj nanometrov. Precipitati so sicer sferičnih oblik, vendar se pri velikih povečavah opazi okrog njih napetostno polje, ki je posledica neujemanja kristalne rešetke precipitata in matice, kar je na sliki vidno kot temna lisa okrog precipitatov.

**Tabela 4.** Sprememba mrežnega parametra pri posameznih zlitinah  
**Table 4.** Lattice parameter changes in alloys

Zlิตina	Razdalja med ravninama d[nm]		Rob osnovne celice [nm]
	(111)	(200)	
A	0,2085	0,1809	0,3612
B	0,2093	0,1813	0,3625
C	0,2085	0,1809	0,3612
D	0,2091	0,1811	0,3621
Hitro strjen baker	0,2084	0,1806	0,3611
Žarjen baker	0,20835	0,1805	0,3610

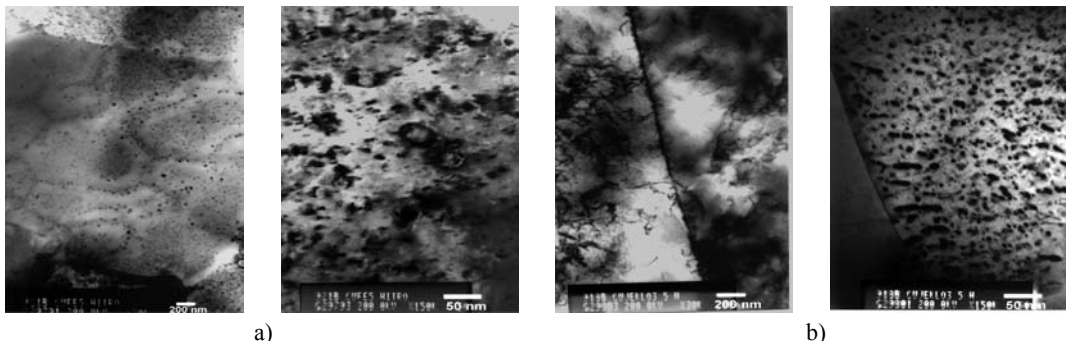
Posnetki mikrostruktur zlitin B in C s TEM so prikazani na sliki 7. V zlitini C je zelo velika gostota dislokacij, ki se kažejo kot drobne in ukrivljene temne črtice. Precipitati

znotraj bakrene matice so bili pri zlitini C izredno drobni (veliki le nekaj nanometrov), tako da smo jih v mikrostrukturi opazili šele pri povečavah nad 100000-krat.



**Slika 6.** Rentgenska strukturna analiza zlitin A, B, C in D ter hitro strjenega in žarjenega tehnično čistega bakra

**Figure 6.** X-ray diffraction analysis results of A, B, C, D alloys, rapidly solidified and annealed technical copper



**Slika 7.** Mikrostruktura zlitin B (a) in C (b), TEM

**Figure 7.** Microstructure of alloy B (a) and alloy C (b), TEM

S pomočjo uklona elektronov v TEM smo dobili uklonske slike, ki so osnova za določitev kristalne strukture in mrežnih parametrov faz oziroma sestavin mikrostrukture. Izmerjene razdalje med ravninami v osnovni celici bakra so se povsem ujemale z rezultati, ki smo jih dobili z rentgensko struktурno analizo. Za precipitate, katerih rentgenska strukturalna analiza ni zaznala, smo ugotovili, da imajo prav tako kot baker kubično ploskovno centrirano kristalno mrežo in da meri rob osnovne celice te kristalne mreže 0,41 nm. Izmerjeni kristalografski parametri precipitatov so podobni železovem oksidu FeO, vendar je verjetnost železovega oksida v zlitini majhna.

## SKLEPI

Mikrostruktura na prečnih prerezih trakov hitro strjenih zlitin je ob kontaktni površini z bakrenim kolutom iz drobnih kristalnih zrn, katerim sledi v notranjost traku cona transkristalnih zrn, ki segajo vse do proste površine.

V mikrostrukturi zlitin ob prosti površini je tako imenovana pasovna podstruktura.

Po izotermnem žarjenju na temperaturi 715 °C kristalna zrna le malo zrastejo. Rast najverjetneje preprečujejo z železom bogati precipitati na kristalnih mejah. Merjenje električne upornosti med toplotno obdelavo trakov hitro strjenih zlitin je bolj učinkovit način sledenja mikrostrukturnih sprememb od metod termične analize.

Razpad prenasičenih trdnih raztopin v zlitinah CuFeC (C, D) začne pri bistveno nižjih temperaturah in traja približno 5-krat dalj kot pri zlitinah CuFe (A, B). S povečanim prenasičenjem se spremene tudi parametri osnovne celice bakrove matice. Hitro strjena zlิตina CuFeC (C) ne predstavlja enofazne, homogene trdne raztopine. Znotraj kristalnih zrn trdne raztopine so drobno dispergirani delci nanometrske velikosti. To smo ugotovili s preiskavo z analitsko TEM.

V hitro strjenih zlitinah se pogosto pojavijo sestavine, katerih kemična sestava je različna od poznanih ravnotežnih in tudi neravnotežnih faz oziroma spojin, ki so že kristalografsko identificirane, zato tudi delcev, ki so po kristalni strukturi podobni FeO, ne moremo pripisati tej spojni brez dodatnih preverjanj.

## CONCLUSIONS

### Synthesis and analysis of rapidly solidified copper alloys ribbons

Microstructure on cross sections of rapidly solidified ribbons is made of undersized crystal grains at contact surface, which pass over in large transcrystalline grains toward free surface.

At free surface of rapidly solidified ribbons a banded substructure can be detected. After isothermal annealing at 715°C the growth of crystal grains is minimal. Their growth is blocked by small precipitates on grain boundaries.

In-situ electric resistance measurements during heat treatment is more accurate method for detecting micro structural changes than methods of thermal analysis.

Decomposition of solid solutions in CuFeC (C, D) alloys starts at lower temperatures and last approximately five times longer as in CuFe (A, B) alloys. With super saturation the lattice parameters also changes. Rapidly solidified alloy C does not represent a homogeneous solid solution. This fact was determined by TEM analysis.

In rapidly solidified alloys often appear constituents with chemical composition different as already known equilibrium and non equilibrium phases that are crystallographically identified.

## LITERATURA

- [<sup>1</sup>] M. BIZJAK: Temperaturna obstojnost hitro strjenih večkomponentnih aluminijevih zlitin, Doktorska disertacija, Univerza v Ljubljani, 1999.
- [<sup>2</sup>] L. A. JACOBSON, J. McKITTRICK: Rapid solidification processing, Materials Science and Engineering, 98, 1988, 1-12.
- [<sup>3</sup>] W. KURZ, R. TRIVERDI: Rapid solidification processing and microstructure formation, Material Science and Engineering, A179/A180, 1994, 46-51.
- [<sup>4</sup>] H. JONES: The critical concentration for formation of segregation-free solid by solute trapping during rapid solidification from the melt; Materials Letters, vol. 6, No. 5, 1987
- [<sup>5</sup>] I. ANŽEL: Notranja oksidacija hitro strjenih bakrovih zlitin, Doktorska disertacija, Univerza v Ljubljani, 1996
- [<sup>6</sup>] J. W. MARTIN, R. D. DOHERTY AND B. CANTOR: Stability of microstructure in metallic systems, 2nd edition, Cambridge University Press, 1997.
- [<sup>7</sup>] ALLOY PHASE DIAGRAMS, ASM INTERNATIONAL HANDBOOK, Vol. 3, Materials Park, Ohio, 1992.
- [<sup>8</sup>] B. KOSEC: Naprava za hitro strjevanje kovinskih zlitin, Euroteh, 5, 2004, 32-33.
- [<sup>9</sup>] W. KURZ, R. Trivedi: Solidification microstructures: Recent developments and future directions; Acta Metall. Mater., vol. 38, No. 1, 1-17, 1990
- [<sup>10</sup>] M. ŠULER: Sinteza hitro strjenih trakov bakrovih zlitin, Diplomsko delo, Univerza v Ljubljani, 2005.
- [<sup>11</sup>] G. LOJEN, I. ANŽEL, A. C. KNEISSL, A. KRIŽMAN, U. UNTERWEGER, B. KOSEC, M. BIZJAK: Microstructure of Rapid Solidified Cu-Al-Ni Shape Memory Alloy Ribbons, Journal of Materials Processing Technology, Vol. 162, No. 15, pp. 220-229, 2005.
- [<sup>12</sup>] L. A. DOBRZANSKI: Technical and Economical Issues of Materials selection, Silesian Technical University, Gliwice, 1997.
- [<sup>13</sup>] M. ŠULER, L. KOSEC, I. ANŽEL, M. BIZJAK, B. KOSEC, A. C. KNEISSL, J. A. AMANGUAL: Synthesis of Rapidly Solidified Ribbons of Copper Alloys, Metalurgija, Vol. 45, No. 3, 230, 2006.

# Some methods of analysing caving processes in sublevel coal mining

## Nekateri načini analiziranja rušnih procesov pri podetažnem odkopavanju premoga

JAKOB LIKAR<sup>1</sup>, EVGEN DERVARIČ<sup>2</sup>, MILAN MEDVED<sup>3</sup>, JURIJ ČADEŽ<sup>4</sup>, GREGOR JEROMEL<sup>2</sup>

<sup>1</sup>Faculty of Natural Science and Engineering, University of Ljubljana, Aškerčeva cesta 12,  
SI-1000 Ljubljana, Slovenia; E-mail: jakob.likar@ntf.uni-lj.si

<sup>2</sup>Premogovnik Velenje, d.d., Partizanska 78, SI-3320 Velenje, Slovenia;  
E-mail: evgen.dervaric@rlv.si, gregor.jeromel@rlv.si

<sup>3</sup>HSE,d.o.o., Koprskra ulica 92, SI-1000 Ljubljana; E-mail: milan.medved@hse.si

<sup>4</sup>Geoportal, d.o.o., Brnčičeva ul.13, SI-1000 Ljubljana; E-mail: jurij.cadez@geoportal.si

Received: October 11, 2006 Accepted: October 20, 2006

**Abstract:** The formation of large disturbed areas around coal mining activities, including sublevel stoping, is due to various factors which directly or indirectly influence the surrounding rocks and soils. Even though the analytical methods for determining these impacts are not strictly determined, the elastic and elastoplastic theory can be successfully applied to calculate the impacts of the caving process on the surrounding mine objects and assessing the intensive caving process height in the hanging wall. In this paper some results of the classic theory calculation of the caving process are presented with the results obtained by 2D and 3D analyses using Finite Difference Method with FLAC 3D computer code. For geometrical data preparation, a special numerical code was developed which allows for rapid and high quality construction of large meshes of the Finite Difference up to 50,000 space elements. Large numerical analyses, which were carried out specifically to analyse the caving processes in the Velenje Coal Mine, show that this type of analytical methods could be used in the future to analyse complex processes in various material models considering multi caving and compressed coal and soil layers.

**Izvleček:** Nastanek obsežnih porušenih območij na širšem prostoru odkopavanja premoga od zgoraj navzdol je posredno odvisen od več faktorjev z direktnim in posrednim vplivom na okoliške hribine. Čeprav način analiziranja teh vplivov ni enolično določen je moč nekatere ravnotežne enačbe elasto in plastomehanike koristno uporabiti za določitev vpliva odkopa na sosednje objekte v jami ter narediti ocene višine intenzivnih rušnih procesov v krovinskih plasteh. Prikazani so rezultati t.i. klasičnih računskih postopkov analiziranja rušnih procesov ter osnovne analize teh procesov z 2D in 3D numerično metodo končnih diferenc. Za geometrično pripravo podatkov je bil v ta namen razvit poseben računalniški program, ki omogoča hitro in kakovostno načrtovanje in uporabo velikih mrež končnih diferenc velikostnega reda več kot 50000 prostorskih elementov. Obsežne simulacije, ki so bile narejene posebej za potrebe analiziranja rušnih procesov pri odkopavanju lignita v Premogovniku Velenje so pokazale, da je v bodoče na takšen način moč analizirati zapletene procese v več materialnih modelih ob upoštevanju večkrat porušene in ponovno komprimirane krovnine.

**Key words:** sublevel mining method, coal, hanging wall, footwall, longwall support system, geotechnical parameters, empirical methods, numerical methods, Finite Difference Method, plastic zones, secondary stress field

**Ključne besede:** podetažna metoda odkopavanja, premog, krovina, talnina, samohodno hidravlično podporje, geotehnični parametri, empirične metode, metoda končnih diferenc, plastična območja, sekundarno napetostno polje

## INTRODUCTION

Sublevel mining of minerals and energy resources triggers various deformation processes in the earth crust which depend on many factors. Deformations, which are the result of caving processes, are defined as partially controlled rock fractures during which mechanical energy is released, which results in crushing of rocks of different sizes (COOK, N. G. W. ET. AL.<sup>[1]</sup>). Caving processes can be rapid or slow, or, are the result of fractured materials, which can cause seismic effects of different size. Since sublevel coal mining methods are designed so that caving processes occur on a wider hanging wall area, which extend high into the layers above coal layers, the effects which have impact on the development of mining (and consequently on the environment), are crucial for engineering appraisal of the situation of a wider impact area. The effects are due to intensive fractures in natural, and in some cases artificial materials, exposed to extreme stress deformation changes.

The physical aspect of fracturing of hanging wall layers of natural and soil or rock materials in sublevel coal mining refers to partially controlled process of caving of these materials into the mined – empty spaces due to the stress deformation field changes which are the result of advancement of mining. Fracturing of hanging wall materials, including coal, occurs in different ways, either continuously or discontinuously, which additionally causes stress in the surrounding rocks. Such discontinuous fractures are frequently due to man-made activities with the purpose of activating caving processes in order to achieve continuous subsiding of

upper hanging wall layers on the layers below and to prevent uncontrolled movement or leaching of mine water and other liquid masses which are located close to the mining operations. Such phenomena or processes in hanging wall layers can significantly change the course of deformation in terms of time and geometrics.

The risk level of the whole mining system in such cases is quite significant due to the possibility of inrush of mine water or liquid masses of natural materials into the caves. Particularly dangerous are inrushes which can hinder the advancement in coal mining or even stop the works for a period of time. In case of a smaller inrush, mining works can still proceed with shorter break intervals. It needs to be noted that inrushes present risk factors not only for the equipment, but also for the people involved in mining operations. In longwall sublevel mining it is important to consider the geometric design of the whole system of coal extraction which depends on the caving height. Geometric design has indirect impacts on fracturing at a certain longwall length, located in the coal layer between the hanging wall and footwall layers with different geomechanical properties. The factors which have direct impacts on technical mining characteristics are geological and geotechnical properties of the layers, the faults which are due to tectonics and structure of layers, hydrogeological conditions, as well as primary stress conditions on a wider working space. From physical point of view, the displacement vectors of hanging wall layers are directed towards the space which is in the phase of hanging wall caving, while the length of displacements is limited by the floor level.

Caving processes can significantly change the structure of a rock or weak rock and cause impacts on mine infrastructure, which plays a particular role and is vital for normal operation of the cave. The supporting systems which are used to reduce the effect of the caving processes on the existing mine infrastructure, are adjusted to real geotechnical conditions and need to have a particular flexibility and adaptability to changeable stress. Therefore, for economic and safe exploitation of coal it is of primary importance to know geotechnical properties of the layers which occur in the rocks and soils in the hanging wall, in the footwall and the properties of coal layers, and mining impact factors. The analyses of stress deformation changes in mining by fracturing the direct hanging wall were made by 2D and 3D numerical analyses by finite difference method (FDM). This method allows for complex calculations in the so called large deformations which occur during caving processes in coal mining. In this article we present the results of extensive numerical analyses, carried out by special computer interfaces which allowed for simulations of mining and fracturing of the hanging wall in 2D and 3D weak rock environment. In this way we obtained good quality geotechnical results of the complex phenomena which occur in a wider area of coal sotping.

### **SOME ANALYTICAL METHODS OF CAVING PROCESSES IN SUB-LEVEL COAL MINING**

The complexity of caving processes in sub-level coal mining is related to time-dependant changes in weak soil layers, including

coal layer, geological and geotechnical properties of weak soil layers, their structural, hydrological and mechanical changes and other natural and technological impacts. The reports in professional literature refer mainly to describing different methods for analysing stress deformation changes in the immediate or wider mining area, with focus on different aspects: studying technical parameters of excavation, e.g. caving height, the height of the immediate soil layer of the hanging wall, caving width, caving length, advancing speed, production loss, etc. The main purpose of this research was to prove suitability of the coal mining method in the given conditions. Further on we present some analyses of the different methods which describes caving processes during coal extraction.

### **Measurements and monitoring of caving processes**

The layer of clay and coal, which breaks in after crossing the face, and which in its loose state fills up the excavated area is slowly subsided by overburden layers the weight of which makes the layer consolidated, depending on the depth and the speed of face retreat. The value of pressure due to compression ranges from very low values (0.1 MPa) to high values of 10 MPa in deeper excavations at a depth of around 500 m. The greatest height of caving-in occurs close behind the face. The scheme of a caving process in coal and clay is shown in Figure 1.

The height of caving-in is determined by computing the mass volume of the caved material, which in its loose state fills up the excavated area KOČAR, F. ET AL.<sup>[2]</sup>, as follows:

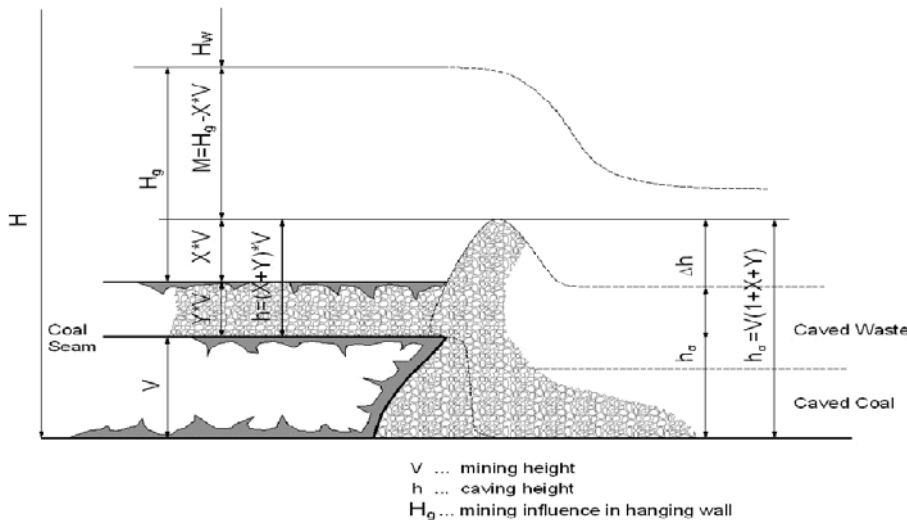


**Figure 1.** Figure of caving process in coal and clay

**Slika 1.** Shematski prikaz rušnega procesa v premogu in glini

The ratio of roof caving height/working height results in:

$$\frac{h}{V} \leq 1.5 \quad \text{or} \quad \frac{h_0}{V} \leq 1.5 \quad (1)$$

The ratio between the caving height and the working height is indicated either by coefficient "X" which is called the coefficient of caving of clay, or by "Y", when the face is deeper in the coal seam. Since the coefficient of caving was measured in situ and has not exceeded the value 1.5 it is accepted as  $X_{\max} = Y_{\max} = 1.5$ .

In case when the face is close under the clay layer, and when the caving-in gob process is completely in the clay, the ratio is as follows:

$$\frac{h}{V} \leq X_{\max}; \quad Y = 0 - h; \quad h = X - Y \quad (2)$$

When the caving-in gob process is completely in the coal and does not cover the clay layer, the relations are as follows:

$$\frac{h}{V} \leq Y_{\max}; \quad X = 0; \quad h = Y \cdot V \quad (3)$$

If the caving process covers also a part of a clay layer the relations are as follows:

$$\frac{h}{V} \leq (X + Y) = 1.5; \quad h = (X + Y) \cdot V \quad (4)$$

In these cases we calculated the thickness of the layer above the face, has been caved and has become loose. To determine the height of the caved bow the working height has to be added to these results. The equation is as follows:

$$h_0 = V \cdot [1 + (X + Y)] \quad (5)$$

The symbols in the equations above have the following meanings:

- H depth of the face floor from the surface [m],
- $H_g$  thickness of isolating clay layer [m],
- $H_w$  depth of water bearing strata [m],
- h height of roof caving - in goaf above the coal face [m],
- $h_0$  maximum height of caving in the goaf from the floor of the face [m],
- $\Delta h$  subsiding of roof layer on the goaf [m],
- $h_c$  goaf height behind the face during the consolidation phase [m],
- X coefficient of caving height of isolating layer [/],
- Y coefficient of caving height of the coal in the roof of the face [/],
- V working height [m],
- M thickness of intact isolating clay layer [m].

## Model laboratory tests

Model laboratory tests are intended for better understanding of caving processes and mechanism of fracturing, which are the constituent part of advancement in coal extracting. Tests can be made by using different materials, e.g. aluminium rods with approx. 4 mm diameter

(3 mm and 5 mm in our case) with length of 50 to 70 mm (in our case 60 mm), sand with different granulation and humidity, glass balls with different diameter, etc. Due to high complexity of the simulation and analyses of caving processes some simplifications were needed (i.e. the measurements during experiments were adjusted to the measuring technique (the use of stationary photo camera, video camera, etc.). Similarly, the quality of measurements during tests depended on the analyses of measurement results and the interpretation of the results of deformation processes.

Figure 2 shows the Taylor-Sneebley simulation model of sublevel coal mining. Model test were performed using aluminium lamellas, representing mining levels. These were drawn against the dispositive framework at constant speed, while the aluminium rods, representing the hanging walls layer were moving – »caving« into the empty space which was formed by the moving framework of the aluminium lamellas (SOVINC, I. and LIKAR, J.<sup>[3]</sup>). We believe that the simulation model of sub-level coal mining is relatively good in that it provides better understanding of physical aspects of the hanging wall caving processes.

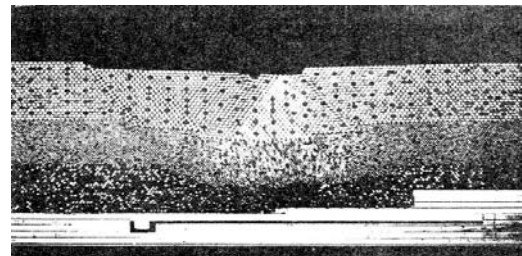
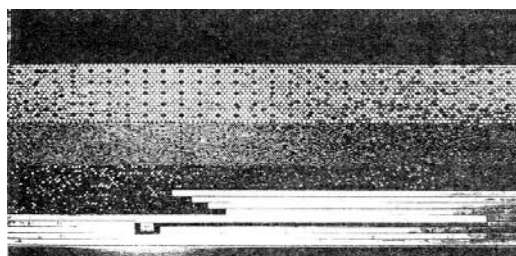


**Figure 2.** Dispositive model of Taylor-Sneebley test before the simulated excavation and during excavation in the third level in a three layer hangingwall

**Slika 2.** Prikaz modelnega poizkusa v Taylor-Sneebleijevem dispozitivu pred simulacijo odkopavanja in v fazi odkopavanja v tretji etaži v triplastni krovnnini

It needs to be emphasized that our research was carried out by using synthetic materials which are different from natural materials, particularly in our case where we were dealing with the friction part of the shear strength and not the cohesive shear strength. The performance of »hanging wall materials« agree well with the Mohr-Coulomb yielding model. The displacement field of measurement points after the simulation of excavation of the upper three levels is shown in Figure 3. The direction of displacement vectors changes with regard to vertical direction.

### VERTICAL STRESS IN THE AREA OF LONGWALL MINING

In professional literature there are several reports on similar studies based on hypotheses, which allow for direct or indirect calculations of stress distribution. WILSON, A.H. [5] made a hypothesis that vertical stress in the caved waste increases linearly from value 0 to the final value, at a distance where it is not pos-

sible to detect the impacts of instability in mine road ways.

WILSON [5] found out that pressure arch changes in the interval between factor 0.2 and 0.3 of the caving depth below the surface. Other authors, e.g. KING, H.J. and WHITTAKER, B.N. [6], CHOI, D.S. and McCAIN, D.L. [6], MARK, C. [7] suggest similar ratios between the values of 0.12, (as suggested by SMART and HALEY<sup>[8]</sup>) and 0.6, as suggested by WILSON<sup>[5]</sup>. It needs to be noted that some studies, where numerical methods were used, indicate opposite results (e.g. TRUEMAN, R. [9] and THIN, I.G.T. ET. AL. [10]), namely that the impact area decreases with the increasing caving depth. The National Coal Board<sup>[11]</sup>, based on extensive studies and measurements in situ found out that the ratio between the size of rock pressures and their geometric distribution with regard to the primary pressure stress depends to a great extent on geotechnical properties of fractured material. This is normal, since the subsiding of hangingwall layers in the caved waste area depends on these properties.

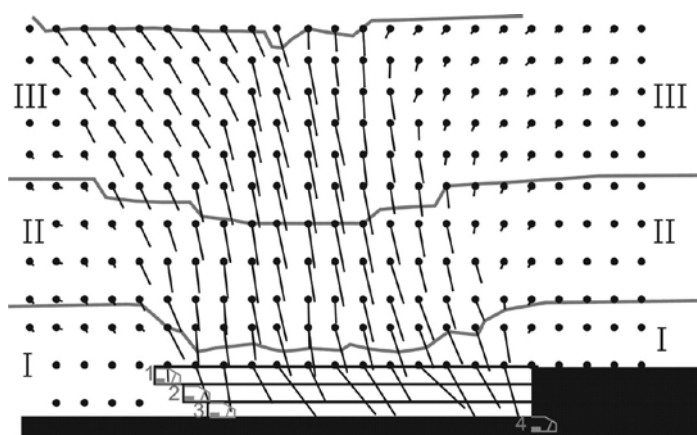


**Figure 3.** Displacement vectors of measurement points in a three-layer hangingwall after the simulation of mining of the first three panels from up to downwards

**Slika 3.** Ugotovljeni vektorji pomikov merskih točk v triplastni krovnnini po končani simulaciji odkopavanja prvih treh etaž od zgoraj navzdol

Figure 4 shows the interpretation of the distribution of vertical stress, around a single longwall face. The vertical stress is zero at the face and the rib side. The stress increases rapidly with distance into the yield zone in the unmined coal, reaching a peak value near the excavation phase. Vertical stress can be in order of four or five times the overburden stress where  $h$  is the mining depth and  $\gamma$  is the volume weight of the hangingwall strata. With the increased distance into the unmined coal, the vertical stress reduces towards the overburden stress.

In the mined region, the stress on hydraulic support is relatively small compared with the area behind the mined region and on the sides of (as shown in profiles B-B and C-C). This is due to the deformability properties of the surrounding layers.

### SIMULATION OF THE CAVING PROCESS BY USING 2D NUMERICAL METHOD

Very complex caving processes of the geological materials which are part of sublevel coal extraction can be analysed using numerical method, i.e. Finite Difference Method,

which we found appropriate for solving such problems. In this way software application using computer code FLAC 2D and FLAC 3D are useful ways for simulating caving processes connected with large displacement. FLAC 3D is also applicable for solving this type of geotechnical problems: in some cases of elements (250.000 or more) and longer computing time.

FLAC is an explicit finite difference program for engineering mechanics computation. This program simulates the behaviour of structures made of soil, rock or other materials that may undergo plastic flow when their yield limits are reached. Materials are represented by elements, or zones, which form a grid that is adjusted by the user to fit the shape of the object to be modelled. Each element behaves according to a prescribed linear or non-linear stress/strain law in response to the applied forces or boundary restraints. The material can yield and flow and the grid can deform (in large-strain mode) and move with the material that is represented. The explicit Lagrangian calculation mode and the mixed-discretization zoning technique used in FLAC ensure that plastic collapse and flow are modelled very accurately. Since no matrices are formed, large two-dimensional

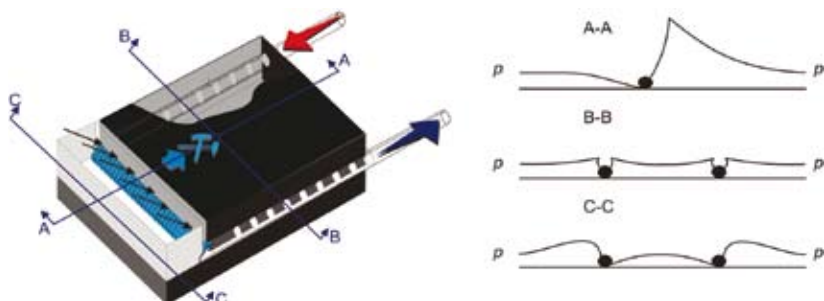


**Figure 4.** Interpretation of the distribution of vertical stress around a single longwall face  
**Slika 4.** Prikaz prerezporeditve vertikalnih napetosti pri širokočelnemu odkopavanju premoga

**Table 1.** Geotechnical properties of geological materials used in the numerical simulations  
**Tabela 1.** Geotehnične lastnosti geoloških materialov uporabljenih v numeričnih simulacijah

Type of the geological layer	Rock (soil) specific weight $\gamma$ (kN/m <sup>3</sup> )	Young modulus E(Pa)	Poisson ratio $\nu$ (/)	Shear modulus G(Pa)	Bulk Modulus K(Pa)	Angle of the internal friction $\phi$ (°)	Cohesion c(Pa)
Protection layer of clay	18.7	5.72E+08	0.32	2.17E+08	5.20E+08	35	2.0E+06
Sand with layers of clay	18.7	5.27E+08	0.32	2.00E+08	4.80E+08	30	7.0E+05
Coal	12.7	4.48E+08	0.33	1.68E+08	4.50E+08	30	1.5E+06
Comprimented coal in the gob	12.7	3.52E+08	0.35	1.30E+08	4.00E+08	25	1.0E+05

calculations can be made without excessive memory requirements. The drawbacks of the explicit formulation (i.e., small time step limitation and the question of required damping) are overcome to some extent by automatic inertia scaling and automatic damping that does not influence the mode of failure.

In the simulation of the caving process during longwall coal mining we used 2D and 3D analyses. The emphasis was on the simulation of the coal extracting by sublevel caving

for different speeds of the coal extracting advancement.

Primary stress state was assumed on the basis of the weight of the handing wall layers. It needs to be emphasized that the primary stress estimation is the result of the analyses which were made in previous decades and were carried out in the Velenje Coal Mine. This refers to the average ratio between primary horizontal and vertical component of stress which is  $K_0 = 0.85$ . The table shows

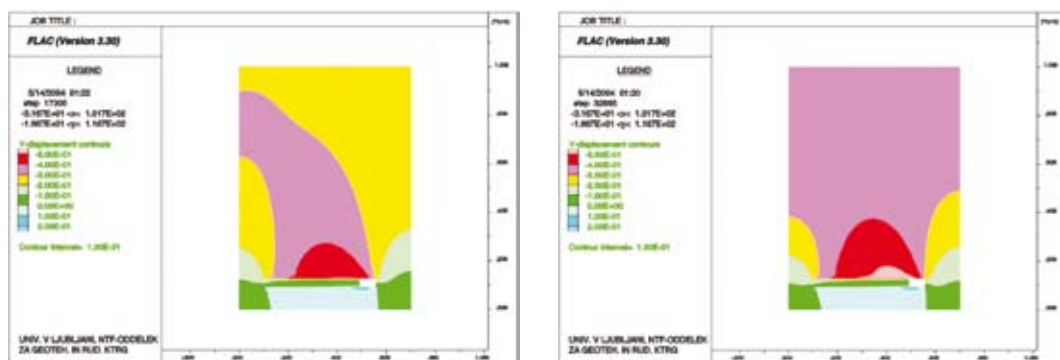


**Figure 5.** Vertical displacements during coal extracting when advancement is 3m/day and displacements when coal extracting has advancement 7m/day, JEROMEL [12]

**Slika 5.** Vertikalni pomiki pri napredku odkopa 3m/dan in vertikalni pomiki pri napredku odkopa 7m/dan, JEROMEL [12]

input data for calculations. In calculations we employed an additional program function FISH, which included the elements which allowed for the simulation of the speed of coal extracting from 1.0 m/day to 8.0 m/day.

### Results of the simulation of caving process in longwall coal extracting

Caving processes of hangingwall in longwall coal mining are more intensive if mechanical properties of coal and the hanging wall are different, particularly when the direct hangingwall is harder than the coal layer. In such cases a spontaneous continuous fracturing of the hangingwall with subsequent large stress concentrations does not occur in the pillar of coal layer and in the immediate hangingwall layers, which is frequently caused by rock bursts (Old Coal Mine Zenica, Kakanj Coal Mine, BiH). In the case which we analysed, the properties of the hangingwall and the coal layer allowed for a continuous hangingwall caving.

A comparison of our analyses was made where we considered an equal distance from the initial point of excavation, meaning that different time periods were needed to reach a certain length of longwall; coal extraction with shorter advancement requires more time to reach a certain distance from the initial point of coal extraction. For this reason, the speed of extraction advancement and changes in secondary deformation fields related to time increases of displacements of the hanging wall layers, which is shown in Figure 5. If we compare the size of the calculated displacements for the advance coal extraction speed of 3 m/day and 7 m/day, we can see that the intensity of caving is significantly larger at a low extraction speed, which results in deformation processes which are less favourable as far as the distribution of plastic yield regions in the hangingwall seams is concerned.

There is less difference in the height and the shape of the area to which individual zones of additional effective vertical stress reach (Figure 6).

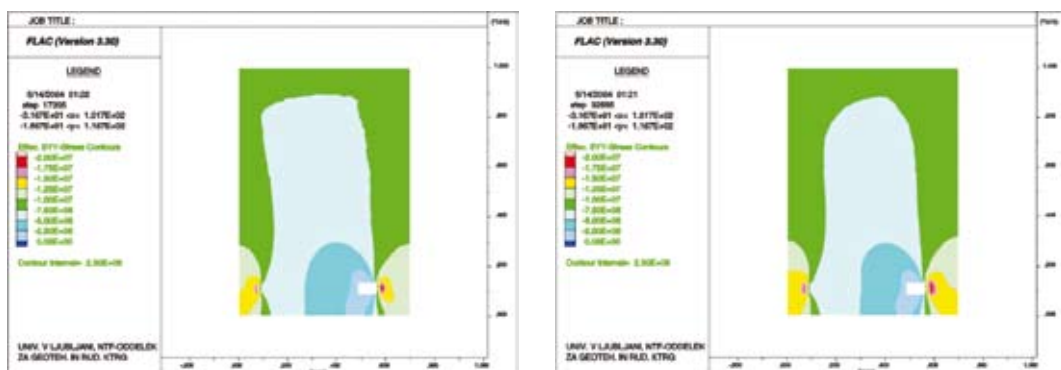


**Figure 6.** Effective vertical stress in the surroundings layers when extraction advancement are 3m/day and 7m/day JEROMEL [12]

**Slika 6.** Efektivne vertikalne napetosti v okoliških plasteh pri napredku odkopa 3m/dan in 7m/dan JEROMEL [12]

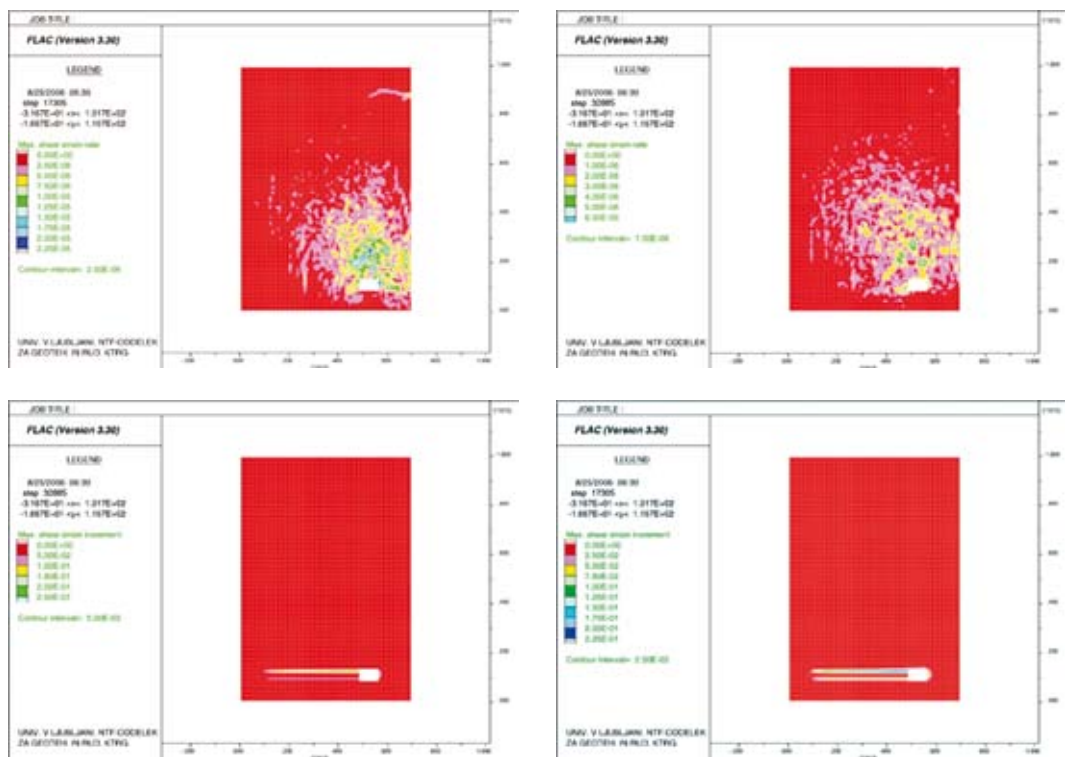


**Figure 7.** Effective shear stress in the hangingwall during coal extraction advance 3m/day and 7m/day JEROMEL [12]

**Slika 7.** Efektivne strižne napetosti v krovini pri napredku odkopa 3m/dan in 7m/dan JEROMEL [12]

## TOP CAVING ANALYTICAL PROCESS BY USING 3D FINITE DIFFERENCE METHOD

Analyses of the stress strain changes were carried out by using real geometrical data of the coal extracting advancement and other parameters which have impact on the coal extracting process in the Velenje Coal Mine. In the Finite Difference Model the following geological/geotechnical and technological units were included:

- hanging wall above clay protection layer,
- clay protection layer,
- coal (exploitation),
- footwall bellow the coal panel .

Mine production levels are situated below the so-called protection layer of clay, which prevents inrush of water, sand and mud into the longwall. In the last few years, excavation of coal has started under thinner layers of clay, which consequently increases the danger for miners working in such rock conditions (Figure 8). The continuous research work performed in the Velenje Coal Mine yielded numerous geotechnical parameters of the lignite seams, rocks and soils in the hanging wall and the footwall. Therefore, the exploitation space is better understood and mechanism of coal production has become the main issue for safe and productive exploitation. In this respect a large body of research

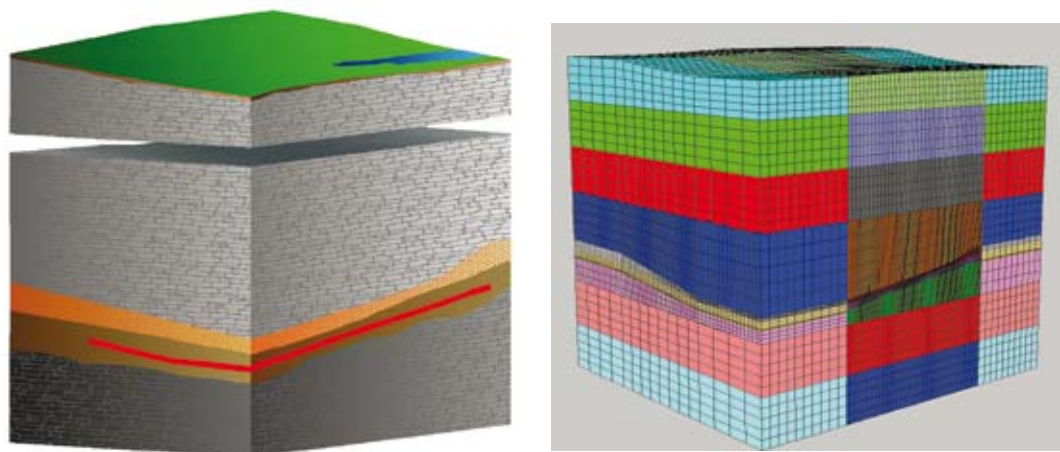


**Figure 8.** Geological profile trough the Velenje coal mine across the exploitation slice G1A and Finite Difference Mesh

**Slika 8.** Geološki profil Velenjskega premoškega nahajališča in odkopne plošče G1A ter mreža končnih diferenc

has been done, and in the past years a 3D numerical model has been developed which describes the mechanism of coal exploitation under a thin layer of protective clay. The numerical model has been developed with *FLAC3D* program.

The numerical model, developed for the coal exploitation analysis in the Velenje Coal Mine, consists of approx. 240,000 elements, and takes into account detailed geology in working space. For that reason, special software has recently been developed to transfer

the geological geometry into the model. Figure 8 shows finite difference mesh and the geological profile through the Velenje Coal Mine across the exploitation slice G1A.

### Input data

Geotechnical properties of coal seam, the hangingwall and the footwall were determined on the basis of laboratory tests and in-situ tests. In our calculations the Mohr-Coulomb failure criterion was used. The geotechnical properties of geological materials are shown in Table 1.

**Table 2.** Geotechnical properties of geological materials  
**Tabela 2.** Geotehnične lastnosti geoloških materialov

Geological material	Density $\rho\mu/\gamma\kappa(^3)$	Bulk modulus K (MPa)	Shear modulus G (MPa)	Cohesion c (kPa)	Internal friction angle $\phi (^0)$	Poisson ratio v(%)	Tensile strength T(kPa)
Protection layer of clay	1960	240	180	700	17	0.20	590
Coal	1290	320	195	700	30	0.25	590
Layers below clay protection	2130	155	50	400	15	0.35	80

## Initial stress state

Primary stress states in virgin rocks and soils were defined on several observations during carried out “in-situ” measurements. In many calculations the ratio between the horizontal and vertical components of stress field 0.85 was used. In same cases the determined values cause doubt. From this reason, value 0.85 needs to be proved in future.

## Excavation geometry

The present analysis simulated the excavation of coal slice G1A, with dimensions approx. 200 m x 300 m. The designed mining height is 4m, and daily exploitation round was about 4m. To simulate the daily exploitation round, a single step in the numerical analysis consisted of elements which were removed inside the zone 200 m x 4 m x 4 m. As a result, 65 steps have been calculated, each step presenting a daily exploitation round. Figure 9 shows the exploitation field G1A within *FLAC3D* grid.

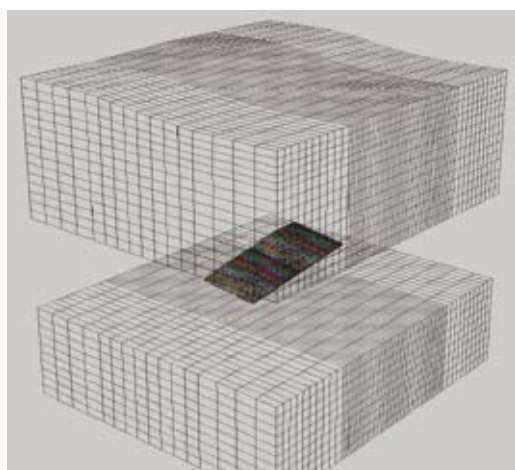


**Figure 9.** Exploitation field G1A within FLAC 3D grid  
**Slika 9.** Odkopno polje G1A v FLAC 3D mreži

## Calculation procedure

Firstly, the primary stress state was calculated under predefined conditions. Subsequently, 65 steps of mining sequences of the exploitation field G1A were carried out.

Each step included:

- Removing elements, which represented each exploitation step,
- Gradual reaching of the equilibrium until the vertical movements has not reached the level of the exploitation height (4 m in our case),
- Inserting the removed elements into the model before starting the subsequent calculation step.

## Analyses of the top caving process

Owing to extensive “in-situ” and laboratory research which has been done in the past, the exploitation process in the Velenje Coal Mine is well studied. Therefore, the results of our numerical analyses could build upon previous experience and comparable parameters could be tested as well.

Some details about the sublevel mining method with caving immediate roof i.e. top caving, which is used in Velenje Coal Mine, regarding the displacement and stress changes are explained below.

According to our experience the hanging-wall failure height is approx. 1.5 - 2.0 times the mining height. This means that for the mining height of 4m the roof failure height is between 6m and 8m, measured from the top of the longwall face. The failure zone is determined, where the specific shear strain is under 3 %. The failure area is finished approx. 0.5 to 0.8 times the mining height behind the supported end. At the height three times the



**Figure 10.** The coal extracting in the Velenje Coal Mine  
**Slika 10.** Odkop v Premogovniku Velenje

value of the caving height, the hangingwall layers were not equally destroyed Figure 10 shows the caving process in the Velenje Coal Mine. About two times the mining height in front of the longwall face a horizontal displacement occurs in magnitude of 0.5 m. In the area with longwall influence, horizontal movements are transformed in to a vertical displacement, the magnitude of which is close to the mining height.

The compression process in the hangingwall soil layers after the coal was mined out, continue to develop behind the longwall face exactly behind the hydraulic support. The caving process fills in the mined out area behind the support and the displacements stops. The stress in the surrounding rocks and soils behind the longwall face tends to increase close to the initial value. The compression part of deformation starts approx. 0.5-0.8 times of the failure height behind the support end, and about 6.0 times of the failure height behind the support-end, where the compression process is practically finished. The volume of mined coal was replaced with caving of the upper layers into

the mining space. The volume loss in upper layers is close to 80 % of the total volume of the mined coal. That means that the deformation process is very intensive and continuous, following the longwall face, which is in the moving state during coal exploitation.

Initial changes of the stress state in the hangingwall, the coal seam and the footwall in front of the longwall, started developing when the extraction panel start to move ahead. Analyses have shown slow upward movements towards the excavation face. Close to the longwall face, the stress field started to increase rapidly from its initial value to about 85 % of overstress. Vertical stress started to increase causing an intensive compression process at the distance which was 0.5-0.8 the times of the mining height behind the longwall. Compaction of caving material from hangingwall is relatively fast. Usually six months were enough to receive suitable compacted material. This fact is very important for designing a new longwall below the current production level. At a distance about 60 m behind the longwall, vertical stress converges to the initial stress

state value. The stress state around the exploitation field is shown in Figure 4.

Vertical stress distribution in the protection layer of coal and in the protection layer of clay in the hangingwall area is an important part of the present analyses. The stress in these layers undergoes similar changes as in the coal production level, but it is distributed in different places, while the stress changes are not so high.

Underground coal mining caused extensive surface movements in a large space above the coal production levels. In the analyzed case, caving and deformation processes moved to the surface vary fast. The impact angle was low and the surface above mine workings was usually damaged, filled with surface water in the form of artificial lake, with the area of about  $1.35 \text{ km}^2$ . Vertical movements are clearly shown in different levels in the hangingwall in Figure 11.

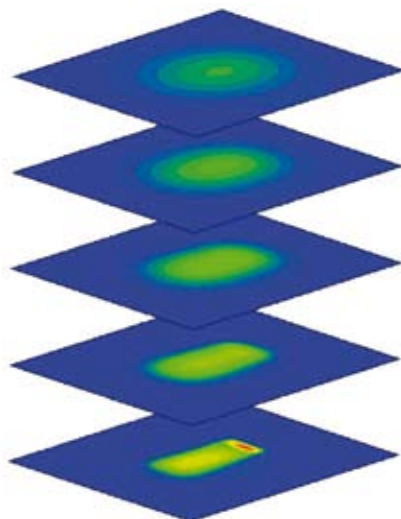


**Figure 11.** Vertical movements in different levels in the hangingwall

**Slika 11.** Vertikalni pomiki na različnih nivojih krovnine

## Other impacts of the exploitation process

Coal mining has strong impacts on other parts of the mine, particularly on its infrastructure, which is located close to the coal production field. The changes of the stress strain were analyzed too, since underground connections (such as main mine roadways) are important for normal and continuous coal production. Sometimes mine roadways urgent reshaping, but that is only later, when stress concentration has decreased.

## Results of numerical analyses

In our experience, the hangingwall failure height is approx. 1.5-2.0 times the mining height. In our case, the mining height was 4m and failure height between 6 m to 8 m, measured from the top of the longwall. However, the hanging wall failure area could be determined using shear strain increment condition. That means, if shear strain exceeded 3 %, a failure in the hangingwall was present. Generally, the hangingwall failure area must stop in the protection layer of coal. The thickness of the protection layer of the coal seam was between 5m and 20m.

Figure 12 shows shear strain increment from 3 % to 10 % in the protection clay layer above the longwall. At the edges of the longwall, the calculated shear strain in the clay protection layer was much higher than expected. This fact shows clear connection with the calculated stress concentration at the edges of the longwall.

The deformations in front of the longwall reached a value of 20-30 cm at the top of exploitation panel, which agrees well with

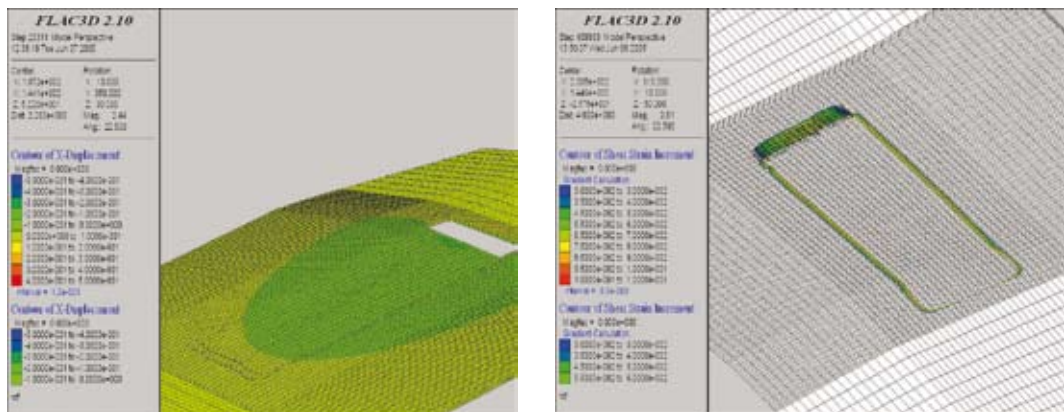


**Figure 12.** Shear strain increment from 3 % to 10 % in the clay protection layer above the longwall and the development of the deformation field in front of the longwall

**Slika 12.** Strižni prirastek od 3% do 10% v glinastem varovalnem sloju nad odkopnim poljem in razvoj deformacijskega polja pred čelom odkopavanja

our previous experience and the “in-situ” measurement results. However, more interesting is the impact area of the mining production process, which was much wider than previously expected. When 25 % of the coal mining of field G1A was finished, the displacements reached the end of the exploitation slice. This fact is shown in Figure 12.

The compression process began immediately behind the longwall hydraulic support. In the numerical analysis, by which we simulated mining and caving process, we used the removed elements which were installed back into the model, when vertical displacement reached the mining height. From this point of view, the stresses in those elements started to increase, depending on the distance

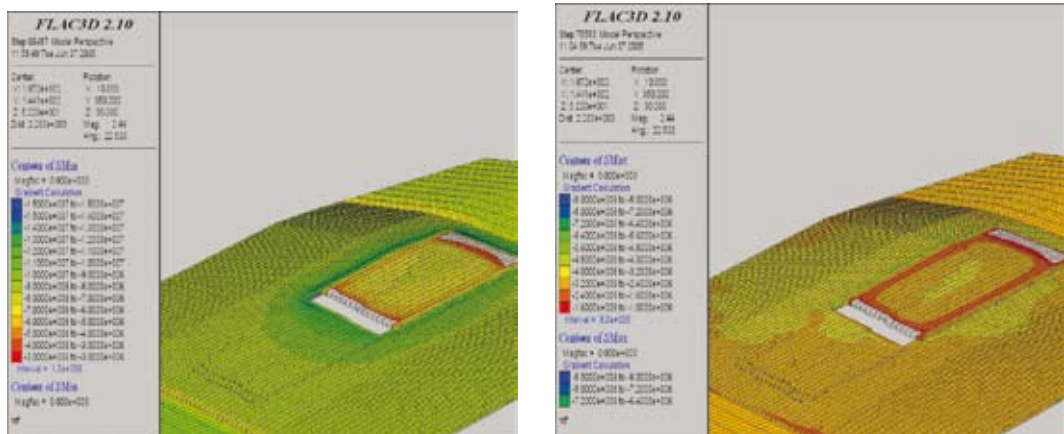


**Figure 13.** Stress  $\delta_{\text{max}}$  and Stress  $\delta_{\text{min}}$  – slice G1A

**Slika 13.**  $\delta_{\text{max}}$  in  $\delta_{\text{min}}$  napetosti – odkopno polje G1A

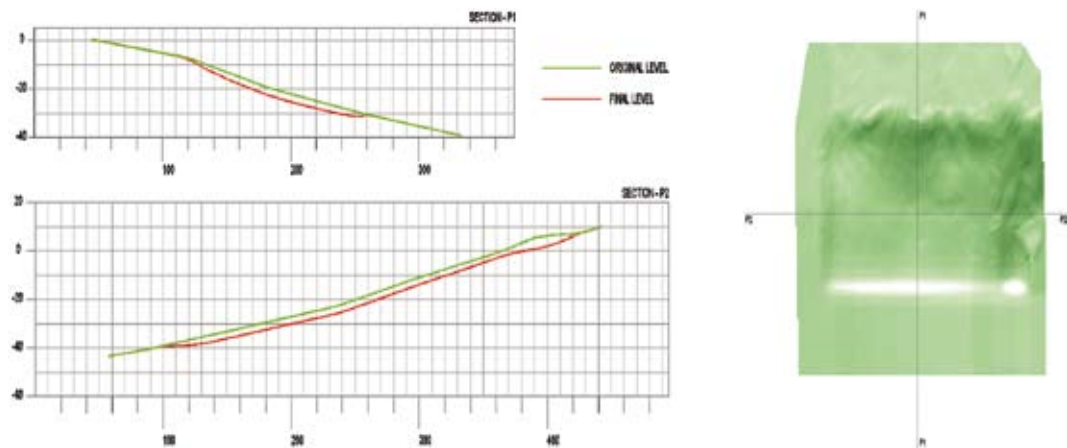


**Figure 14.** Deformed surfaces at the lower part of the clay protection layer

**Slika 14.** Deformirana površina spodnjega dela varovalne plasti gline

between the longwall face and the observation point. The level of the stresses in the caved waste was activated, if the compression of the surrounding damaged rocks and soils material was started. Figure 12 shows the stress convergence to the initial value, when it reached the value close to the initial stress in the surrounding rocks and the coal seam. This finding was in agreement with the observations carried out in our previous research (KOČAR ET.AL.)<sup>[2]</sup>.

The volume, which can be calculated using the difference between the initial position of the specified surface and the deformed surface, is about 80% of the coal excavated volume. Figure 14 shows the deformed surface at the lower part of the clay protection layer. These values are close to the estimations from the observation part of the project.

## CONCLUSIONS

The results of the analyses, based on the modelling by Finite Difference Method, have shown relatively good agreement between the calculated values and the observed data.

Numerical modelling and the results of extensive geotechnical analyses of the longwall mining method, which have been used in the Velenje Coal Mine with safety considerations, represent a contribution to better understanding of complicated stress strain processes in the larger space of the influence of the coal mining.

Strain and stress changes, calculated during the simulation of the longwall coal extraction in the hanging wall, the coal seam and in the footwall, have shown good agreement with our expectations.

There are some differences between the results of numerical analyses and observations regarding the area of deformation impact, caused by coal extraction in the analysed area.

The 3D numerical model will be tested in the future with different input data and elastic-plastic models. Some improvements need to be implemented with considerations to the impacts of underground water and different primary stress states in the cases analysed.

The current model took into account detailed geology and mining production geometry, which allowed for making calculations without usual simplifications.

## Povzetki

### Nekateri načini analiziranja rušnih procesov pri podetažnem odkopavanju premoga

Podetažno odkopavanje premoga je povezano z velikimi deformacijami v okoliških hribinah in predstavlja v geotehničnem pogledu časovno odvisen proces, pri katerem so prisotne različne porušitve hribinskih območij v okolini odkopa. Posamezne faze, ki se odvijajo z napredovanjem odkopavanja,

so pomembne za oceno komprimacijskih učinkov v porušeni krovini za odkopom ter v realnem merilu dajejo osnovo za možna predvidevanja procesov, ki so prisotni pri odkopavanju globlje ležečih etaž. Vsekakor je modeliranje rušnega procesa z metodo končnih diferenc s simulacijo napredovanja odkopa primeren način analiziranja intenzivnih sprememb v porušenih naravnih materialih, kar med drugim omogoča tudi do določene mere boljše vedenje o samem rušnem procesu ter primerjavo rezultatov izračunov z izmerjenimi vrednostmi. Pri tem je potrebno poudariti, da simulacije načina odkopavanja premoga v Premogovniku Velenje narejene z 2D in 3D dajejo možnost nadrobnejšega analiziranja konkretnih primerov odkopavanja, saj je iz dobljenih rezultatov moč relativno hitro preverjati dobljene vrednosti npr. pomikov v zapletenih napetostno deformacijskih procesih, ki se dogajaj v širšem območju, kjer poteka odkopavanje premoga.

Izračunane spremembe napetosti in deformacij pri podetažnem odkopavanju premoga se dobro ujemajo s pričakovanjimi, medtem ko je zaznati manjše neskladje med rezultati numeričnih analiz in opazovanji v velikosti območja deformacij v okoliških hribinah okrog neposrednega zaruševanja krovinskih plasti.

## REFERENCES

- [<sup>1</sup>] B.H.G. BRADY, E.T.BROWN, 1993, Rock Mechanics for Underground Mining; Second edition, Culver Academic Publisher, Dordrecht, Boston, London.
- [<sup>2</sup>] J. LIKAR, Rušni procesi v rudniku lignita Velenje raziskovalna naloga, reports for years 2001, 2002 and 2003, Ljubljana, University of Ljubljana, Faculty of Natural sciences and Engineering.
- [<sup>3</sup>] ITASCA CONSULTING GROUP, 2002 FLAC – 3D manual.
- [<sup>4</sup>] S. JANEŽIČ, Študija za reševanje problematike varnega odkopavanja in določitev kriterijev za projektiranje in odkopavanje premoga pod vodonosnimi plastmi v jamah RLV, Rudnik Lignita Velenje, 1987.
- [<sup>5</sup>] A.H. WILSON, 1981, Stress, stability in coal ridges and pillars. Proceedings of the First Conference on Ground Control in Mining, p.1-12.
- [<sup>6</sup>] H.J. KING, B.N. WHITTAKER, 1971, A review of current knowledge on roadway behavior, especially the problems on which further information is required. Proceedings of the Symposium on Strata Control in Roadways, London, Inst. Min. Met. p 73-87.
- [<sup>7</sup>] D.S. CHOI, D.L McCAIN, 1980, Design of longwall system. Trans Soc Min Eng AIME, 258: 1761-4.
- [<sup>8</sup>] C. MARK, 1990, Pillar design methods for longwall mining, BuMines IC9247, p. 53.
- [<sup>9</sup>] B.G.D. SMART, S.M. HALEY, 1987, Further development of the roof strata tilt concept for pack design and the estimation of the stress development in a caved waste. Min Sci Technol; 5:121-30.
- [<sup>10</sup>] R. TRUEMAN, 1990, Finite element analysis for the establishment of stress development in a coal mine caved waste. Min Sci Technol; 10: 247-52.
- [<sup>11</sup>] I.G.T. THIN, R.J. PINE, R. TRUEMAN, 1993, Numerical modelling as an aid to the determination of the stress distribution in the goaf due to longwall coal mining. Int J Rock Mech Min Sci Geomech Abst. 30:1409-9.
- [<sup>12</sup>] G. JEROMEL, Numerična simulacija rušnih procesov pri odkopavanju premoga, Diplomsko delo, Ljubljana 2004.
- [<sup>13</sup>] NCB. National Coal Board, 1975, Subsidence engineer's handbook, NCB Mining Department; London, p. 111.

# Calculation of volume with the use of “NTF” method

## Izračun volumnov z uporabo “NTF” metode

MILIVOJ VULIĆ<sup>1</sup>, ANES DURGUTOVIĆ<sup>2</sup>

<sup>1</sup>Faculty of Natural Science and Engineering, University of Ljubljana, Aškerčeva cesta 12,  
SI-1000 Ljubljana, Slovenia; E-mail: milivoj.vulic@ntf.uni-lj.si

<sup>2</sup>Oikos d.o.o., Jarška cesta 30, SI-1230 Ljubljana, Slovenia;  
E-mail: anes.durgutovic@oikos.si

Received: October 02, 2006 Accepted: October 20, 2006

**Abstract:** The development of computer science, GPS, up to date instruments and methods for measurement has enabled fast collection and handling of data. Nowadays, we can come across many different programs which, on the basis of input data, give results of the shape volume. However, these programs function on the basis of the black box and we can therefore, only make assumptions about their accuracy. Due to the fact that the results, which we get with the use of programs, differ among themselves, we have made “NTF” method of volume calculation. In this article we wish to present the mentioned method and the mathematical background of the volume calculation.

**Izvleček:** Razvoj računalništva, GPS-a, sodobnih merskih instrumentov ter metod merjenja je omogočil zelo hitro pridobivanje in obdelavo podatkov. Danes lahko srečamo celo vrsto računalniških programov, ki nam na podlagi vhodnih podatkov podajo rezultat o prostornini neke mase. Toda le ti delajo na principu črne skrinjice in o njihovi natančnosti lahko samo ugibamo. Ker se rezultati, ki jih programi podajajo med seboj razlikujejo smo zasnovali metodo izračuna volumnov »NTF«, katero vam v tem prispevku želimo predstaviti. V prispevku vam želimo prikazati, kakšna je zamisel tega načina in njegovo matematično ozadje.

**Key words:** volume calculation, Delauney triangulation, MS Excel, UDF

**Ključne besede:** izračun volumnov, Delaunayeva triangulacija, MS Excel , UDF

## INTRODUCTION

The development of computer science, GPS, up to date instruments and methods for measurement has enabled fast collection and handling of data. Nowadays, we can come across many different programs which on the basis of input data give results of the shape volume. This implies to fast calculation of area or volume calculation. The way of life is also based on the fact that it is important

to acquire results in the short period of time. Due to that people nowadays use the software programs when working on calculation of volume. However, these programs function on the basis of the black box and we can therefore, only make assumptions about their accuracy.

However, the results we get with the use of programs (programs, which enable the calculation of the volume) vary among

themselves. In order to find out why these particular programs give various results we would be bound to the background of their function. Because this would be difficult we have decided to prepare the method of volume calculation in the range of our own capacities. In this way we have made “NTF” method of volume calculation. The basis of this method and the mathematical background of the volume calculation are shown in the article calculation of the volume with the use of “NTF” method.

With the consideration of mathematical principles we have used positive characteristics of program tools MS Excel and with the help of Microsoft Visual Basic for Applications<sup>1</sup>, we have prepared User Defined Functions (UDF), which enable us to define the volume of shape in MS Excel program. The principal of volume calculation, based on Delaunay triangulation, what is also the characteristic of already mentioned programs.

## CALCULATION OF THE VOLUME WITH THE USE OF “NTF” METHOD

Volume of shape (dump, embankment...) can be calculated in different ways. The selection of the way, among others, depends on the shape as well as on the accuracy which we wish to reach at the volume calculation.

For the less complicated geometrical shapes, where it is possible to combine geometrical shape from regular geometrical shape, we can use way of determining the volume by abstracting volume of individual regular geometrical shape. For the volume calculation in practice the most usual principals are:

- Volume calculation from profile,
- Volume calculation from the already carried out triangulation net.

Triangle net is mostly used for modeling of the surface of the area. That is because the triangle net matches measured points on the field. The already carried out Delaunay triangulation of the shape to which we wish to calculate volume with the use of “NTF” method. Delaunay triangulation is the process of calculating a triangle net that tries, among the given points, to find equilateral triangles.

### The idea of the “NTF” method

If we have a series of data about the coordinate points of a particular shape, we can with the help of a suitable program from the series of data carry out Delaunay triangulation. The shape to which we wish to calculate volume, we separate with certain contour line into two parts. We get **upper** and **down** part of that shape.

<sup>1</sup>Visual Basic for Applications (VBA) is the variety of program language Microsoft Visual Basic for programming of macro in applications for Windows operation systems

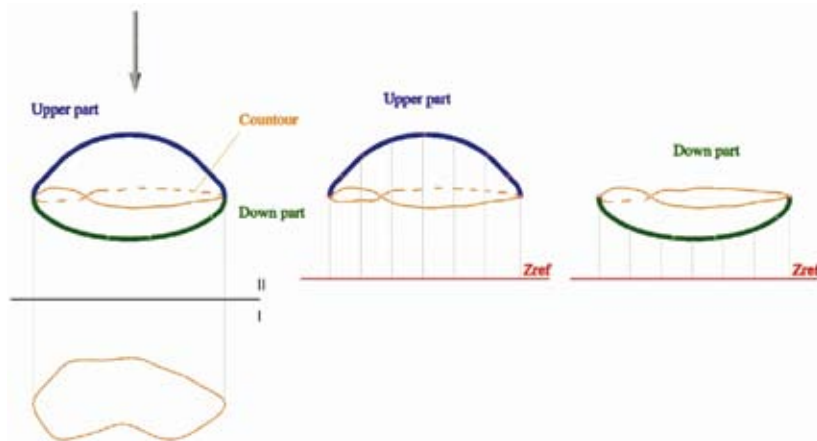


**Figure 1.** The separation of the shape into down and upper part

**Slika 1.** Razdelitev telesa na spodnji in zgornji del

To this shape with the upper and down surface we determine a certain reference high and on that reference high we create horizontal surface. In a mathematical way we can determine reference high anywhere in ending. In a numerical way it is best to choose it there where the partial amount of individual volume is the lowest, or rather where the sum of high differences of the upper and down surface equals zero. We can achieve this by determine the reference high in the centre of gravity, according to one dimension (high). But if for the reference high take minimal high from the set of the lowest location points we will not make a big mistake.

Due to the pretentiousness of determination of the centre of gravity it is recommendable to take minimal high from the set of the lowest location points. With the help of the horizontal surface on the chosen reference high and data about the edges which form triangles of the carried out Delaunay triangulation, we can solve the problem of the volume of the limited space by volume calculation of the final number of vertical triangle prism.

After we have carried out Delaney triangulation of the upper and down surface and chosen the reference high, we can on the basis of already mentioned finding calculate:

- Volume between upper surface of the shape and the surface on the reference high (volume of the upper part of the shape),
- Volume between down surface of the shape and the surface on the reference high (volume of the down part of the shape).

The difference between volumes gives us a final volume of geometrical shape.

## MATHEMATICAL BASIS OF THE “NTF” METHOD

After the carried out Delaney triangulation of the surface we have the limited surface space to which we wish to calculate volume with the help of the horizontal surface on the chosen reference high and data about the edges which form triangles of the carried out Delaney triangulation, we separated on vertical triangle prism.

With this we separated, the volume of limited surface space, by volume calculation of the final number of vertical triangle prism. We are, from the mathematical point of view, interested in the volume calculation of one vertical triangle prism. An example of such prism is given in the picture below.

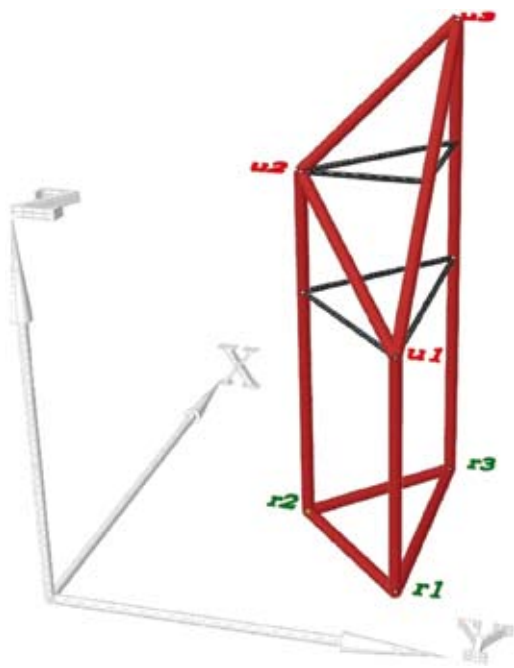


**Figure 2.** Example of triangle prism  
**Slika 2.** Primer tristrane prizme

Coordinates of the given points of basis on the defined surface are:

$$\begin{aligned} u_1 &= (x_{u1}, y_{u1}, z_{ref} + h_1) \\ u_2 &= (x_{u2}, y_{u2}, z_{ref} + h_2) \\ u_3 &= (x_{u3}, y_{u3}, z_{ref} + h_3) \end{aligned} \quad (1)$$

Coordinate points of the second basis, or rather, points on horizontal surface on the reference high which is given by equitation:

$$Z = Z_{ref} \quad (2),$$

Are gained by projecting of points  $u_1$ ,  $u_2$  and  $u_3$  on horizontal surface on the reference high. We get the coordinates of reference points that are:

$$\begin{aligned} r_1 &= (x_1, y_1, z_{ref}) \\ r_2 &= (x_2, y_2, z_{ref}) \\ r_3 &= (x_3, y_3, z_{ref}) \end{aligned} \quad (3)$$

Because of the easier volume calculation of the mentioned triangle prism, we separate this prism into three different geometrical shapes. We get two tetrahedron and one regular prism as it is shown in the picture below:

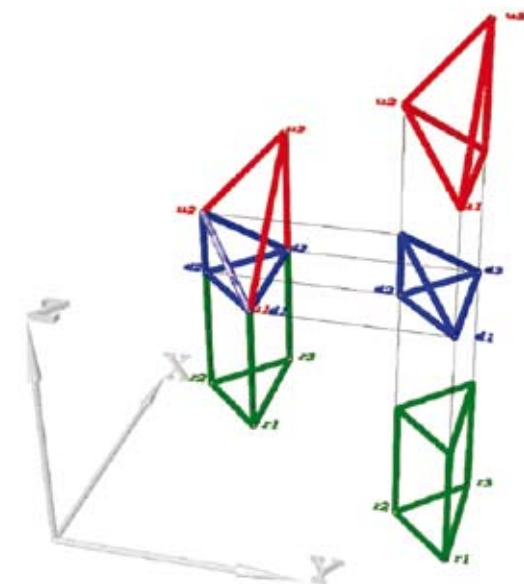


**Figure 3.** Separate prism  
**Slika 3.** Razdeljena prizma

## Volume calculation of separated triangle prism

Because of the better understanding and more simple way of calculation, we name the shapes after colors which are presented in Figure 3. That we get:

- Green prism (GP),
- Blue tetrahedron (BT),
- Red tetrahedron (RT).

Volume of the green prism, which is formed by edges  $r_1, r_2, r_3, u_1, d_1, d_3$ , we can write with a following formula:

$$V_{GP} = BASE_{norm} \cdot h_1 \quad (4),$$

At which the “ $BASE_{norm}$ ” area of normal section, therefore triangles  $r_1, r_2, r_3$  or triangles  $u_1, d_1, d_3$ . Formula for area of normal section is:

$$BASE_{norm} = \frac{\begin{vmatrix} x_{u1} & y_{u1} & 1 \\ x_{u2} & y_{u2} & 1 \\ x_{u3} & y_{u2} & 1 \end{vmatrix}}{2!} \quad (5).$$

Volume of blue tetrahedron which is formed by edges  $u_1, d_2, d_3, u_2$ , we can write with:

$$V_{(BT)u_1d_2d_3u_2} = BASE_{norm} \cdot \frac{h_2 - h_1}{3} \quad (6).$$

It is known that the volume of pyramid dose not change if the top of this pyramid moves on the surface which is paralleled to basis. Due to this the volume of red tetrahedron which is formed by edges  $u_1, u_2, d_3, u_3$  will not change if it will parallel with the surface  $u_1, d_3, u_3$  point  $u_2$  move into point  $d_2$ . That is:

$$V_{(RT)u_1u_2d_3u_3} = V_{(BT)u_1d_2d_3u_2} = BASE_{norm} \cdot \frac{h_3 - h_1}{3} \quad (7).$$

If we calculate the volume of green prism, red tetrahedron and blue tetrahedron, we get final volume of mentioned triangle prism which is presented on the Figure 2. We write this as:

$$V = V_{BT} + V_{RT} + V_{GP} = BASE_{norm} \cdot \frac{h_1}{2} + BASE_{norm} \cdot \frac{h_2 - h_1}{3} + BASE_{norm} \cdot \frac{h_3 - h_1}{3}$$

$$V = BASE_{norm} \cdot \frac{h_1 + h_2 + h_3}{3} \quad (8).$$

If we now also take into consideration for the surface of normal section “ $BASE_{norm}$ ”, equation 5 we get:

$$V = \begin{vmatrix} x_{u1} & y_{u1} & 1 \\ x_{u2} & y_{u2} & 1 \\ x_{u3} & y_{u3} & 1 \end{vmatrix} \cdot \frac{h_1 + h_2 + h_3}{3!} \quad (9).$$

With the purpose of simplifying the calculation on the basis of conclusion of the above described mathematical way of volume calculation in the program MS Excel we have prepared “UDF” for volume calculation with “NTF” method.

### Representation of the correct volume calculation

We carry out volume calculation with the use of NTF method in MS Excel program. For this we have, on the basis of the above mentioned findings, prepared “UDF” which enable realization of volume calculation with the use of MS Excel program.

With the purpose of examining the correctness of the volume calculation with the use of already mentioned tools. We have carried out tests in the computer program MS Excel. To this purpose we have used the prism model which is shown in the Figure 2. Data about

**Table 1.** Coordinate points of edge

**Tabela 1.** Koordinatne točke oglišč obeh trikotnikov

<b><math>z_{ref}</math></b>	<b>Volume UP</b>	<b>Volume DOWN</b>	<b>Accurate volume <math>AV=V_D-V_U</math></b>
90	4000	7000	3000
45	-500	2500	3000
40	-1000	2000	3000
35	-1500	1500	3000
20	-3000	-0	3000
15	-3500	-500	3000
10	-4000	-1000	3000
5	-4500	-1500	3000
0	-5000	-2000	3000

coordinate points of edges of both basis are presented in the Table 1.

With the use of UDF »*point3VolumeW*« in the program MS Excel we have calculated the volume of the given prism for various reference highs. For the use of the calculation we have chosen several different values of reference high, because we wished to check if the mentioned UDF will give the same value of the volume regardless the value of reference high. Results which we have gained are presented in the Table 2.

As seen from the table above, with the use of UDF »*point3VolumeW*«, we get the same final value of the volume regardless the chosen reference high value. Due to this we can hide the reference high. In order to avoid eventual machine error it is recommended to take reference high as the smallest high from the set of given points.

**Table 2.** Chosen reference high value

**Tabela 2.** Prikaz izbranih vrednosti referenčnih višine in prikaz končnega rezultata

<b><math>z_{ref}</math></b>	<b>Volume UP</b>	<b>Volume DOWN</b>	<b>Accurate volume <math>AV=V_D-V_U</math></b>
90	4000	7000	3000
45	-500	2500	3000
40	-1000	2000	3000
35	-1500	1500	3000
20	-3000	-0	3000
15	-3500	-500	3000
10	-4000	-1000	3000
5	-4500	-1500	3000
0	-5000	-2000	3000

In order to check whether written UDF »*point3VolumeW*« in the program MS Excel gives a correct result we have separated the presented prisms shape into three regular geometrical shapes in Figure 1. We calculate the volume of mentioned geometrical shapes with the use of standard mathematical forms.

$$V = V_{RT} + V_{MT} + V_{ZP} = 333,333 + 666,666 + 2000 = 3000 \quad (10)$$

From the above written result we can see that we get the same value of the volume of the prism shape as well as by the use of the above mentioned UDF »*point3VolumeW*«.

## CONCLUSION

On the basis of the above mentioned finds we see that the final value of the volume will not change on the dependence of reference point value. No matter the value of the reference high we always get the same result. UDF also gives us the right value of the shape which we have proved in the example above. We can

with the adding up the calculated volume of the individual vertical prisms which form the volume surface limited space we calculate the final shape volume.

The way we carry out calculation on a practical example and the way of using UDF for the volume calculation with the use of NTF method will be given in the next articles.

## REFERENCES

- [<sup>1</sup>] J. N. BRONŠTEJN-K. A. SEMENDJAJEV, Matematični priručnik, Tehniška založba Slovenije v Ljubljani, 1978. 683 str.
- [<sup>2</sup>] JOSEPH O'ROURKE, Computational geometry in C. Cambridge university press, 1997 350 str.
- [<sup>3</sup>] VULIĆ, MILIVOJ, »User Defined Function«, februar 2005
- [<sup>4</sup>] VULIĆ, MILIVOJ, Matematične osnove določanja prostornin tristranih prizem (interna predavanja), marec 2005
- [<sup>5</sup>] VULIĆ, MILIVOJ, Osnove Delaunay-eve triangulacije in Voronoi diagramov (interna predavanja), februar 2005.



# **Permsko-triasna meja ter zgornjepermски in spodnjeskitski skladi na jugovzhodnem obrobju Ljubljanskega Barja, osrednja Slovenija**

## **Permo-Triassic boundary and Upper Permian as well as Lower Scythian Beds in the Southeastern Borderland of the Ljubljana Marsh, Central Slovenia**

MATEJ DOLENEC<sup>1\*</sup>, STEVO DOZET<sup>2</sup>, SONJA LOJEN<sup>3</sup>

<sup>1</sup>Faculty of Natural Sciences and Engineering, University of Ljubljana,  
Department of Geology, Aškerčeva 12, SI-1000 Ljubljana, Slovenia;  
E-mail: matej.dolenec@s5.net

<sup>2</sup>Geological Survey of Slovenia, Dimičeva 14, SI-1000 Ljubljana, Slovenia;  
E-mail: stevo.dozet@geo-zs.si

<sup>3</sup>Jožef Stefan Institute, Jamova 39, 1000 Ljubljana, Slovenia;  
E-mail: sonja.lojen@ijs.si

**Received:** September 18, 2006      **Accepted:** October 20, 2006

**Izvleček:** V tem in naslednjih člankih skušamo z različnimi raziskovalnimi metodami potrditi obstoj zgornjepermских skladov na območju južne Slovenije in natančneje opredeliti permsko-triasno mejo v pestrem zaporedju sedimentov na južnem obrobju Ljubljanskega Barja. V zgornji perm smo uvrstili paket temnosivih dolomitov ter bolj ali manj dolomitiziranih apnencov z redkimi vložki dolomitnih laporovcev in lapornih glinavcev, ki leže konkordantno pod pisanim karbonatnim in klastičnim zaporedjem skitske serije. Peščeni sedimenti spodnjetriasne serije vsebujejo vložke sljudnih peščenjakov in laporovcev, navzgor pa prehajajo v več deset metrov debel horizont oolitnega apnanca s polžkom *Holopella gracilior* (Schauroth). Spodnji del zgornjepermских sedimentov je prekrit s kvartarnimi usedlinami. Izotopska sestava kisika in ogljika v zgornjepermских karbonatnih kamninah je dokaj konstantna.  $\delta^{18}\text{O}$  ima vrednosti v razponu od -1,30 ‰ do + 0,43 ‰ medtem ko se  $\delta^{13}\text{C}$  spreminja od + 3,22 ‰ do + 4,35‰ (V-PDB), kar je značilno za karbonatne kamnine zgornjega perma. Precej drugačna je izotopska sestava kisika in ogljika v sedimentnih skitske serije. Tako nad predvideno permsko-triasno mejo se pojavi v karbonatih skitske serije negativna ogljikova anomalija, ki znaša 6,78 ‰, nad mejo so povprečne vrednosti parametra  $\delta^{13}\text{C}$  okrog = -2,56 ‰, parametra  $\delta^{18}\text{O}$  pa okrog -4,21 ‰. Sinteza rezultatov izotopske, sedimentološke in favnistične analize ter primerjalnih metod je pokazala, da na jugovzhodnem obrobju Ljubljanskega Barja leži meja med permskim in triasnim sistemom znotraj zaporedja temnih pretežno karbonatnih kamnin, natančneje med ploščastimi dolomiti (zgornji perm) in konkordantno na njih ležičimi temnimi plastnatimi apnenci.

**Abstract:** In this and next papers we try to confirm with various research methods the existence of the Upper Permian beds in Southern Slovenia and to define the Permian-Triassic boundary in the pretty heterogeneous stratigraphic sequence in the southern borderland of the Ljubljana Marsh. In Permian is ranged a packet of the dark grey dolomites and more or less dolomitized limestones with rare interbeds of dolomitic marlstones and marly claystones lying concordantly under the variegated carbonate and clastic succession of the Scythian series. Sandy sediments of the Lower Triassic series contain interbeds of sandstones and marlstones, passing upwards into several ten metres thick horizon of oolitic limestones with the gastropod *Holopella gracilior* (Schauroth). The lower part of the Upper Permian sediments is covered by the Quaternary deposits. The stable isotope composition of oxygen and carbon in the Upper Permian carbonate rocks are pretty constant.  $\delta^{18}\text{O}$  exhibit values in the interval from -1,30 ‰ to +0,43 ‰, whereas  $\delta^{13}\text{C}$  range from +3,22 ‰ to +4,35 ‰ (V-PDB) characteristic for Upper permian carbonate rocks. The isotope composition of oxygen and carbon in sediments of the Scythian series are much more variable. Right above the proposed P/T boundary a global negative carbon isotope anomaly in the range of 6,78 ‰ appears. Above the P/T boundary mean isotopic composition of  $\delta^{13}\text{C}$  is around -2,56 ‰ and  $\delta^{18}\text{O}$  around -4,21 ‰. A synthesis of the results of isotope, sedimentological and faunistical analysis as well as of correlation metohods showed, that in the Southeastern Bordeland of the Ljubljana Marsh the boundary between the Permian and Triassic system lies within the succession of dark prevalently carbonate rocks, more precise between the platy dolomites (Upper Permian) and concordantly overlying dark bedded limestones (Lower scythian).

**Ključne besede:** karbonatne in klastične kamnine, zgornji perm in spodnji skit, meja, litostatigrafija, izotopska sestava, kisik, ogljik, Zunanji Dinaridi, osrednja Slovenija

**Key words:** carbonate and clastic rocks, Upper Permian and Lower Scythian boundary, lithostratigraphy, isotope composition, oxygen, carbon, Outer Dinarides, Central Slovenia

\*Corresponding author. Tel.: +00386-1-4707620; Matej Dolenc

## Uvod

V okviru geološkega kartiranja za izdelavo geološke karte Slovenije na listu Grosuplje 1:50 000 smo na širšem območju med Ortnekom, Sodažico, Blokami, Ljubljano in Ivančno Gorico opazili nekaj izdankov temnih karbonatnih kamnin, ki leže konkordantno pod skitskimi sedimenti in navidezno konkordantno na grödenskih klastičnih kamninah, za katere menimo, da pripadajo zgornjemu permu. Za začetek reševanja tega problema smo izbrali razmeroma dobro odkrit profil Skopačnik na južnem obrobju Ljubljanskega Barja, kjer so razgajljene vrhne zgornjepermske karbonatne kamnine ter spodnji in srednji del skitskega karbonatno-

klastičnega zaporedja z nenavadno debelim horizontom oolitnega apnenca na vrhu. Sedimentno zaporedje zgornjepermskih in skitskih sedimentov je stratimetrijsko izmerjeno, sedimentološko raziskano in litostatigrafsko razčlenjeno. Vzeli smo tudi precej vzorcev kamnin za izotopsko, konodontno, mikrofacijalno in biofacijalno analizo.

V geografskem pogledu pripada raziskovano ozemlje južnemu obrobju Ljubljanske kotline v paleogeografskem pogledu Slovenski karbonatni platformi, v geotektonskem pogledu pa Dolenjsko-Notranjskim mezozojskim grudam oziroma natančneje tektonski enoti Krimsko-Mokrškega hribovja (BUSER, 1974).

V tem članku podajamo rezultate začetnih raziskav problematike zgornjepermskih skladov na območju južne Slovenije s posebnim poudarkom na določanju permsko-triasne meje. Na raziskovanem ozemlju ta meja ni doslej niti litološko niti paleontološko detajljne določena. V ta namen smo vzorčevali tako v zgornjepermskih kot v skitskih plastihih in nabrali okoli 105 vzorcev za različne laboratorijske raziskave.

## DOSEDANJE RAZISKAVE

KOSSMAT (1913) je odkril najpopolnejši razvoj zgornjepermskih skladov v Loških in Polhograjskih hribih v okolici Žažarja in Vrzdenca.

Po HERITSCH-u (1939) predstavljajo zgornjepermski skladi v Loških in Polhograjskih hribih ekvivalent belerofonske stopnje v Južnih Tirolah z jasno zvezo z indijskim *Productus* apnencem, žažarska favna pa zvezo med favnama Južnih Tirolov in zahodne Srbije.

ŠLEBINGER (1953) je ugotovil zgornjepermske sklade v ortneškem paleozoiku na Dolenjskem v apnenčevem in dolomitnem razvoju, ki se brez prekinitve sedimentacije nadaljujejo v sedimente spodnjetroiasne starosti. V ortneškem paleozoiku je ohranjen popoln profil permskih plasti. Najdene so trogkofelske plasti, ki jih je paleontološko dokazala V. KOSTIĆ – PODGORSKA s koralo *Sinophyllum pendulum* Grabau. Razen tega je tam v obliki belih in rdečkastih kremennovih konglomeratov in peščenjakov razvit tudi groden. Belerofonski skladi so v ortneškem paleozoiku zelo podobni velebitskemu razvoju.

GERMOVŠEK (1955) je pri kartirjanju jugovzhodnega obrobja Ljubljanskega Barja pripisal temnosivemu debeloploščastemu dolomitu za senikom Rebolove kmetije in okoli Skopačnika verjetno werfensko starost. Strnjen kompleks sivega in rdečega sljudnega lapornega skrilavca s polami rdečega oolitnega apnanca med Sarskim na severu in Rebolovo kmetijo na jugu je uvrstil v zgornji werfen.

Leta 1956 je GERMVŠEK menil, da geološke razmere ob koncu permske dobe niso bile enake po vsem slovenskem ozemlju. Werfenske plasti leže namreč na zgornjepermskem peščenjaku ali na belerofonskem apnenu oziroma dolomitu. Ob začetku triasne dobe pa so se že povsod odlagale približno enake usedline.

RAMOVŠ (1956) je pisal, da so med permskimi skladi najbolj razprostranjeni grödenski skladi. Vrhni del grödenskih skladov sestavljajo rdeči, vijolični in zeleni skrilavi glinavci, ki se blizu zgornjepermskih skladov menjavajo z belerofonskim dolomitom in tako postopoma prehajajo v zgornjepermske sklade. Najmlajši permski stratigrafski člen sestavljajo na Slovenskem zgornjepermski skladi, ki so zaradi bogatih najdišč indoarmenske favne pri Žažarju in Vrzdencu vzbujali veliko pozornost raziskovalcev.

RAMOVŠ (1958a) je zgornjepermske sedimente na ozemlju Loških in Polhograjskih hribov ter na Cerkljanskem razčlenil v tri serije z dvanajstimi horizonti.

RAMOVŠ (1958b) je menil, da imamo v zgornjem permu na ozemlju Slovenije dve, mogoče celo tri facije in sicer: žažarsko (Škofjeloško-Polhograjsko hribovje, Cerkno),

južnotiolsko (Julijiske Alpe) in karavanško. Na ozemlju Posavskih gub in vzhodne Slovenije pa je bilo verjetno kopno.

RAMOVŠ (1982) je smatral, da je permsko triasna meja tam, kjer je konec sedimentacije permskega značaja (črni in temnosivi plastnati dolomit ali apnenec z drobnimi foraminiferami (*Gymnocodiaceae*) in tankimi laporнимi in glinenimi plastmi.

BUSER (1962) je sklepal, da leže skitske plasti pri Skopačniku pri Želimaljih normalno na zgornjepermškem dolomitu ter da se končajo ob prelomu, kjer je zgornjetriaspni dolomit narinjen na spodnjetriaspnega.

Na Osnovni geološki karti, list Ribnica 1:100 000 (BUSER, 1969) leže spodnjetriaspne plasti diskordantno na permokarbonskih klastičnih kamninah.

BUSER (1974) je v tolmaču lista Ribnica 1:100 000 navedel, da pri vasi Obla Gorica severno od Primskovega leži na rdečkastem kremenovem peščenjaku, ki predstavlja ekvivalent grödenskih skladov, 10 m debel temnosiv dolomit, ki verjetno pripada zgornjemu permu oziroma žažarskim skladom. To bi bila takrat prva najdba žažarskih skladov na ozemlju Posavskih gub, ki so tu bile po njegovem prav gotovo odloženi, vendar so bili kasneje zopet erodirani.

BUSER (1976) je za projekt Mezozoik v Sloveniji pri opisu triasnih plasti na listu Ribnica napisal, da leže skitske plasti pri Skopačniku blizu Želimalj normalno na zgornjepermškem dolomitu. Temnosivi permski dolomit prehaja navzgor najprej v rjavosiv skladovit (20-50 cm) dolomit, ki vsebuje na lezikah sljudo in se menjava z do 20 cm debelimi

plastmi sivorjavega sljudnatega meljevca in peščenjaka. Sledi okoli 30 m debel paket sljudnatega meljevca in peščenjaka z več debelejšimi plastmi sivega in rožnatega oilitnega apneca, za katerega je menil, da leži v nižjih delih skitskih plasti in ne v srednjem delu, kakor so menili poprej.

BUSER in sodelavci (1986) so opisali stratigrafske, paleontološke in sedimentološke značilnosti zgornjepermških sedimentov. Na ozemlju Slovenije so razlikovali dva razvoja zgornjepermških plasti. Zahodno od Ljubljane je razvita žažarska formacija, v južnih Karavankah in v Posavskih gubah (vzhodno od Ljubljane) pa imamo karavanško formacijo.

OGORELEC in GRAD (1986) sta med drugim opisala tudi zgornjepermško zaporedje karbonatnih kamnin na Žirovskem in ga razdelila v tri litološke enote. Meja med permскimi in skitskimi plastmi ni ostra in poteka v 120 m debelem paketu svetlejšega tankoplastnatega dolomita z redko detritično primesjo. Zgornjepermški del skladovnice sta pripisala žažarski formaciji.

RAMOVŠ (1989) je poročal, da permsko-triadsna meja v severnih Julijskih Alpah ni nikjer razločna. Še najbolj jasne so razmere med obema členoma južno od Save v Podkorenju, to je severno od Rutiča, kjer je v vrhnjem zgornjem permu ploščast, dimnatosiv, luknjičav, peščen dolomit, sivi plastnati dolomit nad njim z vložki sljudnega laporovca pa je skitski.

MUŠIČ (1992) je nadrobno raziskal zgornjepermške in spodnjetriaspne kamnine pri Skopačniku v Želimaljski dolini. Opisal je njihove petrografske in paleontološke značil-

nosti, sedimentacijsko okolje in diagenetske spremembe. Menil je, da predstavljajo te plasti litološki ekvivalent tretje dolomitne enote (zgornje dolomitne plasti) v južnih Karavankah (Tržič). Zgornjepermski del profila je razdelil na tri litološke enote (od spodaj navzgor: 1) – spodnja dolomitna enota, 2) – zgornja dolomitna enota in 3) – prehodna P/T enota.

## MATERIALI IN METODE DELA

Geološki podatki, ki so uporabljeni za ta članek, so bili pridobljeni pri geološkem kartiraju za Geološko karto Slovenije na listu Grosuplje 1:50 000, ki ga v tem delu Slovenije izvaja Geološki zavod Slovenije. Najnovejši podatki so dobavljeni pri stratimetrijskem profiliranju in sedimentološki obdelavi profila Skopačnik na jugovzhodnem obrobju Ljubljanskega Barja.

Istočasno s stratimetrijskimi meritvami je potekalo vzorčevanje zgornjepermских in spodnjega dela skitskih kamnin za izotopske meritve in druge laboratorijske raziskave. Vzorci so jemani v svežih kamninah, ki niso preperele ali rekristalizirane.

Karbonatne kamnine so določene po FOLKovi (1959) in DUNHAM-ovi (1962) klasifikaciji. Barva kamnin je določena po GSA Rock-Color-Chart barvni lestvici, ki jo je ustvaril Rock Color-Chart Committee, izdala pa Geological Society of America, Boulder, Colorado.

Vzorci za masnospektrometrične analize izotopske sestave kisika in ogljika so bili odvzeti na podlagi nadrobne mikroskopske raziskave z alizarin rdeče obarvanih prepa-

ratov karbonatnih kamnin, ki so omogočili podrobnejšo oceno vsebnosti dolomita v apnencih oziroma kalcita v dolomitu in s tem vpliva postsedimentacijskih procesov. Ti lahko bistveno spremenijo prvotno izotopsko sestavo obeh prvin v karbonatih. Za analizo smo izbrali najmanj dolomitizirane in rekristalizirane apnence ter najmanj kalcitizirane dolomite in iz njih pripravili prah z velikostjo delcev  $< 63 \mu\text{m}$ .

Praškaste vzorce (40 mg) karbonatnih kamnin smo najprej evakuirali, nato pa preliminarno raztopili z 2 ml  $> 100\% \text{ H}_3\text{PO}_4$  po postopku, ki ga je razvil McCREA (1950). Reakcija je potekala 2 ur pri temperaturi  $55 \pm 0,5^\circ\text{C}$ , kar omogoča tudi popolno raztopljanje dolomita. Pri reakciji med kislino in karbonatom je nastal  $\text{CO}_2$ , ki smo ga zamrznili v posebni pasti pri temperaturi  $-70^\circ\text{C}$  in tako očistili preostalih plinov, ki bi lahko vplivali na pravilnost meritve. Tako očiščenemu  $\text{CO}_2$  smo nato izmerili izotopsko sestavo kisika in ogljika z masnim spektrometrom Europa 20-20 (Europa Scientific LTD). Dobavljeni rezultati predstavljajo povprečno izotopsko sestavo kisika in ogljika vseh generacij karbonatov, prisotnih v merjenem vzorcu apnence oziroma dolomita. Vsak vzorec smo pripravili in merili 4 do 5 krat, nato pa izračunali povprečje meritve. Kot standard smo uporabili mednarodni standard IAEA-CO-1, ki ima  $\delta^{18}\text{O}$  vrednost  $-2,44\text{\textperthousand}$ , za  $\delta^{13}\text{C}$  pa  $+2,48\text{\textperthousand}$ . Dobljene vrednosti za izotopsko sestavo kisika in ogljika podajamo kot relativne vrednosti izražene v promilih (‰) glede na mednarodni standard V-SMOW oziroma V-PDB (Vienna - PeeDee Bellemnita Americana). Natančnost meritve za  $\delta^{18}\text{O}$  in  $\delta^{13}\text{C}$  je boljša od  $\pm 0,1\text{\textperthousand}$  ( $1\sigma$ ). Izotopske analize kisika in ogljika v karbonatih so bile napravljene na Inštitutu Jožef Stefan v Ljubljani.

## REZULTATI RAZISKAV

### Litologija in litostratigrafska razčlenitev

Za študij problematike zgornjopermskih plasti in meje med permskimi in skitskimi sedimenti smo izbrali okoli 150 m dolg profil na jugovzhodnem obrobju Ljubljanskega Barja (Slika 1). V profilu je razkrit vrhnji del zgornjopermskih karbonatnih sedimentov ter spodnji del karbonatnih in klastičnih skitskih skladov z nekaj deset metrov debelim horizontom oolitnega apnenca na vrhu.

#### *Zgornji perm*

Okoli 20 m debel najspodnejši del obravnavanega sedimentnega zaporedja, ki ga štejemo za zgornji perm, je sestavljen iz temnega ploščastega in plastnatega dolomita z redekimi tankimi vložki dolomitnega laporovca in laporne glinavce.

#### *Ploščasti dolomikrit, dolomitni laporovec in laporni glinavec (H-1):*

V najmlajši litostratigrafski zgornjopermski enoti prevladujejo ploščast (5-10 cm), siv, srednjesiv in srednje temnosiv gost dolomit oziroma dolomikrit. Mestoma je tankoplastnat (10-20 cm), zrnat in oolitičen. Ponekod vsebuje tanke vložke sivega in olivnosivega laporovca in laporne glinavce, redka zrna pirita in kremena ter ostanke drobnih foraminifer in alg. Pogosto je bolj ali manj rekristaliziran. Vezivo je mikritno ali mikrosparitno. Izmerjena debelina najstarejše zgornjopermske litostratigrafske enote znaša 20 metrov, vendar je v resnici večja, ker je precejšnji del plasti, ki leže spodaj, prekrit s kvartarnimi sedimenti in odsekani s prelomom.

### *Spodnji skit*

V litostratigrafskem pogledu smo spodnjeskitsko skladovnico razdelili v štiri horizonte (od spodaj navzgor):

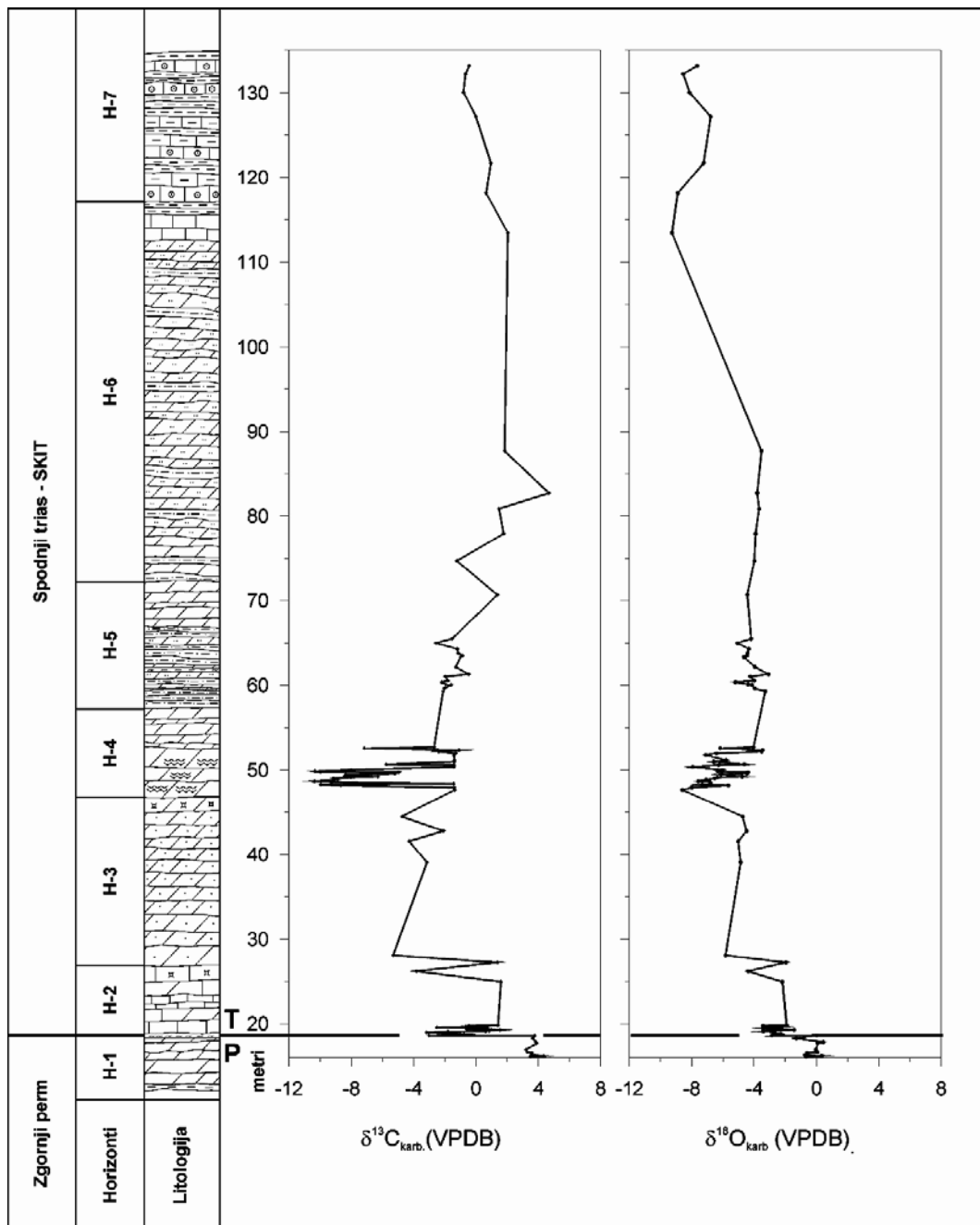
- 1) plastnati apnenec, dolomitni apnenec in apnenčev laporovec (H-2),
- 2) plastnati sparitni dolomit (H-3),
- 3) plastnati stromatolitni dolomit (H-4),
- 4) sajske plasti (H-5).

#### *Plastnati apnenec, dolomitni apnenec in apnenčev laporovec (H-2):*

Spodnjeskitski apnenec je srednjesiv do sivkastočrn, zelo drobno do drobnozrnat, plastnat (20-45 cm) in redkeje ploščast (5-10 cm) karbonatni sediment. Po strukturi je mikriten, (mudstone) redkeje biomikriten (wackestone), zelo redko biospariten ali intrabiospariten (packstone). Vezivo je mikritno in mikrosparitno, redko sparitno. Praviloma je bolj ali manj dolomiten. Vsebuje ostanke foraminifer in alg ter drobne bele kalcitne žilice. Debolina paketa plastnatega apneneca, apnenčevega laporovca in dolomitnega apnenca je 8 metrov, posamezne plasti pa so debele 10-30 cm. Kemično je čist, saj vsebuje le nekaj procentov detritičnega kremena, sljud in mineralov glin. Mestoma je nekoliko rekristaliziran.

#### *Plastnati sparitni dolomit (H-3):*

Spodnjeskitski bazalni dolomit je temnorjavosiv, bledorjavkastosiv in srednje svetlosiv, plastnat (15-35 cm), pogosto luknjičast srednje- in debelozrnat karbonatni sediment s peščenim otipom. V spodnjem delu je debeloplastnat, v zgornjem pa srednje- do tankoplastnat. Mestoma vsebuje drobne vključek belega kalcita. Po strukturi je dolosparit, biodolosparit in intrabiodolosparit. Vsebuje zrna



Slika 1. Litološki stolpec in izotopska sestava kisika in ogljika v permsko-triasni mejni sekvenci iz profila Skopačnik (osrednja Slovenija)

Figure 1. Lithology and depth profile of oxygen and carbon isotope composition across the Permo-Triassic boundary in the Skopačnik section (Central Slovenia)

pirita ter ostanke foraminifer in alg. Debelina spodnjega dela je 12,5 metrov zgornjega pa 7,5 metrov, skupaj torej 20 metrov.

#### *Plastnati stromatolitni dolomit (H-4):*

Enoti plastnatega stromatolitnega dolomita pripada okoli 11 metrov debela skladovnica srednje svetlosivega do zelo svetlosivega, plastnatega, v vrhnjem delu debeloploščastega in tankoplastnatega (5-20 cm), izredno kompaktnega in čvrstega, izrazito stromatolitnega dolomita. V stromatolitnem dolomitu ne opazujemo prepokanosti niti paralelepi-pedske krojitve. Površine plastovnih ploskev so ravne do rahlo valovite.

Sparitni plastnati dolomit, ki leži nad spodnjeskitskim temnim apnencem, je nastal v rahlo razgibani morski vodi, o čemer priča mnogokrat precejšnja izpranost tega sedimenta, in z pozdnodiagenetsko rekristalizacijo prvotnega sedimenta, zaradi česar je ta sediment srednje- in debelozrnat in peščenega otipa. Piritna zrna in organska snov v dolomitu in apnencu govorijo za občasno lokalno redukcijsko okolje.

Stromatolitni dolomit je izrazito valovito in nepravilno laminiran sediment, ki je nastajal v zelo plitvi morski vodi. Nastopa v plasteh in debelejših ploščah. Njegova izredna kompaktnost in trdota sta posledica mikritizacije, ki je bila istočasna s sedimentacijo, ali pa se je zgodila po litifikaciji karbonatnega mulja.

#### *Sajske plasti (H-5):*

Vrhni del spodnjeskitskega zaporedja sedimentov pripada sajskim plastem. Gre najprej za okoli 15 metrov debel paket ploščastih rumenkastosivih, oranžnorumenih in oranžnorjavih, pogosto laminiranih ali

pasastih peščenih (sljudnih) laporovcev z interkalacijami in redkeje vložki ploščastega in plastnatega rumenkastosivega bolj ali manj peščenega dolomita. Približno v sredini opisanega karobantnega zaporedja je 20 do 50 cm debel vložek temnosivega do sivkastočrnega, ploščastega, progastega in pasnatega laporne glinavca ozira dolomitnega laporovca.

Nad repernim vložkom temnosivega do črnega ploščastega progastega in pasnatega laporne glinavca ozira dolomitnega laporovca je ena do dva metra debel horizont ploščastega in tankoplastnatega oolitenga dolomita.

Opisano bazalno sajsko zaporedje prehaja navzgor postopno najprej v 7,5 m debel paket sivega, ploščastega in tankoplastnatega (3-25 cm), tu in tam laminiranega peščenega dolomita z redkimi interkalacijami dolomitnega laporovca. Nato sledi 15 m debel interval rumenkastosivega in plastnatega (5-20 cm) peščenega dolomita z vložki dolomitnega laporovca. Na vrhu litostratigrafske enote peščenih dolomitov leži 23 m debela skladovnica rožnatorumenega, bledo do rožnatorjavega, ploščastega in tankoplastnatega, močno peščenega (sljudnatega) dolomita z vložki peščenega dolomitnega laporovca in interkalacijami (20-35 cm) debeloplastnatega peščenega dolomita.

Nad 60,5 m debelim sajskim zaporedjem pisanih peščenih dolomitov (H-5 in H-6) leži litostratigrafska enota oolitnih apnencev (H-7). Raziskali smo spodnji del te enote, ki sestoji iz dveh paketov. V spodnjem 10 m debelem paketu se menjavajo sivi in srednjesivi, ploščasti in plastnati zrnati apnenec, laporni apnenec in apnenčev laporovec.

Apnenec je tudi oospariten in kaže navzkrižno plastičnost. V zgornjem paketu (7,5 m) so zelen ploščast laporovec, temnordeč srednjezrnat oolitni apnenec s številnimi preseki polžka *Holopella gracilior* (Schauroth) in temnoolivnozelen apnenčev laporovec.

### Sedimentacijsko okolje zgornjepermskih in spodnjeskitskih skladov

V zgornjem permu in spodnjem skitu je prevladovala sedimentacija plitvega zaprtega šelfa oziroma plitve lagune.

Temni apnenec je nastajal v plitvem zaprtem šelfu oziroma plitvi laguni. Izsuševanje lagune je bilo močno, zaradi česar je apnenec praviloma bolj ali manj dolomiten. Močno izparevanje je narekovalo večjo slanost morja in slabe pogoje za življenje zlasti večjih in bentonskih organizmov, zato so zgornjepermski sedimenti na jugovzhodnem obrobju Ljubljanskega Barja zelo revni z makrofosili. K slabim ohranjenosti fosilov pa sta prispevala tudi zgodnja in pozna dolomitizacija. Občasno odpiranje lagune je nekoliko razgibalo lagunsko vodo, kar je bilo ugodno za rast alg in drobnih foraminifer ter za nastanek ooidov in oolitnih plasti. Piritna zrna v apnencu govore za redukcijsko okolje.

Zgornjepermski dolomit je nastal z zgodnjediagenetsko dolomitizacijo apnenčevega mulja. Usedanje karbonatnega mulja je bilo tu in tam prekinjeno z donosom zelo drobnega terigenega materiala (glina, melj) s kopnega, o čemer pričajo tanjši vložki glinenega laporovca in lapornega glinavca. Zgornjepermski dolomit je v celoti zgodnjediagenetskega izvora, piritna zrna v njem pa govore za občasno redukcijsko okolje. Zgodnja dolomitizacija je potekala po evaporitnem modelu, kar potrjujejo tudi izotopske preiskave.

### Biofacijalna analiza

Omenili smo že, da je zgornjepermsko morje zaradi majhne globine, močnega izsuševanja in posledično prevelike slanosti bilo dokaj neugodno za razvoj zlasti večjih organizmov. Toda zgornjepermsko morje se je občasno odpiralo, kar je omogočilo rast nekaterih alg in drobnih foraminifer, vendar je s pomočjo le-teh nemogoče opraviti zanesljivo biostratigrafsko razčlenitev.

Prvo mikrobiofacijalno analizo na jugovzhodnem obrobju Ljubljanskega Barja je opravil Mušič (1992). V spodnji dolomitni enoti je ugotovil mikroforaminiferne rodove *Ammodiscus* in *Hemigordius*. Poleg teh so tu prisotne še druge nedoločljive oblike malih foraminifer, ostanki iglokožcev, briozojev in problematik rodu *Tubiphytes*. V temnosivem kompaktnem dolomitu zgornjedolomitne enote je precej drobcev rdečih alg iz družine *Solenoporaceae* in spongijs rodu *Carta*. Od ostalih fosilnih ostankov so prisotni še preseki talusov dazikladacej, problematik rodu *Tubiphytes*, ploščice ehinodermov ter redke male foraminifere od katerih je bil določljiv le primitivni rod *Staffella*. V 25 metrov debeli prehodni P/T litološki enoti sivega do svetlosivega in srednje- do debeloplastnatega (20-200 cm) dolomita niso najdeni nobeni fosili, tako da starost te enote in meja med permom in triasem nista dokazani.

Sto petdeset metrov debelo skladovnico spodnjetriaspnih karbonatnih kamnin je razdelil v dve litološki enoti: 1) – apnenčeva enota in 2) – dolomitna enota.

Starost spodnjega dela dolomitne enote s fosili ni bila dokazana. Prvi fosilni ostanki se pojavijo razmeroma visoko. V lečah

apnenca so nedoločljivi fragmenti moluskov in ehinodermov, v dolomitu pa so le posamezne hišice mikroforaminifer *Ammodiscus* sp. Mejo med griesbachijem in nammalijem je postavljena pod biomikrosparitnim apnencem (packstone) s številnimi polžki rodov *Coleostylina* in *Natica*. V vrhnjem delu profila je najdeno nekaj presekov polža *Natiria* sp., ki se na ozemlju Slovenije pojavljajo v vrhnjem delu spodnjega triasa (spathij). Najdbe polžev vrste *Natiria costata* v spodnjetroiasnih kamninah pri Skopačniku omenja BUSER (1974).

### Izotopska sestava kisika in ogljika v zgornjepermiskih in spodnjeskitskih skladih

#### Izotopska sestava kisika ( $\delta^{18}\text{O}$ )

Izotopska sestava kisika, v zgornjepermiskih dolomitih – horizont (H-1) niha od  $-1.30\text{\textperthousand}$  do  $+0.43\text{\textperthousand}$  s srednjo vrednostjo  $\delta^{18}\text{O}_{\text{Mean}} = -0.25\text{\textperthousand}$ , v spodnjeskitskih dolomitih (horizonti H-2, H-3, H-5 in H-6) pa od  $-5.83\text{\textperthousand}$  do  $-1.95\text{\textperthousand}$  s srednjo vrednostjo  $\delta^{18}\text{O}_{\text{Mean}} = -4.21\text{\textperthousand}$ . Izjema so dolomiti iz horizonta H-4, kateri so močno obogateni z lahkim kisikovim izotopom. Njihova sestava se spreminja od  $-8.60\text{\textperthousand}$  do  $-3.46\text{\textperthousand}$  s srednjo vrednostjo  $\delta^{18}\text{O}_{\text{Mean}} = -6.05\text{\textperthousand}$ . Spodnjeskitski apnenci horizonta H-2 nad P/T mejo so v primerjavi z zgornjepermiskimi dolomiti obogateni z lahkim kisikovim izotopom in imajo vrednosti  $\delta^{18}\text{O}$  v razponu od  $-4.40\text{\textperthousand}$  do  $-1.43\text{\textperthousand}$  s srednjo vrednostjo  $\delta^{18}\text{O}_{\text{Mean}} = -2.75\text{\textperthousand}$  v primerjavi s spodnjeskitskimi dolomiti pa obogateni s težkim kisikovim izotopom ( $\Delta\delta^{18}\text{O}_{\text{Mean(APNENEC)} - \text{Mean(DOLOMIT)}} = 1.45\text{\textperthousand}$ ). Oolitni in lapornati apnenci iz horizonta H-7 vsebujejo izmed vseh karbonatov profila

Skopačnik največ lahkega kisikovega izotopa. Njihove vrednosti so v razponu od  $-9.27$  do  $-6.79\text{\textperthousand}$ , srednja vrednota  $\delta^{18}\text{O}_{\text{Mean}}$  pa znaša  $-8.08\text{\textperthousand}$ .

#### Izotopska sestava ogljika ( $\delta^{13}\text{C}$ )

Variabilnost izotopske sestave kisika in ogljika je podana na sliki 1, iz katere so razvidne tudi litološke značilnosti raziskanega profila, katerega smo razdelili na 7 horizontov.

Iz slike 1 je razvidno, da je izotopska sestava ogljika v zgornjepermskem dolomitu – horizont H-1, relativno homogena in da je ta horizont obogaten s težkim ogljikovim izotopom. Njegov  $\delta^{13}\text{C}$  se spreminja od  $+3.22\text{\textperthousand}$  do  $+4.35\text{\textperthousand}$  (VPDB) s srednjo vrednostjo  $\delta^{13}\text{C}_{\text{Mean}} = +3.66\text{\textperthousand}$ . Te vrednosti sovpadajo z razponom vrednosti, ki jih navajata MAGARITZ in HOLSER (1991) za Belerofonsko formacijo (ekvivalent Žažarski in Karavanški formaciji ter horizontu H-1) in znaša od  $+2\text{\textperthousand}$  do  $+3.5\text{\textperthousand}$ . V vseh ostalih horizontih (od H-2 do H-7) pa se  $\delta^{13}\text{C}$  spreminja od  $-10.36\text{\textperthousand}$  do  $+4.68\text{\textperthousand}$  (V-PDB) s srednjo vrednostjo  $\delta^{13}\text{C}_{\text{Mean}} = -2.56\text{\textperthousand}$ . Krivulja  $\delta^{13}\text{C}$  na prehodu iz perma v trias kaže drastičen padec vrednosti  $\delta^{13}\text{C}$  in sicer od  $+3.77\text{\textperthousand}$  do  $-3.01\text{\textperthousand}$ . Gre za glavno ogljikovo anomalijo na P/T meji v velikosti  $6.78\text{\textperthousand}$ , ki je posledica povečane vsebnosti lahkega ogljikovega izotopa v apnencu. Negativna ogljikova anomalija se pojavi tik nad horizontom H-1 (slika 1) 1 cm pod temno sivo do 3 cm debelo plastjo gline. Podobna anomalija je bila ugotovljena tudi na drugih lokacijah v Sloveniji tako v zahodni Sloveniji v profilu Masore (M. DOLENEC, 2004; T. DOLENEC, et al., 2000; 2004) in profilu Idrijca (M. DOLENEC, 2004; M. DOLENEC and OGORELEC, 2001; T. DOLENEC, et al., 2001;

T. DOLENEC and RAMOVŠ, 1998), kakor tudi v Karavankah v profilu Košutnikov graben in profilu Brsnina (M. DOLENEC, 2004; M. DOLENEC, et al., 2003; T. DOLENEC, et al., 1998; 1999).

Za spodnji skit so poleg glavne negativne anomalije značilne tudi sekundarne anomalije. Od njih je najbolj izrazita pa tudi največja negativna ogljikova anomalija 30 m nad predpostavljenou P/T mejo (horizont H-4). Iz slike 1 je razvidno, da krivulja med horizontom H-3 in H-4 kaže drastičen padec vrednosti  $\delta^{13}\text{C}$  od  $-1,4\text{ ‰}$  do  $-8,67\text{ ‰}$  in na 50 m doseže vrednost  $-10,35\text{ ‰}$ . Omenjena sekundarna anomalija je bila najdena tudi v profilu Idrijca (M. DOLENEC, 2004; T. DOLENEC and RAMOVŠ, 1998) in v profilu Brsnina (DOLENEC M. et al., neobjavljeno). V profilu Idrijca se omenjena sekundarna negativna ogljikova anomalija pojavi 15 m in 20,7 m nad mejo v profilu Brsnina pa 30 m na P/T mejo. Nad horizontom H-4 sledi nato obogatitev s težkim ogljikovim izotopom. Vrednosti naraščajo od  $-2,54\text{ ‰}$  na začetku horizonta H-5 do  $+4,68\text{ ‰}$  na 83 m v horizontu H-6. Srednja vrednost horizontov H-5 in H-6 je  $\delta^{13}\text{C}_{\text{Mean}} = -0,43\text{ ‰}$ . Izotopska sestava ogljika v oolitnih apnencih horizonta H-7 je dokaj konstantna. Vrednosti  $\delta^{13}\text{C}$  se gibljejo od  $-0,8\text{ ‰}$  do  $+2,05\text{ ‰}$  s srednjou vrednostjo  $\delta^{13}\text{C}_{\text{Mean}} = +0,25\text{ ‰}$ .

## RAZPRAVA IN PRIMERJAVE

### Tektonika

Razmeroma plitvi sedimentacijski prostor, v katerem so nastajali spodnjepermски karbonatni sedimenti, se je pričel proti koncu spodnjega perma v času saalskih premikanj

dvigati, tako da so bili nekateri predeli južne Slovenije to je Kočevske, Bele Krajine in Gorskega Kotarja v srednjem in zgornjem permu kopno (DOZET, 1989). Na tem ozemlju v tem času ni bilo pomembnejšega gubanja. Pri počasnem dviganju je nastalo sorazmerno ravno kopno, zgrajeno iz glinenih sedimentov z vložki peščenjakov in konglomeratov. To kopno je bila posledica delovanja zadnjih sunkov ugašajoče hercinske orogeneze. Dviganje omenjenega ozemlja je spremljala prelomna tektonika, v Gorskem Kotarju (SAVIĆ and DOZET, 1985) pa tudi šibka magmatska aktivnost. Na kopno med srednjim permom in triasom sklepamo tudi po stratigrafski vrzeli; skitske plasti leže namreč diskordantno na spodnjopermskih. Na tektonsko-erozijski značaj te meje in na kopno kaže tudi okoli 20 cm debela limonitna skorja precejšnje razsežnosti v Gorskem Kotarju (SAVIĆ, et al., 1982) na meji med mlajšimi paleozojskimi in triasnimi sedimenti, ki predstavlja produkt razkrojevanja v izrazito oksidacijskih pogojih. Dviganje obravnavanega ozemlja, ki se je pričelo že na meji med spodnjim in srednjim permom v času saalske faze, se je neprekiniteno nadaljevalo v pfalsko fazo, s katero se je v Alpah končal hercinski tektogenetski ciklus. Le-ta se je na ozemlju Kočevske, Bele Krajine in Gorskega Kotarja kazal v obliki šibkih, počasnih pozitivnih epirogenetskih premikanj. Po PREMRUJU (1974) je nanj vezana močna srednjjetriaspna transgresija. Hercinski orogenezi je na območju Zunanjih Dinaridov sledilo splošno pogrezanje, temu pa transgresija spodnjetriasnega morja. V pogojih bolj ali manj plitvega morja in visokega oksidacijskega potenciala je na Slovenski karbonatni platformi nastajala pretežno karbonatna sedimentacija z občasnimi donosi večjega ali manjše količine terigenega materiala s kopnega.

### Stratigrafija in sedimentologija

Stratimetrijske in sedimentološke raziskave so pokazale, da leže zgornjepermske plasti na jugovzhodnem obrobju Ljubljanske kotline konkordnatno in brez prekinitve sedimentacije pod skitskimi bazalnimi temnimi apnenci. Sestavljeni so iz različnih dolomitov, dolomitnih apnencev, apnencev in laporovcev. Slednji so močno podrejeni. Izmerjena debelina zgornjepermskega litološkega stolpca je okoli 20 m, pri tem pa je treba poudariti, da v tem profilu niso ohranjeni sedimenti spodnjega dela zgornjepermskih kamnin. Po litološki sestavi in stratigrافski legi lahko primerjamo opisane zgonjelpermske sklade s podobnimi razvoji teh plasti v profilih Planica pri Čepuljah in Križna gora z območja Škofjeloškega hribovja (DEMŠAR and DOZET, 2002). Člen ploščastega dolomita v profilu na jugovzhodnem obrobju Ljubljanskega Barja ustrezava četrtemu členu zgornjepermskih plasti v profilu Planica pri Čepuljah, kjer prevladuje apnenčev dolomit. Če primerjamo izbrani profil Skopačnik s profilom zgornjepermskih plasti Križna gora, bi dolomikritni člen našega profila ustrezal prvemu členu to je dolomitiziranemu apnencu z algo *Vermiporella nipponica* Endo Križne gore. Člen dolomitnega apnanca Skopačnika bi odgovarjal drugemu členu t.j. apnenčevemu dolomitu z vrsto *Vermiporella nipponica* Endo Križne gore, plastnati sparitni dolomit Skopačnika pa tretjemu členu t.j. plastnatemu dolomitu Križne gore, ki se konča s 4 m debelim horizontom plastnatega apnanca in apnenčevega dolomita z algo *Vermiporella nipponica* Endo in redkimi preseki korale *Waagenophyllum indicum* Waagen et Wenzel.

Po facijalnih značilnostih opisanega sedi-

mentnega zaporedja lahko primerjamo izbrani profil tudi z žažarskim razvojem (RAMOVŠ, 1958b), natančneje s tretjo apnenčev dolomitno serijo s tremi horizonti tega razvoja, kjer je spodaj dolomitno apnenčev horizont z apnenčevimi algami, redkimi ostanki kriroidov in s koralo *Waagenophyllum* sp. Nad njim leže luknjičavi dolomitizirani apnenci, apnenčevi dolomiti in pasnati apnenčevi dolomiti, vsi brez fosilnih ostankov, najmlajši zgornji perm pa sestavljajo dolomiti, tudi brez fosilnih ostankov.

Če primerjamo skitski del raziskanega profila na jugovzhodnem obrobju Ljubljanskega Barja s klasičnim razvojem teh plasti v Južnotirolskih vzhodnih Dolomitih lahko rečemo, da oolitni horizont v našem profilu ni razvit, oziroma da je kvečjemu zelo neizrazit in da morda obsega najzgornjejni del zgornjepermskega temnega ploščastega dolomita in najspodnejši del spodnjeskitskega temnega plastnatega apnanca. Njegova debelina ne presega nekaj metrov. Enoto temnega apnanca, dolomitnega apnanca in apnenčevega laporovca primerjamo z enoto Mazzin v Vzhodnih Tirolskih Dolomitih, horizontu Andraz pa najverjetneje pripadata obe naslednji enoti našega profila, to je temni plastnati sparitni dolomit in na njem konkordnatno ležeči svetli plastnati stromatolitni dolomit. Sajska člen je na obravnavanem območju sestavljen iz pisanih peščenih dolomitov, peščenih dolomitnih laporovcev, laporih peščenjakov in peščenih lapornih glinavcev, leži pa konkordnantno pod gastropodnimi oolitom, ki vsebuje številne polžke vrste *Halopella gracilior*.

*Izotopska sestava kisika*

Podatki o izotopski sestavi kisika (slika 1) v profilu Skopačnik kažejo, da so karbonati na prehodu iz perma v trias - horizonta H-1 in H-2, obogateni z lahkim kisikovim izotopom. Obogatitev znaša okrog 2,5 ‰ in je lahko posledica izmenjave z izotopsko lažjo porno vodo pri postsedimentacijskih procesih. Ti so delno zabrisali prvotno izotopsko sestavo v kamnini značilno za morske karbonate, medtem ko se izotopska sestava ogljika ni spremenila (T. DOLENEC and RAMOVŠ, 1998). Izotopska sestava kisika v recentnem morskom karbonatu je okrog 0 ‰ (FAURE, 1977), apnenci nad P/T mejo v horizontu H-2 pa imajo vrednosti okrog – 2,8 ‰. V primerjavi z spodnjeskitskimi apnenci so dolomiti iz vrhnjega dela zgornjepermских plasti horizonta H-1 manj spremenjeni, kar je lahko posledica večje odpornosti proti izotopski izmenjavi z izotopsko lažjo porno vodo (FAURE, 1977) ali pa dejstva, da so nastali v evaporitnem okolju, v katerem je morska voda obogatena zaradi efekta evaporacije s težkim kisikovim izotopom. Zato imajo dolomiti iz teh okolij višje δ<sup>18</sup>O vrednosti kot morski apnenci. Manjše vrednosti δ<sup>18</sup>O iz profila Skopačnik v horizontu H-4 in horizontu H-7 si lahko razložimo kot posledico kasnejših diagenetskih procesov ali dotoka sladke vode v evaporitno okolje v času njihovega nastajanja, pa tudi manjše evaporacije (BRAND and VEIZER, 1981; M. DOLENEC, 2004; MAGARITZ and HOLSER, 1991). Kljub temu lahko iz poteka krivule δ<sup>18</sup>O sklepamo na negativni trend parametra δ<sup>18</sup>O v zgornjem permu in na prehodu iz perma v trias. Ta lahko nakazuje klimatske spremembe in sicer toplejšo klimo v spodnjem skitu v primerjavi z zgornjim permom in nenadno povečanje temperature na samem prehodu iz perma v trias.

*Izotopska sestava ogljika*

Variabilnost izotopske sestave ogljika (slika 1) v karbonatih je predmet večine člankov, ki obravnavajo ne samo P/T mejo ampak tudi spremembe v ogljikovem ciklusu v drugih časovnih obdobjih (ERWIN, 1993 in referenčne v knjigi). Rezultati dosedanjih raziskav na profilu Idrijca (T. DOLENEC and RAMOVŠ, 1998) in raziskav variabilnosti izotopske sestave ogljika v karbonatih od zgornjega karbona do spodnjega triasa (M. DOLENEC, et al., 2003) kažejo, da so zgornjepermски karbonati močno obogateni s težkim ogljikovim izotopom, kar je globalni fenomen. Podobne vrednosti v razponu od 3 ‰ do 4 ‰ namreč navajajo za zgornjepermiske karbonate v zahodni Tetidi pa tudi drugod po svetu, številni raziskovalci P/T meje (BAUD, et al., 1989; HEYDARI, et al., 2000; HOLSER and MAGARITZ, 1985; HOLSER, et al., 1989; KRULL, et al., 2004; MAGARITZ, et al., 1988; MAGARITZ and HOLSER, 1991; MUSASHI, et al., 2001; SHAO, et al., 2000).

Potek krivilje δ<sup>13</sup>C nakazuje drastične spremembe v ogljikovem ciklusu na prehodu iz perma v trias. Globalno ogljikovo anomalijo na meji P/T med horizontom H-1 in H-2 si lahko razložimo s teorijo o nenadnem fluksu ogljikovodikov predvsem metana iz morskih sedimentov v atmosfero. Ta teorija v zadnjem času vse bolj pridobiva na veljavi. Prva raziskovalca, ki sta predpostavila, da so tako drastične spremembe v ogljikovem ciklusu na prehodu iz perma v trias lahko posledica nenadnega fluksa metana v atmosfero sta bila KVENVOLDEN (1988) in ERVIN (1993). Izotopska sestava ogljika v recentnih ogljikovodikih je okrog – 65 ‰ (DICKENS, et al., 1997). Zaradi povečane temperature lahko pride do oksidacije ogljikovodikov v morskem okolju

ali v atmosferi. Pri tem nastane  $\text{CO}_2$ , ki je močno obogaten z lahkim ogljikovim izotopom. Ta vpliva na izotopsko sestavo  $\text{CO}_2$ , tako v morski vodi kot v zračnem  $\text{CO}_2$  (KATZ, et al., 1999). BERNER (2002) smatra da lahko nenaden fluks metana iz morskih sedimentov povzroči nenaden padec  $\delta^{13}\text{C}$  vrednosti v morskem okolju za 7 do 8 %. Glede na podatke iz profila Skopačnik predpostavljamo da drastičen padec vsebnosti  $\delta^{13}\text{C}$  za 6,78 % v karbonatih med horizontom H-1 in H-2 predstavlja P/T mejo, ki je podobno kot v Idrijci (M. DOLENEC, 2004) tudi tu vezana za plast gline (PTB – plast). Neneaden drastični padec vrednosti  $\delta^{13}\text{C}$  je značilen tudi za P/T mejo drugod v Tetidi (BAUD, et al., 1989), pa tudi na Kitajskem (SHAO, et al., 2000; XU and ZHENG, 1993) in Japonskem (MUSASHI, et al., 2001). Poleg globalne negativne ogljikove anomalije na sami meji je pomembna tudi sekundarna ogljikova anomalija med horizontom H-3 in H-4 30 m nad P/T mejo, ki pa zaenkrat še ni zadovoljivo pojasnjena. Gre za drugo močno negativno anomalijo, opaženo tudi v profilu Idrijca 15 in 20,7 m nad mejo (M. DOLENEC, 2004; T. DOLENEC and RAMOVŠ, 1998) in profilu Brsnina 30 m nad mejo (M. DOLENEC, neobjavljeno). Lahko si jo razložimo kot posledico pospešenega razkroja organskih komponent pri postdesimentacijskih procesih. Pri njihovem razpadu se sprošča  $\text{CO}_2$  s podobno izotopsko sestavo ogljika, kot je sestava te prvine v rastlinah (CERLING, et al., 1989). Ta  $\text{CO}_2$  je lahko znižal  $\delta^{13}\text{C}$  vrednosti v stromatolitnih dolomitih horizonta H-4.

## SKLEPI

Za začetek študija problematike zgornjepermских skladov južne Slovenije je na jugovzhodnem obrobju Ljubljanskega Barja izbran profil, ki v geotektonskem oziru pripada enoti Dolenjsko-Notranjskih mezozojskih grud natančneje tektonski enoti Krimsko-Mokrškega hribovja (BUSER, 1974).

V zgornji perm je uvrščen najspodnejši del skladovnice karbonatnih kamin (temni dolomikrit z vložki dolomitnega laporovca in lapornega glinavca), ki leži konkordantno in brez znakov prekinitve sedimentacije pod pisanimi skitskimi sedimenti.

V zgornjepermском litološkem stolpcu močno prevladujejo karbonatne kamnine (dolomit, dolomitni laporovec), ki so nastale na območju supralitorala in v mirnem okolju zatišnega plitvega šelfa oziroma v plitvi laguni.

Na podlagi izotopske analize lahko sklepamo, da poteka meja med permскими in triasnimi (skitskimi) sedimenti na meji med najspodnejšim ploščastim dolomitom in paketom temnega apnenca, dolomitnega apnenca in apnenčevega laporovca. Za točno določitev meje bi bile potrebne tudi podrobne paleontološke in geokemične analize. Dvajset metrov debelemu zgornjepermском zaporedju karbonatnih kamin na jugovzhodnem obrobju Ljubljanskega Barja pripada le najstarejša lithostratigrafska enota temnega dolomita z vložki dolomitnega laporovca in lapornega glinavca, skitski serijski pa pripadajo enota temnega apnenca, dolomitnega apnenca ter apnenčevega laporovca, enota temnega plastnatega sparitnega dolomita, sajske plasti ter enota oolitnih apnencev.

## Acknowledgements

The authors are much obliged to the Ministry of High Education, Science and Technology as well as to the Geological Survey of Slovenia and Faculty of Natural Sciences and Technics – Geology Department – University of Ljubljana for financial support of their research work in the field and laboratory.

## SUMMARY

### **Permo-Triassic Boundary and Upper Permian as well as Lower Scythian Beds on the Southeastern Borderland of the Ljubljana Marsh, Central Slovenia**

The scope of this paper is to report on definition of the Permo-Triassic boundary in the Dolenjsko district with stratigraphical and isotopic methods, to describe lithological units developed at this boundary and to correlate them with the classic development in the Eastern Tyrol Dolomites. For the beginning of solving of these problematics the cross-section Skopačnik on the southeastern borderland of the Ljubljana Marsh has been chosen where the topmost Upper Permian as well as the lower and middle part of the Scythian carbonate-clastic sedimentary succession is exposed.

From the geographical point of view the considered area belongs to the southern borderland of the Ljubljana Marsh, paleogeographically to the Slovenian Carbonate Platform and geotectonically to the Dolenjsko-Notranjsko Mesozoic Blocks (Buser, 1974), more precisely to the Krim-Mokre Mountains tectonical unit (BUSER, 1974).

In the Skopačnik sedimentary sequence the following lithostratigraphic units have been found: 1) dark platy dolomite, dolomitic marlstone and marly claystone, 2) – dark bedded limestone, dolomitic limestone, limy marlstone, 3) – dark bedded sparitic dolomite, 4) – light bedded stromatolitic dolomite, 5) – Seis Beds and 6) – Gastropod Oolite.

In the Skopačnik cross-section on the southeastern borderland of the Ljubljana Marsh the boundary between the Permian and Triassic system has been established by isotope method. It is placed into the point between the first and second lithostratigraphic horizon of the Skopačnik sedimentary succession, i.e. between the dark platy dolomite (Upper Permian – H-1) and the overlying dark bedded limestone (H-2), representing, accordingly, the basal lithostratigraphic unit of the Scythian stratigraphic sequence in this part of Slovenia. For more precise determination of the P/T boundary further paleontological and geochemical analyses are required.

Lithological composition as well as textural, structural, mineralogical and chemical characteristics of the researched sedimentary succession showed, that in the Upper Permian and Lower Scythian, sedimentation of a shallow restricted shelf, a shallow lagoon respectively, has been prevailed.

The dark limestone was formed in a shallow restricted shelf, a shallow lagoon respectively. Evaporation of the lagoon was strong. Therefore the limestone is, as a rule, more or less dolomitic. The strong evaporation caused greater salinity of the sea and bad life-conditions especially for bigger organisms; for that reason the dark Upper Permian and Lower Scythian sediments on the southern

borderland of the Ljubljana Marsh are poor in macrofossils. To the bad preservation of fossils contributed very much an early and late dolomitization as well. Periodical opening of the lagoon agitated its water what was favorable for growth of algae and very small foraminifers as well as for formation of ooids and oolitic beds. Accordingly, to the Upper Permian belongs only the first (the oldest) lithostratigraphic unit; other four units belong to the Lower Scythian. The Upper Permian beds can be compared with pretty similar developments of these beds; in the cross-sections Planica at Čepulje and Križna gora from the Škofja Loka Mountains area (DEMŠAR and DOZET, 2002) as well as with the Žažar development (RAMOVŠ, 1956) more precisely with the third limestone-dolomite series with three horizons of this development.

If we compare the Scythian part of the researched cross-section on the southeastern borderland of the Ljubljana Marsh at

Skopačnik with the classic development of these beds in the Southern Tyrol Dolomites, it can be said, that the oolite horizon in our cross section is not developed, at the most, it is very unexpressive comprising probably the topmost part of the Upper Permian dark platy dolomite and the lowermost part of the Lower Scythian dark bedded micritic limestone. Moreover, its thickness do not exceed some metres. The unit of the dark limestone, dolomitic limestone and limy marlstone is compared with the Mazzin unit in the Eastern Tyrol Dolomites, and to the horizon Andraz belong most probably the next two units of our cross-section, i.e. dark bedded sparitic dolomite and the concordantly overlying light bedded stromatolitic dolomite. The Seis Member is in the considered region composed of variegated sandy dolomites, sandy dolomitic marlstones, marly sandstones and sandy marly claystones lying concordantly under the Gastropod Oolite, which contain numerous gastropods of the species *Hallopella gracilior*.

## LITERATURA

- BAUD, A., MAGARITZ, M. & HOLSER, W. T. (1989). Permian-Triassic of the Tethys: Carbon isotope studies. *Geol. Rdsch.*, 642-677.
- BERNER, R. A. (2002). Examination of hypotheses for the Permo-Triassic boundary extinction by carbon cycle modeling. *Proceedings of the National Academy of Sciences of the United States of America* 99, 4172-4177.
- BRAND, U. & VEIZER, J. (1981). Chemical diagenesis of a multicomponent carbonate system - 2: stable isotopes. *J. Sediment. Petrol.* 51, 987-997.
- BUSER, S. (1962). Geološke razmere na listu Ig-Ribnica 52-25/1, 40.
- BUSER, S. (1969). List Ribnica, *Osnovna geološka karta SFRJ 1:100.000*.
- BUSER, S. (1974). Triasne plasti na listu Ribnica, 1. faza., *Mezozoik v Sloveniji*, 70.
- BUSER, S. (1976). Tolmač lista Ribnica, *Osnovna geološka karta SFRJ 1:100.000*, 60.
- BUSER, S., GRAD, K., OGORELEC, B., RAMOVŠ, A. & ŠRIBAR, L. (1986). Stratigraphical, paleontological and sedimentological characteristics of Upper Permian beds in Slovenia, NW Yugoslavia. *Mem. Soc. Geol. It.* 34, 195-210.
- CERLING, T. E., QUADE, J., YANG, W. & BOWMAN, J. R. (1989). Carbon isotopes in soils and palaeosoils as ecology and palaeoecology indicators. *Nature* 341, 138-139.
- DEMŠAR, M. & DOZET, S. (2002). Nekaj razvojev zgornjopermskih plasti zahodno od Škofje Loke. *Geologija* 54, 189-200.
- DICKENS, G. R., CASTILLO, M. M. & WALKER, J. C. G. (1997). Direct measurement of in situ methane quantities in a large gas-hydrate reservoir. *Nature* 385, 426-428.

- DOLENEC, M. (2004). Permsko-triasna meja v Karavankah in zahodni Sloveniji: sedimentološki, izotopski in geokemični vidiki globalnih sprememb v zahodni Tetidi, *Oddelek za geologijo*, Doktorska disertacija, 110.
- DOLENEC, M. & OGORELEC, B. (2001). Organic carbon isotope variability across the P/Tr boundary in the Idrijca Valley section (Slovenia : a high resolution study = Variabilnost izotopske sestave organskega ogljika na permsko-triasni meji v dolini Idrijce : detajljna študija). *Geologija* 44, 331-340.
- DOLENEC, M., OGORELEC, B. & LOJEN, S. (2003). Upper carboniferous to lower triassic carbon isotopic signature in carbonate rocks of the Western Tethys (Slovenia). *Geologica Carpathica* 54, 217-228.
- DOLENEC, T., BUSER, S. & DOLENEC, M. (1998). The Permian - Triassic boundary in the Karavanke Mountains (Slovenia) : stable isotope variations in the boundary carbonate rocks of the Košutnik Creek and Brsnina section = Permsko - triasna meja v Karavankah : variabilnost izotopske sestave v karbonatnih kamninah Košutnikovega potoka in Brsnine. *Geologija* 41, 17-27.
- DOLENEC, T., LOJEN, S., BUSER, S. & DOLENEC, M. (1999). Stable isotope event markers near the Permo-Triassic boundary in the Karavanke Mountains (Slovenia). *Geologia Croatica* 52, 77-81.
- DOLENEC, T., LOJEN, S. & DOLENEC, M. (2000). The Permian - Triassic boundary in the Idrijca valley (western Slovenia) : isotopic fractionation between carbonate and organic carbon at the P / Tr transition = Permsko - triasna meja v dolini Idrijce (zahodna Slovenija) : izotopska frakcionacija med karbonatnim in organskim ogljikom na prehodu iz perma v trias. *Geologija* 42, 165-170.
- DOLENEC, T., LOJEN, S. & RAMOVŠ, A. (2001). The Permian-Triassic boundary in Western Slovenia (Idrijca Valley section) : magnetostratigraphy, stable isotopes, and elemental variations. *Chemical Geology* 175, 175-190.
- DOLENEC, T., OGORELEC, B., DOLENEC, M. & LOJEN, S. (2004). Carbon isotope variability and sedimentology of the Upper Permian carbonate rocks and changes across the Permian-Triassic boundary in the Masore section (Western Slovenia). *Facies* 50, 287-299.
- DOLENEC, T. & RAMOVŠ, A. (1998). Isotopic changes at the Permian-Triasic boundary in the Idrijca Valley (W. Slovenia). *RMZ - Materials and Geoenvironment* 45, 405-411.
- DOZET, S. (1989). Tektonika premikanja na Kočevskem v mlajšem paleozoiku in mezozoiku (južna Slovenija). *Rud.-metal. zb.* 36, 663-673.
- DUNHAM, R. J. (1962). Classification of Carbonate rocks according to depositional texture, V: HAM, W. E. (Ed.) *Classification of carbonate rocks, a symposium*, Am. Assoc. Petrol. Geol. Memoir, pp. 108-122 (Tulsa).
- ERWIN, D. H. (1993). The great Paleozoic crisis: Life and death in the Permian. *Columbia University Press*, 327.
- FAURE, G. (1977). *Principles of Isotope Geology*. (John Wiley & Sons), pp. 464.
- FOLK, R. (1959). Practical petrographic classification of limestones. *Bull. Am. Ass. Petrol. Geol.* 43, 2-38.
- GERMOVŠEK, C. (1955). Poročilo o kartiraju jugovzhodnega obroblja Ljubljanskega barja. *Geologija* 3, 235-239.
- GERMOVŠEK, C. (1956). Razvoj mezozoika v Sloveniji, Paper presented at the *Prvi jugoslovanski geološki kongres*.
- HERITSCH, F. (1939). Karbon un Perm in den Sudalpen und Sudost Europa. *Geol. Rdsch.* 30, 528-588.
- HEYDARI, E., HASSANDZADEH, J. & WADE, W. J. (2000). Geochemistry of central Tethyan Upper Permian and Lower Triassic strata, Abadeh region, Iran. *Sedimentary Geology* 137, 85-99.
- HOLSER, W. T. & MAGARITZ, M. (1985). The Late Permian carbon isotope anomaly in the Bellerophon basin, Carnic and Dolomite Alps. *Jb. Geol. B.* 128, 75-82.
- HOLSER, W. T., SCHÖNLAUB, H. P., BOECKELMANN, K. et al. (1989). A unique geochemical record at the Permian/Triassic boundary. *Nature* 37, 39-44.
- KATZ, M. E., PAK, D. K., DICKENS, G. R. & MILLER, K. G. (1999). The source and fate of massive carbon input during the latest Paleocene thermal maximum. *Science* 286, 1531-1533.
- KOSSMAT, F. (1913). Die adriatische Umrandung in den alpinen Faltenregion. *Mitt. Geol. Ges.*, 61-65.
- KRULL, E. S., LEHRMANN, D. J., DRUKE, D. et al. (2004). Stable carbon isotope stratigraphy across the Permian-Triassic boundary in shallow marine carbonate platforms, Nanpanjiang Basin, south China. *Palaeogeography, Palaeoclimatology, Palaeoecology* 204, 297-315.

- KVENVOLDEN, K. A. (1988). Methane hydrates and global climate, V: McCARTHY, J. J. (Ed.) *Spacial section on Methane Biogeochemistry. Global Biogeochem. Cycles* 221-229.
- MAGARITZ, M., BAR, R., BAUD, A. & HOLSER, W. T. (1988). The carbon-isotope shift at the Permian-Triassic boundary in the Southern Alps is gradual. *Nature* 331, 337-339.
- MAGARITZ, M. & HOLSER, W. T. (1991). The Permian-Triassic of the Gartnerkofel-1 Core (Carnic Alps, Austria): Carbon and Oxygen Isotope Variation. *Abh. Geol. Bundesanst.* 45, 149-163.
- MCCREA, J. (1950). The isotopic chemistry of carbonates and a paleotemperature scale. *Jour. Chem. Phys.* 18, 849 - 857.
- MUSASHI, M., ISOZAKI, Y., KOIKE, T. & KREULEN, R. (2001). Stable carbon isotope signature in mid-Panthalassa shallow-water carbonates across the Permo-Triassic boundary: evidence for 13C-depleted superocean. *Earth and Planetary Science Letters* 191, 9-20.
- MUŠIĆ, B. (1992). Zgornjepermske in spodnjetrijasne kamnine pri Skopačniku v Želimeljski dolini. *Rud.-metal. zb.* 39, 241-259.
- OGORELEC, B. & GRAD, K. (1986). Zgornjepermske, skitske in anizične kamenine na Žirovskem ozemlju, Paper presented at the *Peti skup sedim. Jugosl. Brioni. Abstracts.*, Brioni.
- PREMRU, U. (1974). Triasni skladni v zgradbi osrednjega dela Posavskih gub. *Geologija* 17, 262-297.
- RAMOVŠ, A. (1956). Razvoj paleozoika na Slovenskem, Paper presented at the *Prvi jugosl. geol. kongres*, Ljubljana.
- RAMOVŠ, A. (1958a). Die Entwicklung des Oberperms im Bergland von Škofja Loka und Polhov Gradec. *Razprave SAZU* 4, 455-462.
- RAMOVŠ, A. (1958b). O faciesih v zgornjem wordu in zgornjem permu v Sloveniji. *Geologija* 4, 188-192.
- RAMOVŠ, A. (1982). The Permian-Triassic boundary in Yugoslavia. *Rud.-metal. zb.* 29, 29-31.
- RAMOVŠ, A. (1989). Razvoj skitskih plasti (spodnji trias) v severnih Julijskih Alpah. *Rud.-metal. zb.* 36, 623-636.
- SAVIĆ, D. & DOZET, S. (1985). Tumač za list Delnice, *Osnovna geološka karta SFRJ 1:100.000*, 62.
- SAVIĆ, D., DOZET, S. & SARKOTIĆ, M. (1982). Odnos permskih i gornjotriaskih naslaga na području Gorskog Kotara, Paper presented at the *Zbornik radova 10. jub. kongr. geol. Jugosl.*, Budva.
- SHAO, L., ZHANG, P., DOU, J. & SHEN, S. (2000). Carbon isotope compositions of the Late Permian carbonate rocks in southern China: their variations between the Wujiaping and Changxing formations. *Palaeogeogr. Palaeoclimatol. Palaeoecol.* 161, 179-192.
- ŠLEBINGER, C. (1953). Obvestilo o kartiranju listov Cerknica 1 in 2. *. Geologija* 1.
- XU, D. Y. & ZHENG, Y. (1993). Carbon isotope and iridium event markers near the Permian/Triassic boundary in the Meishan section, Zhejiang Province, China. *Palaeogeogr. Palaeoclim. Palaeoecol.* 104, 171-176.

# Some Considerations on the Series Solution of Differential Equations and its Engineering Applications

LEVENT YILMAZ

Technical University of Istanbul, Civil Engineering Department,  
80626, Maslak, Istanbul, Turkey; E-mail: lyilmaz@itu.edu.tr

Received: October 08, 2006 Accepted: October 20, 2006

**Abstract:** The ordinary linear differential equations with constant coefficients can be solved by the algebraic methods and the solutions are obtained by elementary functions. In practice, the class of this kind of differential equations is rather narrow. The most of the differential equations met in mathematics, physics and engineering sciences remain out of this class. In such cases, it is searched for solutions in form of infinite series. A new theory of functions named as higher transcendent functions or special functions were set up. The Legendre and Bessel equations are of this type. They appear in problems on vibrations, electric field, heat conduction, fluid flow, etc.

In this paper the authors intend to show by means of four interesting applications from the field of structural and mechanical engineering how still a powerful tool is the method of series solutions, beside the algebraic and numerical methods; how easy can the problems be handled by this method using the computer softwares prepared especially for mathematics. The results are compared with the numerical solutions.

**Key words:** Differential Equations, series solution, material and strength, engineering applications

## INTRODUCTION

The ordinary differential equations whose coefficients are constant can be solved by the algebraic methods and the solutions are obtained by elementary functions. Except that the ordinary linear differential equations and the differential equations which reducible to this type, the other ordinary linear differential equations can not be solved in terms of algebraic and transcendent functions known as elementary functions, like trigonometric functions, trigonometric invert functions, transcendent and logarithmic functions. In practice, the class of the differential equations which can be reduced to the ordinary linear differential equations with constant

coefficients is rather narrow. The most of the differential equations met in mathematics, physics and engineering science remain out of this class. In such cases, it is searched for the solutions in form of infinite series. In this point, beyond the elementary functions, a new theory of functions named as higher transcendent functions or special functions come out. This theory was developed by the mathematicians in 18<sup>th</sup> and 19<sup>th</sup> centuries in perfect form. (WYLIE and BARRET (1985), KREYSZIG (1993), AYRES (1952), RICHTER (1968), KoçAK (1983)).

The method of separation of variable for the solution of the partial differential equations often leads to ordinary differential equations

with variable coefficients whose solutions are obtained either in the form of infinite series in term of special functions. The Legendre's and Bessel's equations are of this type. These and other equations and their solutions play an important role in applied mathematics; they appear in problems of vibrations, electric field, heat conduction, fluid flow etc. The Bessel equations are always to be expected when partial differential equations are used in the study of configurations possessing cylindrical symmetry. On the other hand, they arise in numerous applications when neither cylindrical symmetry nor partial differential equations are involved. The Legendre equations appear in problems showing spherical symmetry.

In this paper, the authors, who are self engineers, will try to show by four applications from the fields of structural and mechanical engineering, stability, dynamic, theory of plates and fluid mechanics how still a powerful tool is the method of the series solutions beside the algebraic and the numerical methods and how easy can the problems be handled by this method using the softwares (Mathematica(6), PC-Matlab (7)) prepared particularly for mathematics in the computer medium in our century and the results will be compared with the numerical solutions.

## METHOD OF SOLUTION

Lets consider the differential equation given by equation (1).

$$y'' + p(x) y' + q(x) y = 0 \quad (1)$$

If the functions  $p(x)$  and  $q(x)$  of equation (1) is analytic at  $x = x_0$ , the every solution is analytic at  $x = x_0$  and can be represented by a power series with radius of convergence  $R > 0$ .

$$y(x) = \sum_{m=0}^{\infty} a_m (x - x_0)^m \quad (2)$$

The Legendre differential equation is

$$(1 - x^2)y'' - 2xy' + n(n+1)y = 0 \quad (3)$$

whose coefficients are analytic at  $x = 0$ . Thus the solution by the power series method gives Legendre polynomials of degree  $n$

$$P_n(x) = \sum_{m=0}^M (-1)^m \frac{(2n-2m)!}{2^m m! (n-m)! (n-2m)!} x^{n-2m} \quad M = \begin{cases} n/2 & ; n \text{ even} \\ (n-1)/2 & ; n \text{ odd} \end{cases} \quad (4)$$

which satisfy the orthogonality relations with respect to the weight function  $p(x)=1$

$$\int_{-1}^1 P_m(x) P_n(x) dx = \begin{cases} 0 & ; m \neq n \\ 2/(2n+1) & ; m = n \end{cases} \quad (5)$$

If at least one of the functions  $p(x)$  and  $q(x)$  is not analytic at  $x=x_0$ , but the functions defined by the products  $(x-x_0)p(x)$  and  $(x-x_0)^2 q(x)$  are analytic at  $x=x_0$ , then there is at least one solution which can be represented by a extended power series (Frobenius method) with radius of convergence  $0 < |x - x_0| < R$

$$y(x) = |x - x_0|^r \sum_{m=0}^{\infty} a_m (x - x_0)^m \quad (6)$$

Depending on the roots of the indicial equation

$$r(r-1) + p_0 r + q_0 = 0 \quad (7)$$

there can be three cases in the solution.

The Bessel differential equation of order  $v$  with a parameter  $\lambda$

$$y'' + \frac{1}{x} y' + (\lambda^2 - \frac{v^2}{x^2}) y = 0 \quad (8)$$

whose coefficients are not analytic at  $x = 0$ . If the independent variable of this equation is changed by the substitution of the new variable  $t = \lambda x$ , it is obtained

$$y'' + \frac{1}{t} y' + (1 - \frac{v^2}{t^2}) y = 0 \quad (9)$$

The solution of this equation by the extended power series method gives the Bessel functions of the first kind of order

$$J_v(t) = \sum_{m=0}^{\infty} \frac{(-1)^m t^{v+2m}}{2^{v+2m} m! \Gamma(v+m+1)} \quad (10)$$

The Bessel and modified Bessel functions of the other kinds of order are derived by manipulating of these equations.

For each fixed nonnegative integer for  $v = n$ , the Bessel functions satisfy the orthogonality relations with respect to the weight function  $p(x) = x$

$$\int_0^R x J_n(\lambda_i x) \cdot J_n(\lambda_j x) dx = 0 \quad (i \neq j) \quad (11)$$

Eigenvalue problems can be written in form of the Sturm-Liouville equation with boundary conditions that includes the Legendre and Bessel differential equations. The solution of this equation gives the eigen values and the corresponding eigen functions which have the orthogonality properties. This leads to eigen function expansions.

## APPLICATIONS

I - As a first application the buckling load of a simply supported steel column with variable cross-section (Figure1) will be determined.

The moment of inertia of the cross section in column varies according to the rule given as

$$J(x) = J_A(1+ax)^2 \quad (12)$$

where  $\delta = \delta_B / \delta_A$  ,  $a = (\delta - 1)/l$ .

The differential equation of this stability problem is

$$EJ_A(1+ax)^2 y'' + P y = 0 \quad (13)$$

By changing of a variable by  $e^z = 1+ax$  , this equation is transformed into

$$y'' - y' + \beta^2 y = 0 , \quad \beta^2 = \frac{P}{a^2 E J_A} \quad (14)$$

The boundary conditions are:

$$y = 0 \quad \text{at} \quad z = 0 \quad (15)$$

$$y = 0 \quad \text{at} \quad z = \ln(1+al) \quad (16)$$

This homogenous linear differential equation of second order with constant coefficient can also be solved by the series method. If the power series

$$y = \sum_{m=0}^{\infty} a_m z^m \quad (17)$$

If the power series is put into the differential equation, it is derived for the coefficients of the independent variable z the recurrence formula

$$a_{m+2} = \frac{(m+1)a_{m+1} - a_m \beta^2}{(m+1)(m+2)} ; \quad m \geq 0 \quad (18)$$

and the solution is

$$y = a_0 [1 - \frac{1}{2} \beta^2 z^2 - \frac{1}{6} \beta^2 z^3 + \frac{1}{24} (-\beta^2 + \beta^4) z^4 + \frac{1}{120} (-\beta^2 + 2\beta^4) z^5 + \dots] + \\ a_1 [z + \frac{1}{2} z^2 + \frac{1}{6} (1 - \beta^2) z^3 + \frac{1}{24} (1 - 2\beta^2) z^4 + \frac{1}{120} (1 - 3\beta^2 + \beta^4) z^5 + \dots] \quad (19)$$

The condition for the non-trivial solution of the homogeneous equation system which is obtained by applying the boundary conditions to the above equation gives  $\beta^2 = 64.46$ . With this value, the critical load is calculated as  $P_{cr} = 406.1$  kN. The value is % 7 higher than the value obtained by the analytical solution as 379.5 kN.

This problem is solved by the finite element method with a computer program coded by the second author. In this program the stiffness matrix of the column element is derived by accounting the second order effect of the axial forces.

The column is divided 10 finite elements. Beginning with a selected axial force the numerical value of the determinant of system stiffness matrix is calculated. This axial force value is increased giving an appropriate increment and this determinant is calculated at each step. The resulted axial force is the buckling force when the sign of the value of this determinant changed. All the operations are performed by the program. By this way the buckling force of this column is obtained as 382.6 kN. This value is %0.8 higher than the value obtained by the analytical solution and %6 less than the obtained value by the series solution.

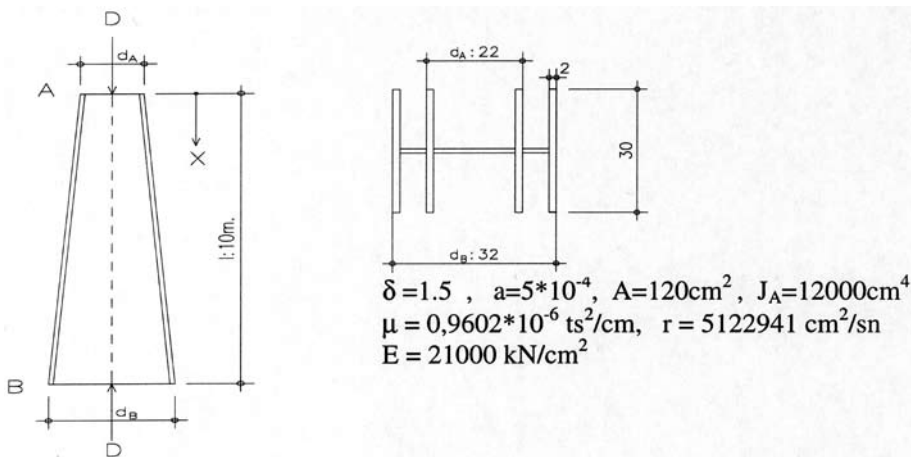


**Figure 1.** The properties of the material and strength of the first example of the steel structure

II – The eigen frequencies of the simply supported steel column given in (Figure 1.) will be determined for the transverse vibration.

The differential equation of motion [NOWACKI (1974)] given as

$$E \frac{\partial^2}{\partial x^2} (J(x) \frac{\partial^2 y}{\partial x^2}) + \mu \frac{\partial^2 y}{\partial x^2} = 0 \quad (20)$$

where  $\mu$  is mass per unit length ( $= A\gamma / g = \text{constant}$ ). By the method of separation of variables,  $y(x, t) = Y(x) e^{i\omega t}$ , the partial differential equation is transformed into an ordinary differential equation as

$$\frac{d^2}{dx^2} (EJ(x) \frac{d^2 Y}{dx^2}) - \mu\omega^2 Y = 0 \quad (21)$$

which can be written in another form

$$[\frac{1}{\mu} \frac{d}{dx} (\sqrt{\mu EJ(x)} \frac{d}{dx}) + \omega] [\frac{1}{\mu} \frac{d}{dx} (\sqrt{\mu EJ(x)} \frac{d}{dx}) - \omega] y = 0 \quad (22)$$

The solution of this equation is

$$Y(x) = C_1 J_0(z) + C_2 Y_0(z) + C_3 I_0(z) + C_4 K_0(z) \quad (23)$$

where  $J_0$ ,  $Y_0$ ,  $I_0$ ,  $K_0$ : The Bessel and modified Bessel functions of the first and second kinds of order zero, and

$$z = 2\lambda\sqrt{1+ax} \quad , \quad \lambda^2 = \omega/(ra^2) \quad , \quad r = \sqrt{EJ_A/\mu} = \text{constant}$$

The four boundary conditions are

$$Y(0) = 0 \quad , \quad EJ(x)Y''(0) = 0 \quad \text{at } x=0 \quad (24)$$

$$Y(l) = 0 \quad , \quad EJ(x)Y''(l) = 0 \quad \text{at } x=l \quad (25)$$

If these boundary conditions are applied to the solution, it comes out a homogeneous equation with the unknowns  $C_i$ . The eigen frequencies are calculated by using a computer software prepared for mathematics from the condition that the determinant of the coefficients matrix must be zero:  $\omega_1 = 61.86 \text{ rad/s}$ ,  $\omega_2 = 249.23 \text{ rad/s}$ , etc.

This problem is solved by the finite element method by using the well known structural analysis program package (SAP90)<sup>[13]</sup>. Dividing the column to ten elements the angular frequencies are obtained as  $\omega_1 = 52.64 \text{ rad/s}$ ,  $\omega_2 = 105.90 \text{ rad/s}$ , etc.

III– As the third application the deflections and the internal forces of a circular plate embedded on elastic foundation subject to vertical central load will be determined.

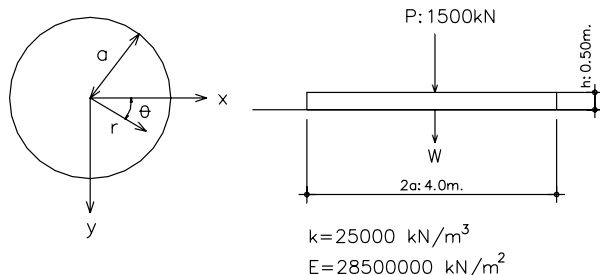


**Figure 2.** The plate, the coordinate system and the loading

The plate, the coordinate system and the loading are shown in Figure 2. The differential equation of the plate in polar coordinate system (Timoshenko (1964)) is

$$D\left(\frac{\partial^2}{\partial r^2} + \frac{1}{r}\frac{\partial}{\partial r} + \frac{1}{r^2}\frac{\partial^2}{\partial \theta^2}\right)^2 w(r, \theta) = q(r, \theta) - k w(r, \theta) \quad (26)$$

where D is the rigidity of the plate and expressed with  $D = Eh^3/[12(1-\nu^2)]$ .

The differential equation will be independent on  $\theta$ , if the loads act axisymmetric. Thus the equation will be

$$D\left(\frac{d^2}{dr^2} + \frac{1}{r}\frac{d}{dr}\right)\left(\frac{d^2 w}{dr^2} + \frac{1}{r}\frac{dw}{dr}\right) = q - kw \quad (27)$$

For the case that the plate is loaded in the center by a concentrated load P, q will be zero, except at the origin, and by using the new variables  $\lambda^4 = D/k$ ,  $z = w/\lambda$ ,  $t = r/\lambda$  the differential equation takes the form as

$$\left(\frac{d^2}{dt^2} + \frac{1}{t}\frac{d}{dt}\right)\left(\frac{d^2 z}{dt^2} + \frac{1}{t}\frac{dz}{dt}\right) + z = 0 \quad (28)$$

or with Nabla or delta operators

$$\Delta \Delta z + z = 0 \quad \text{or} \quad \nabla^4 z + z = 0 \quad (29)$$

The solution of this equation is

$$z(t) = \bar{C}_1 J_0(\sqrt{i} t) + \bar{C}_2 Y_0(\sqrt{i} t) + \bar{C}_3 I_0(\sqrt{i} t) + \bar{C}_4 K_0(\sqrt{i} t) \quad (30)$$

The boundary conditions are

$$\text{i)} \quad M_r = -D \left( \frac{d^2 w}{dr^2} + \frac{1}{r} \frac{dw}{dr} \right)_{r=a} = 0 \quad (31)$$

$$\text{ii)} \quad Q_r = -D \frac{d}{dr} \left( \frac{d^2 w}{dr^2} + \frac{1}{r} \frac{dw}{dr} \right)_{r=a} = 0 \quad (32)$$

iii) The deflection at the center of the plate remains finite.

$$\text{iv)} \quad \int_0^{2\pi} (Q_r r d\theta)_{r=\varepsilon} + P = 0 \quad \text{or} \quad -k\lambda^4 \frac{d}{dr} \left( \frac{d^2 w}{dr^2} + \frac{1}{r} \frac{dw}{dr} \right)_{r=\varepsilon} 2\pi\varepsilon + P = 0 \quad (33)$$

where  $\varepsilon$  is the radius of an infinite small cylinder in the middle of the plate.

Considering the third boundary condition, the solution is written in Thomson's and Kelvin's functions which are obtained by inserting the independent imaginer variable  $\sqrt{i} t$  in the Bessel functions and separating the real and imaginer terms:

$$z(t) = C_1 ber_0 t + C_2 bei_0 t + C_3 kei_0 t \quad (34)$$

where

$$ber_0 t = \sum_{k=0}^{\infty} \frac{(-1)^k t^{4k}}{2^{4k} [(2k)!]^2} \quad (35)$$

$$bei_0 t = \sum_{k=0}^{\infty} \frac{(-1)^k t^{4k+2}}{2^{4k+2} [(2k+1)!]^2} \quad (36)$$

$$kei_0 t = \text{Int.} bei_0 t + \sum_{k=1}^{\infty} \frac{(-1)^k t^{4k-2}}{2^{4k-2} [(4k-2)!]^2} \sum_{n=1}^{2k-1} \frac{1}{n} \quad (37)$$

by using the remaining boundary conditions, the unknown coefficients  $C_1, C_2, C_3$  are determined.

The entire operations have been programmed by using a computer software prepared for mathematics<sup>[6]</sup>.

Comparison of the deflections which are calculated by the method given in this paper and the finite element method is given in Figure 3. In the finite element method, due to axial symmetry the plate is considered as one dimensional element in the radial direction. A finite element program written for this purpose is given in<sup>[14]</sup>. In this way 20 finite elements embedded on elastic foundation is considered.

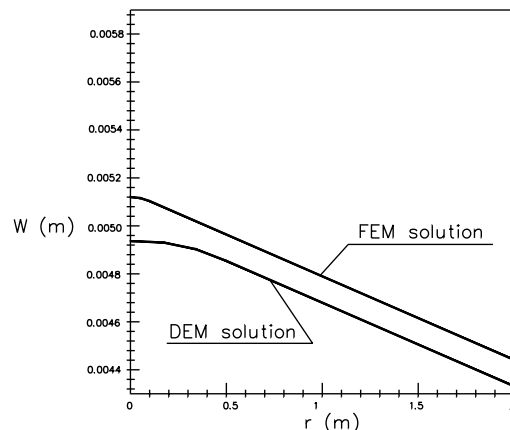


**Figure 3.** Comparison of the deflections which are obtained by the FEM and the dif.eq. method

IV – A fluid (wind) with a velocity 50 km/h flows uniformly over a spherical dome having a radius 5 m. The upstream pressure and temperature are equal to those inside the dome. The upward force on the dome will be estimated.

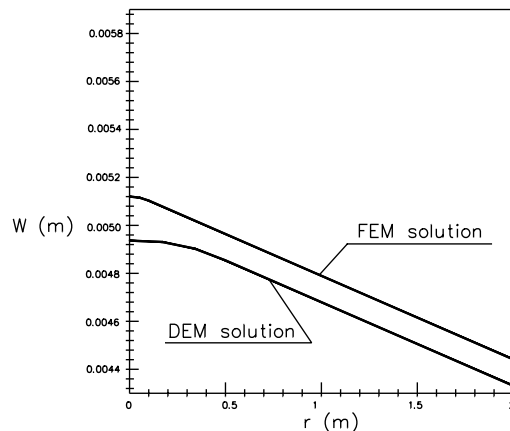


**Figure 4.** An uniform fluid acting on a spherical dome ( $\rho = 1.225 \text{ kg/cm}^3$ )

The velocity potential function,  $\Phi$ , satisfies the Laplace equation. This equation is written in spherical coordinates as<sup>[12]</sup>

$$\Delta\Phi = \frac{1}{r^2} \frac{\partial}{\partial r} \left( r^2 \frac{\partial^2 \Phi}{\partial r^2} \right) + \frac{1}{r^2 \sin\theta} \frac{\partial}{\partial\theta} \left( \sin\theta \frac{\partial\Phi}{\partial\theta} \right) + \frac{1}{r^2 \sin^2\theta} \frac{\partial^2 \Phi}{\partial\varphi^2} = 0 \quad (38)$$

The velocity components are:

$$V_r = \frac{\partial\Phi}{\partial r} \quad (39)$$

$$V_\theta = \frac{1}{r} \frac{\partial\Phi}{\partial\theta} \quad (40)$$

$$V_\varphi = \frac{1}{r \sin\theta} \frac{\partial\Phi}{\partial\varphi} \quad (41)$$

The velocity field satisfies the boundary conditions:

$$V_r = 0 \quad \text{at} \quad r = R \quad (42)$$

$$V_r = V_\infty \sin\theta \sin\varphi \quad \text{at} \quad r \rightarrow R \quad (43)$$

$$V_\varphi = V_\infty \cos\varphi \quad \text{at} \quad r \rightarrow R \quad (44)$$

The solution of the equation by the method of separation of variables,  $\Phi(r,\theta,\varphi) = P(r)\Psi(\theta)\Omega(\varphi)$ , gives three ordinary differential equations:

$$\Omega''(\varphi) + m^2\Omega(\varphi) = 0 \quad (45)$$

$$r^2 P''(r) + 2rP'(r) - n(n+1)P(r) = 0 \quad (\text{Euler differential equation}) \quad (46)$$

$$\sin^2\theta\Psi''(\theta) + \sin\theta \cos\theta\Psi'(\theta) + [n(n+1)\sin^2\theta - m^2]\Psi(\theta) = 0 \\ (\text{Associated Legendre eq.}) \quad (47)$$

The solutions of this equation give

$$\Phi(r,\theta,\varphi) = \sum_{n=0}^{\infty} \left( a_n r^n + \frac{b_n}{r^{n+1}} \right) \sum_{m=0}^n P_n^m(\cos\theta) [A_{nm} \cos m\varphi + B_{nm} \sin m\varphi] \quad (48)$$

where  $P_n^m(\cos\theta)$  is Legendre polynomial. By using the boundary conditions, and for  $m=n=1$  the velocity potential is obtained as

$$\Phi = V_\infty \left( r + \frac{R^3}{2r^2} \right) \sin\theta \sin\varphi \quad (49)$$

If the Bernoulli equation is applied adjacent to the surface of the sphere where  $V_r = 0$ , it is written

$$\frac{p_\infty}{\rho} + \frac{V_\infty^2}{2} = \frac{p_s}{\rho} + \frac{V_\theta^2}{2} \quad (50)$$

from which it is obtained

$$p_s - p_\infty = \frac{\rho V_\infty}{8} [4 - 9 \cos^2 \theta \sin^2 \theta] \quad (51)$$

The upward force is calculated by integration of the pressure over the surface as

$$L = \int_s (p_s - p_\infty) \vec{n} \cdot \vec{k} ds = \rho \frac{V_\infty^2}{8} \int_0^{2\pi} \int_0^{\pi/2} (4 - 9 \cos^2 \theta \sin^2 \theta) \cos\theta R^2 \sin\theta d\theta d\varphi = \frac{7\pi\rho R^2 V_\infty^2}{32} \quad (52)$$

where  $ds$  is surface element,  $\vec{k}$  and  $\vec{n}$  are unit vectors in the z axis and perpendicular to the surface. In this calculation it is assumed that the shear force  $\tau_w = 0$ . For the given numerical values, this force is calculated as 40.6 kN.

## RESULTS AND CONCLUSIONS

In this paper four applications from the fields of structural and mechanical engineering, stability, dynamic, theory of plates and fluid mechanics are solved. In all applications, firstly, the differential equations and boundary conditions are given. From this point of view, these equations are considered as Sturm-Liouville equations.

In the first application, the buckling load of a simply supported steel column with vari-

able cross-section are calculated. The Euler differential equation is transformed into the linear differential equation with constant coefficients by changing of variable, and this equation is solved by applying the power series to demonstrate the usage and practicality of the method.

In the second application, the eigen frequencies for the transverse vibration of the column given in the first application are calculated. The partial differential equation of motion is transformed into an ordinary linear dif-

ferential equation of the fourth order whose solution is given by the Bessel functions. The eigen frequencies are calculated from the determinant of the coefficients matrix by using a computer software prepared for mathematics which has generally higher trancendant functions in its files.

In the third application, the deflections and the internal forces of a circular plate embedded on an elastic foundation and subject to a single load in its centre. Because of the circular symmetry of the plate, the partial differential equation of the plate reduces to the ordinary linear differential equation of the fourth order with variable coefficients. The solution of this equation is given under consideration of the boundary conditions in Thomson's and Kelvin's functions. The

whole operations have been performed by using a computer software. The deflections of the plate obtained by the series solution method are compared with the deflections obtained by the finite element method.

The last application belongs to a problem of fluid mechanics. The solution of the Laplace equation of velocity potential function written in spherical coordinates by the method of separation of variables gives three ordinary linear differential equation, Euler's differential equation and Legendre equation; the solutions of these equations give the potential function. The upward force is obtained by applying the Bernoulli equation and then integrating the pressure over the surface of the spherical dome.

## APPENDIX

### Notations

$a_m$	Coefficients in the series expansions
$C_i, \bar{C}_i$	Indefinite coefficients in the solution of the differential equations
$ds$	Surface element
$D$	Constant or longitudinal load
$E$	Modulus of elasticity
$g$	Acceleration of gravity
$i$	Imaginary unit
$J_0, Y_0, I_0, K_0$	Bessel, modified Bessel functions of first and second kinds of order zero
$J(x)$	Variation of the moment of inertia as a function of $x$
$J_A$	Moment of inertia at cross-section A
$k$	Modulus of subgrade reaction, real number, unit vector
$m, M, n$	Real numbers, unit vector perpendicular to the surface
$M_r$	Moment
$p_s$	Pressure of the fluid
$p_0, q_0$	Coefficients in the series expansions
$q(r, \theta)$	Lateral load
$Q_r$	Shear force

r	Exponent in the series expansions
R	Radius of convergence
t	Time, independent variable
T	Temperature of the fluid
$V_r, V_\theta, V_\phi$	Velocities in the radial, longitudinal and latitudinal directions
w	Deflection
Y(x)	Amplitude
x,y,z	Dependent and independent variables
$\gamma$	Density of the steel per unit volume
$\Gamma$	Gamma function
$\Delta$	Delta operator
$\nabla$	Nabla operator
$\mu$	Mass per unit length
v	Poisson's ratio
$\rho$	Density of the fluid
$\omega$	Angular frequency

## REFERENCES

- [1] WYLIE CR,BARRET LC .,1985,Advanced Engineering Mathematics, Mc.Graw – Hill, International Edition,pp.562-638.
- [2] KREYSZIG E.,1993,Advanced Engineering Mathematics, John Wiley and Sons Inc., pp.197-260.
- [3] AYRES F.JR.,1952,Theory and Problems of Differential Equations, Schaum's Outline Series, Mc.Graw-Hill Book Comp.,pp.197-230.
- [4] RICHTER EW.,1968,Höhere Mathematik für den Praktiker,Johann Ambrosius Barth, Leipzig, pp.375-388 and 404-409.
- [5] KOÇAK C.,1983,Higher Mathematics (in Turkish), Library of Istanbul Technical University,pp322-404.
- [6] Mathematica, a system for doing mathematics by computer. Addison-Wesley.
- [7] PC-Matlab for MS-DOS Personal Computers.,Version 4.1-PC,The Math. Works Inc.
- [8] PETERSEN C.,1980,Statik und Stabilität der Baukonstruktionen, Friedr. Wieweg and Sohn.,pp.446-459.
- [9] INAN M.,1965,Strength of Materials (in Turkish),Library of Istanbul Technical University pp.521-526.
- [10] NOWACKI W.,1974,Baudynamik, Springer Verlag,pp.166-172.
- [11] TIMOSHENKO S.,1964,Theory of Plates and Shells (translated in Turkish), Library of Istanbul Technical University, pp.244-273.
- [12] GERHART PM.,GROSS R.J. AND HOCHSTEIN J.I.,1993,Fundamentals of Fluid Mechanics, Addison-Wesley Publ.Company,pp.584-749.
- [13] SAP90 (Structural Analysis Program), 1990, Habibullah A.,Wilson E.L.
- [14] AYDOĞAN M., 1997, The Analysis of the Common Shell of Revolution-Circular Plate Systems, Prof.Dr.R.Yarar Symposium, Turkish Earthquake Foundation Publ.,Vol.1, pp.365-377,Istanbul,Turkey.
- [14] SAP90 (Structural Analysis Program), 1990, Habibullah A., Wilson E.L.



## Zbirka ulitkov profesorja Milana Trbižana

### Castings collection of professor Milan Trbižan

KATARINA TRBIŽAN<sup>1</sup>, RADOMIR TURK<sup>2</sup>, MIRKO JUTERŠEK<sup>3</sup>,  
REINHARD DÖPP<sup>4</sup>, BOŠTJAN ŽEKŠ<sup>5</sup>, MILAN TRBIŽAN<sup>2</sup>

<sup>1</sup>Inštitut ISC d.o.o., Dunajska 186, 1000 Ljubljana, Slovenija

E-mail: institut.isc@t-2.net

<sup>2</sup>Naravoslovnotehniška fakulteta, Aškerčeva 12, 1000 Ljubljana, Slovenija

E-mail: rado.turk@ntf.uni-lj.si; milan.trbizan@ntf.uni-lj.si

<sup>3</sup>Martinova pot 13, 1000 Ljubljana, E-mail: mjutersek@volja.net

<sup>4</sup> Tehnična Univerza Clausthal, Robert-Koch-Straße 42, D-38678 Clausthal-Zellerfeld

E-mail: giessereitechnik@tu-clausthal.de

<sup>5</sup>Slovenska akademija znanosti in umetnosti, Novi trg 3, 1000 Ljubljana, Slovenija

E-mail: sazu@sazu.si

Received: September 21, 2006

Accepted: October 20, 2006

**Izvleček:** Dne 21. junija 2006 je bila v prostorih Oddelka za materiale in metalurgijo Naravoslovnotehniške fakultete Univerze v Ljubljani, Lepi pot 11, odprta stalna razstava »Zbirka ulitkov profesorja Milana Trbižana«. Uvodni govor je imel dekan Naravoslovnotehniške fakultete in predstojnik Oddelka za materiale in metalurgijo prof. dr. Radomir Turk, zbirko je ocenil umetnostni zgodovinar prof. dr. Mirko Juteršek, v imenu Tehnične Univerze v Clausthalu je govoril prof. dr. Reinhard Döpp, sledil je kratek nagovor avtorja zbirke prof. dr. Milana Trbižana, poglobljeno oceno je na zaključku podal predsednik Slovenske akademije znanosti in umetnosti akademik prof. dr. Boštjan Žekš, ki je tudi otvoril razstavo.

**Abstract:** On 21st June 2006 was at Department for Materials and Metallurgy, Faculty of Natural Sciences and Engineering, University of Ljubljana, Lepi pot 11, opened permanent exhibition »Casting collection of Professor Milan Trbižan«. Introductive speech had dean of Faculty of Natural Sciences and Engineering and principal of Department for Materials and Metallurgy Prof. Dr. Radomir Turk, the collection estimated art historian Prof. Dr. Mirko Juteršek, in the name of Technical University Clausthal spoke Prof. Dr. Reinhard Döpp, following had short speech author of collection Prof. Dr. Milan Trbižan, deep estimation gave at the end president of Slovenian Academy of Sciences and Arts Academician Prof. Dr. Boštjan Žekš, who also opened the exhibition.

**Ključne besede:** zbirka, umetniški ulitki, donacija, mednarodno sodelovanje

**Key words:** collection, art castings, donation, international collaboration

## Uvod

KATARINA TRBIŽAN, UNIV. DIPLO. INŽ.

Prisotnih je bilo nad 110 udeležencev, med njimi je bilo več delegacij iz tujine, najbolj številna je bila iz Nemčije, saj je bilo samo iz TU Clausthal sedem profesorjev pod vodstvom bivšega rektorja prof. dr. G. Müllerja in podpredsednice dr.-inž. Schwarz, češko livarstvo je zastopal doc. dr. J. Roučka iz TU Brno, generalni sekretar Avstrijskega društva livarjev in urednik Giesserei Rundschau dipl.-inž. E. Nechtelberger, hrvaško prof. dr. F. Unkić iz Sveučilišta u Zagrebu in predsednik Hrvatskog Udruženja za ljevarstvo mag. M. Galič, medtem ko se poljska delegacija odprtja zaradi drugih obveznosti ni mogla udeležiti.

Razstavni eksponati so donacija umetniških in okrasnih ulitkov, ki jih je avtor prejemal več desetletij kot priznanja za delovanje v različnih forumih, za predavanja na jubilejnih kongresih ali kot osebna darila. Takih eksponatov je v zbirki največ in posredujejo zapis o strokovni povezanosti livarjev Slovenije s svetom. Drugi sklop predstavljajo stvaritve domačih avtorjev, ki so nastale na pobudo Katedre za livarstvo, ko je bilo potrebno predstaviti in obeležiti posebne dogodke, npr. ob ustanovitvi samostojne države.

Odločitev o donaciji te osebne zbirke ni bila težka, saj je bila podprta s strani Oddelka za materiale in metalurgijo in Naravoslovnotehniške fakultete, predvsem dekana prof. dr. R. Turka. Z njo predstavlja Fakulteta lивarsko in metalurško stroko na povsem drugačen način: umetniško oblikovana ulita kovina trajno sporoča o lepoti, ki si jo je zamislil ustvarjalec in dovršeno izvedel livar.

Poleg eksponatov so razstavljeni tudi panoji s tremi izstopajočimi dosežki na področju umetniškega litja v preteklih 300 letih. V prvi vrsti gre za pogosto prezrto delo J. V. Valvazorja na področju livarstva. Na kratko nekaj podatkov: Leta 1681 je ulil 2,5 m visok kip Marije v enem kosu s tanko steno, ki se nahaja pred cerkvijo sv. Jakoba v Ljubljani. Nato je leta 1687 v Philosophical Transactions, glasilu angleške akademije Royal Society, objavil članek o litju tankostenskih kipov, ki je prvi slovenski tehnični dokument in je pomemben prispevek k razvoju livarstva. V istem letu je postal tudi član Royal Society. Razvoj litja tankostenskih ulitkov se je torej začel že tedaj in je enako aktualen še danes. Prispevek Valvazorja na področju livarstva je premalo poznan in naloga stroke je, da ga uveljavi kot pomemben del kulturno-tehnične identitete Slovenije.

Drugi pano podaja prispevek Železarne in železolivarne na Dvoru pri Žužemberku (1795 - 1891) pri razcvetu umetniškega litja železove litine v prvi polovici 19. stoletja v tedanji Avstroogrski monarhiji in Nemčiji. Ulivali so okrasne krožnike in predmete, s katerimi so se enakovredno vključevali med tedanje vodilne livarne, po lastnih osnutkih pa so ulivali tudi spomenike, grbe in ploše. Ker je Železarna leta 1891 v celoti prenehala delovati, ne da bi se ohranil vsaj del proizvodnje, se je v nasprotju z drugimi tedanjimi livenami ohranilo le malo ulitkov, modeli pa so se v celoti izgubili. Zato ti dosežki niso postali, tako kot v drugih državah, del nacionalne identitete, na katere opozarjajo z reprodukcijami v obliki visokovrednih daril. Najbolj značilno se to vidi pri razstavljenih okrasnih krožnikih iz prve polovice 19. stoletja, ki izvirajo iz štirih držav nekdanje Avstroogrške monarhije, medtem ko ostajajo domači unikatni eksponati nepoznani.

Le po zaslugi nekaterih zgodovinarjev, ki so opisovali Dvor pri Žužemberku, je danes Železarna prikazana v tuji literaturi kot ena tedaj vodilnih. Z reprodukcijami kot tudi z lastnimi kreacijami, predvsem pa s povsem enakovredno tehnično dovršenostjo okrasnih in umetniških ulitkov, se je vključevala v te danje umetniške trende pri ulivanju železove litine. To gibanje, ki se je nenavadno hitro razširilo najprej po Nemčiji, nato pa še po Avstroogrski monarhiji, je v obdobju med 1820 in 1860 doseglo po kakovosti ulitkov iz litega železa zaenkrat še nepresežen vrhunec. Zaradi vojn z Napoleonom tedaj ni bilo na razpolago brona, zato je mogoče, da je na kontinentu ravno to vzpodbudilo razvoj kupolk, ki so omogočile kakovostno pretaljevanje že pridobljenega železa, ki je bil dotedaj prvenstveno namenjeno za kovanje jekla na fužinah. Lito železo iz kupolk ima evtektično sestavo z bistveno več ogljika, posledica je neprimerno nižje tališče in odlična livnost. Na ta način je bila talina vedno dosegljiva, ne samo kot dotedaj ob kampanijah na fužinah. Za arhitekte je pomenilo lito železo z značilno črno barvo, ki je omogočilo litje zelo tankih sten z debelino celo samo 2 – 3 mm, nov izziv in novo področje ustvarjanja. Da bi čim bolje spoznali in izkoristili njegove prednosti, so se poglabljali v tehniko izdelave lивarskih modelov, lивarsko tehnologijo, cizeliranje in površinsko obdelavo litoželeznih ulitkov. Seveda je bilo litje železove litine poznano že več kot dva tisoč let preje, vendar ne v tako razširjeni obliki ter v taki umetniški in tehnološki dovršenosti. Nastali so litoželezni paviljoni in cerkve, spomeniki, okrasne ograje, okrašene peči, nagrobni križi, okvirji za zrcala in še vrsta drugih predmetov. Okoli leta 1860 je ta trend sicer pričel ponehavati, ohranila pa se je močna tradicija, ki pa jo je

pri nas potrebno še oživiti in ji v naši javnosti dati svoje mesto.

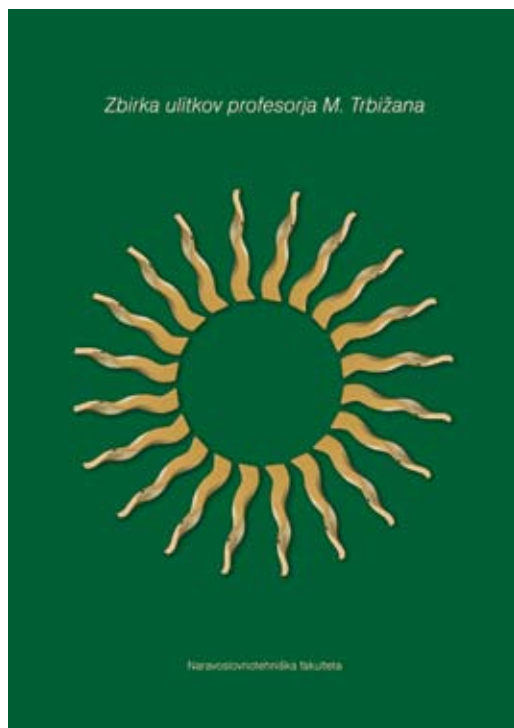
Tretji pano prikazuje liveno zvonov družinskega podjetja Samassa (1767 - 1917), ki je z mednarodno uveljavljenostjo ravno tako presegala tedanje državne meje in je pri nas nekoliko bolj poznana. Leta 2004 so v Italiji izdali o njej brošuro z bogatim slikovnim materialom, v strokovnem komiteju je sodeloval tudi dr. M. Žargi kot predstavnik Narodnega muzeja v Ljubljani; tekst, ki je sicer v italijanskem, je preveden tudi v slovenski in furlanski jezik.

## RAZSTAVNI KATALOG

KATARINA TRBIŽAN, UNIV. DIPLO. INŽ.

Panoji so le povzetek opisov iz uvodnega dela kataloga, ki je izšel ob odprtju razstave na 138 straneh, njegov osrednji del je namenjen predstavitvi posameznih eksponatov (65 umetniških in okrasnih predmetov, 9 miniaturnih portretov znamenitih Slovencev ter 35 medalj in plaket). Obsežno in zahtevno uredniško delo skupaj s fotografijami in zamudnim zbiranjem podatkov je prevzela Katarina Trbižan, univ. dipl. inž. O vsakem eksponatu so zbrani podatki, kot: naziv, podatki o avtorju, liveni, v kateri je bil ulit original in reprodukcija, dimenzijski ulitka, liveni material, postopek litja in darovalec. Ker je večina darovalcev iz tujine, so podatki v dveh jezikih, v slovenščini in angleščini. V predgovorih sta katalog ocenila prof. dr. R. Turk kot dekan Naravoslovnotehniške fakultete s stališča metalurške in livenke stroke ter univerze, v drugem predgovoru je umetnostni zgodovinar prof. dr. M. Juteršek podal vsebinski vidik in kategorizacijo zbirke.

V uvodnem delu so opisani tudi tehnološki postopki litja umetniških ulitkov, ki so bili poznani tudi na prostoru Slovenije, le nekateri od njih so bili na osnovi najnovejšega razvoja bistveno izboljšani. Povsem so opuščeni postopki z uporabo glinastih peskov, ki so zahtevali večdnevno sušenje. Vendar se pri tem pozablja, da so tedaj ulivali v sušene forme, ki so bile ogrete na 300 °C in popolnoma brez vlage, to pa je izboljšalo livnost. Zato lahko nekatere tankostenske ulitke izdelujemo danes le z bolj zahtevnimi tehnološkimi postopki.



**Slika 1.** Razstavni katalog; na naslovniči je kompozicija žarkov akademskega kiparja Tomaža Kolariča  
**Figure 1.** Exhibition catalogue; on the title page is composition of sunbeams by academic sculptor Tomaž Kolarič

## OTVORITVENI GOVOR

PROF.DR.RADOMIR TURK, DEKAN NARAVOSLOVNOTEHNIŠKE FAKULTETE

Zbirka ulitkov prof. Trbižana, ki jo danes otvarjam, ima več pomenov. Je del izdelkov metalurgije širšega evropskega prostora, je plod sodelovanja eksperta - livarja pri tehniški realizaciji zamisli umetnika, je spomin na nešteta mednarodna znanstvena in strokovna sodelovanja strokovnjakov - livarjev, in kjer je bil prof. Trbižan izjemno ploden, govorí o visoki tehnološki strokovnosti slovenskih livarjev ter opozarja na več kot 300 letni kulturno-tehnični dokument o tradiciji livarstva in metalurgije na Slovenskem. Imamo malo znanstvenih člankov, ki bi na takoj visokem nivoju že v času Valvazorja, seveda pa po njegovi zaslugi, seznanjal angleško akademijo Royal Society o litju tankostenih ulitkov v Ljubljani. Ne nazadnje, zbirka bo ostala v teh naših prostorih, t.j. prostorih Oddelka za materiale in metalurgijo Naravoslovnotehniške fakultete Univerze v Ljubljani v nagovor mlajšim generacijam, da je izbira poklica življenjska odločitev, kjer se združujejo tako razumski, kot tudi duhovni potenciali človekove celovitosti. In to ta stroka gotovo je.

Da bi razumeli pomen celovitosti, je treba iti časovno daleč nazaj.

Odločajoč pohod človeka se je pričel, ko se je naučil oblikovati materijo. Več kot deset tisoč let ta proces že poteka in mu ni videti konca. Pričel se je spontano in skoraj sočasno na treh, povsem ločenih predelih modrega planeta, na bližnjem vzhodu, na severu Kitajske in visoko v goratih Andih. Pohod časovno pridobiva eksponentno na dinamiki in postaja vse bolj neobvladljiv. Danes je globaliziran, v vsak, še tako zakotni



**Slika 2.** Različne upodobitve sv. Barbare – zaščitnice montanistov

**Figure 2.** Different designs of St. Barbara – patroness of miners and metallurgists



**Slika 3.** Pogled na sklop z okrasnimi krožniki, večina izvira iz 19. stoletja

**Figure 3.** View to ornamental plates, most of them from 19th century

del, lahko seže katerakoli informacija v trenutku. To je vsekakor zasluga neslutenega razvoja materialov. Je pa zato postal svet tudi ranljiv kot še nikoli poprej.

V ospredju tega razvojnega pohoda je že v samem začetku izstopal kovač. Prvotno je združeval vse, bil je talivec, livar, oblikovalec. Bil je umazan, prepoten. Stvari,

ki jih je počel, pa so bile uporabne in lepe. Posedoval je tudi moč bogov, spreminjal je naravo substance. Spreminjal je brezoblično kamenino v bleščečo kovino. Po lastni volji jo je utekočinjal ali strjeval, ji dal togost ali pa jo napravil kovno. Metal je ljudi fasciniral, hkrati je bil skrivnosten. Grški filozofi so se spraševali, kaj se s kovino dogaja, ko jo kovač segreje. Prišli so na atomistično predstavo. Ostali, manj zainteresirani na filozofiji, so kovino enostavno občudovali in uporabljali, in z njeno uporabo so ustvarjali to, čemur danes rečemo civilizacija. V začetku so oblikovali predmete, ki so jih že poznali, kasneje so oblikovali orodja za kmetovanje, lonce za kuho, orožje za vojne in nakit za religiozne in slavnostne namene.

Rezultati uporabe kovin so bili presenetljivi. Njihova vloga in nasploh vloga tehnike na razvoj človeka je premalo znana in ni ovrednotena. Priče tehničnega razvoja tega niso spremljale in zapisale z besedami. Shranjen je le v ohranjenih objektih in predmetih. Pa še v teh tega vselej ne prepoznamo. Današnja znanost mora vse to šele rekonstruirati, analizirati in smiselno povezati.

Vsekakor pa že vemo, da človek kovine ni odkril zato, da bi z njo nadomestil kameno orodje, da bi zato imelo orodje boljše lastnosti. Kovina se je pojavila v zavesti človeka zaradi človekove umetniške senzibilnosti, ko je pred tisoči let postal pozoren na lep kamen. Ne glede na to, da je kasneje industrijska revolucija razvila gromozanske industrije, da so kovine v začetku vplivale skoraj na vsako fazo človekovega razvoja, pa so do približno pred dvesto leti, ena za drugo nastajale nove metode oz. tehnologije oblikovanja kovin skorajda vedno iz umetniško dekorativnih vzgibov.

Mnogo tisoč let zatem, ko je človek že koško hladno preoblikoval kovine, je odkril moč ognja za zmehčanje kovine in njeno lažje preoblikovanje. Navdih iznajdljivosti in racionalnosti ga je cca 3000 do 3500 p.kr. vodil do ulivanja predoblik, te tehnike je izpopolnjeval in nekatere kot npr. precizno litje s pomočjo voščenih modelov, ki so še danes zelo uporabne, je uporabil za oblikovanje nesmrtnih umetniških del. Omenil sem že, da tovrstni postopki niso bili v davnini zavestno zapisani, je pa človeško opravilo slikovno vklesano v kamnite bloke, je priča v obliki podob, ki so vžgane v glineno posodje. Mnogi najdeni predmeti so prave umetnine in priča razvite tehnike obdelave in predelave kovin skozi tisočletja. Knjige zaenkrat še niso zakladnica razumevanja vseh tehničnih postopkov davnine, so pa muzeji in nekatere zbirke pravi zakladi, ki še čakajo na znanstveno metalurško in arheološko razlago.

Šola, posebno še univerza, lahko tu stori mnogo. Same informacije in togo sklepanje še niso garancija za snovanje novih materialov, novih izdelkov in tehnologij. Razvijati je potrebno intuicijo tistih odločitev, ki so človeka varno vodile v njegovem razvoju tisočletja, brez škode na rušenje okolja, kot npr. nizkotemperature tehnologije, ponovna uporaba materiala ipd. Tu pa se imamo kaj učiti iz preteklosti. In tudi ta zbirka je zato izziv.

Prof. dr. Milanu Trbižanu, našemu rednemu profesorju livarstva, se zahvaljujem, ne le za širokogrudnost pri snovanju, postavitvi in podaritvi zbirke, pač pa za jasno sporočilo, ki ga predaja na mlajše in bodoče pedagoške delavce in metalurške inženirje, kar je tudi temelj prenove univerzitetnih izobraževalnih

programov po bolonjskih načelih, t.j. da je bodoči intelektualce osebnost s kompetenčami, ki združujejo znanje, kreativnost in podjetnost, ter ob uporabnem tehničnem znanju tudi širino humanista - svetovljana.

## KAKO JE ZBIRKA NASTALA IN NJENO

### MESTO V LIKOVNI UMETNOSTI

PROF.DR.MIRKO JUTERŠEK

-UMETNOSTNI ZGODOVINAR

Obstojijo najrazličnejše zbirke iz vseh mogočih področij in v vseh razberemo neko preteklost, tudi med tistimi, ki segajo v naš čas. Sedanjosti in naših dni se dotika tudi zbirka ulitkov profesorja Milana Trbižana, ki bo od današnje predaje javnosti stalno na ogled na Oddelku za materiale in metalurgijo Naravoslovnotehniške fakultete Univerze v Ljubljani.

Najprej bi rad opozoril, da sestavlja zbirko ulitki, ki so nastali večinoma namensko ob raznih strokovnih srečanjih livarjev in z njimi povezanih strok. V zbirko vključeni predmeti so nastali v znak pozornosti in bili izročeni udeležencem iz vidika spoštovanja svojim kolegom pa tudi ponosa darovalcev v dokaz o njihovih lastnih organizacijskih in livaarskih zmožnostih.

Ulitke, pridobljene ob raznih priložnostih, vsi niso tako z veseljem shranjevali, kot je to počel profesor Milan Trbižan. Tovrstno zbiranje ulitkov odraža pri njem predvsem zanimanje za stroko in seveda tudi spoštovanje do kolegov in vseh, ki so povezani z livaarstvom. Vsak v razstavo vključen predmet ima svojo zgodbo. Po svoje odraža tudi povezavo Milana Trbižana s številnimi priatelji, kolegi in znanci, strokovnjaki s področja livaarstva številnih evropskih dežel.

Milan Trbižan se je že na kamniški gimnaziji usmerjal v metalurško stroko, tako kot jaz v umetnost! Dolgo osemletno šolsko tovarištvo in nazadnje še izbirni maturitetni izpit iz kemije je prijateljstvo med nama le še utrdilo. Pri medsebojnem zanimanju za najino delo mi je njegova poklicna predanost nenehno vzbujala spoštovanje. Ni bilo kovinskega predmeta, kot so ulite ograje, pokrovi jaškov, kandelabri in podobni predmeti iz bližnjega okolja, da mu Trbižan ne bi posvetil vsaj kanček strokovne pozornosti. Pri tem je zanimivo, da za obliko in zunanjo podobo teh kovinskih ulitkov, ki je predvsem mene zanimala, ni bil gluh.

Spomnim se, kako mi že v začetku sedemdesetih let ni bilo vseeno, ko je z zanimanjem sprejel moje visoko mnenje npr. o slikarju, zdaj vodilnem profesorju na likovni akademiji Emeriku Bernardu, se pravi v času, ko umetnostna stroka še ni hotela vedeti zanj. Pritegnilo me je tudi njegovo občudovanje in s tem povezano hranjenje slikovitejših livaarskih modelov, posebno iz peska narejenih livaarskih jeder. Občudoval je njihovo zanimivo, z votlimi prostori povezano obliko. Iz estetskega vidika je livaarske modele, predvsem jedra upošteval tudi kot del opreme svojega kabineta in to veliko preden so se slovenski umetniki in teoretički v likovnem ustvarjanju pričeli navduševati nad programskim postavljanjem t.i. prostorskih instalacij in performansov. Trbižanovo občudovanje form iz livaarskega sveta je v nečem mogoče primerjati z likovno dejavnostjo, hočem le opozoriti na njegov odnos in občutljivost do nevsakdanjega okolja, ki mu ga je nudilo livaarstvo. Želim le opozoriti na odprtost in sprejemljivost Milana Trbižana do vsega, kar je kdo ustvaril v livaarstvu.

Zbirka ulitkov je bila zanj torej privlačna kot rečeno tako iz spominskega kot tudi strokovnega vidika, in ne nazadnje tudi nam predstavlja dokument dosežkov in raven ulivanja. Zgovorni so pa tudi iz povsem oblikovno umetniškega vidika. Ko so v zadnjih letih njegovi strokovni kolegi spoznali, kaj mu ulitki pomenijo, so mu s še toliko večjo pozornostjo poklanjali tovrstne predmete.

Ideja, da bi te ulitke Milan Trbižan poklonil fakulteti, kot zaključeno osebno zbirko, je dozorevala počasi do odločitve, ko je končno odkril smisel in pomen svojega s stroko povezanega zbiranja.

Fakulteta se je hitro odločila in sprejela njegovo ponudbo, saj z zbirko ulitkov posreduje enkraten dokument o njihovi strokovni povezanosti z livarstvom v svetu v obliku, ki nekaj velja le kot celota, kot nek določen časovni izsek iz njihove pedagoške in praktične dejavnosti. Zbirka ne propagira posameznih ulitkov, na način drugih številnih zbirk v svetu in tudi v Sloveniji. Opozarja na vključnost fakultete in njihovih učiteljev v stroko, hkrati pa odseva v zbirki tudi strokovna raven livarstva, v bronu in sivi litini na primerih umetniško zanimive male plastike.

Zbirko ulitkov spreminja razstavni katalog, glede na vsebino pa so ulitki urejeni po sklopih.

Zaradi tesnejše vsebinske povezanosti z livarstvom bi kot posebno zanimivost lahko izpostavili kiparske upodobitve sv. Barbarre kot zaščitnice rudarjev. V zbirki je več upodobitev te svetnice. Barbari s krono na glavi in stolpom ob nogah ter z metalurškim simbolom, kladivom in kleščami, sta na-

stali pred kratkim in sta umetniški izdelek kiparja Jureta Smoleta, učitelja – tehnologa livarstva na Akademiji likovnih umetnosti v Ljubljani.

Med malo plastiko s področja figuralike so tesneje z livarstvom povezani mali kipci livarjev s težkimi posodami za ulivanje taline v rokah. Po izgledu teh težakov, po izdelanosti, obliki, mdr. stilizaciji, lahko ugotavljamo čas njihovega nastanka.

S praktičnim namenom, se pravi igri, so bile v zbirko ulitkov vključene male, v 19. stoletju nastale, šahovske figure iz jeklene litine, katerih originalni primerek je hrانjen v graškem Joaneum muzeju v Avstriji, praktični predmeti so še zvonci, posoda in svečniki.

Poseben niz sestavlja upodobitve živali. V primerih lahko prepoznamo privlačne in simpatične ulitke male plastike, ki so izdelani v raznih stilih 19. in 20. stoletja, od realističnega prikaza živali kot so npr. v umetnosti pogosto skozi tisočletja najrazličnejše upodobljeni levi in bizoni, do moderno, stiliziranih in shematisiranih podob sov, simbola učenosti, v našem primeru vsi v velikosti namiznih obtežilnikov.

V sklop figuralne plastike z moderno oblikovanim ženskim torzom ali ekspresionistično poenostavljeno čepečo ženo postavimo lahko tudi niz miniaturnih portretnih upodobitev slovenskih znamenitih mož, izdelke kiparja Mihe Kača. Sem lahko uvrstimo tudi sodobno oblikovano skledo, okrašeno z odtisom prave slovenske oziroma idrijske čipke.

V zbirki je še nekaj okrasno uporabnih ulitih predmetov, od velikih ploščatih krožnikov

z renesančno motiviko do po videzu čipkasto lahkočnih krožnikov 19. stoletja, ko so nekatere ulivali tudi pri nas na Dvoru pri Žužemberku.

Umetnostno zanimiva je še serija medalj in plaket, posamično prave mojstrovine medaljerstva v svetu, ulite, a včasih podobne kovanim novcem. Med moderno oblikovanimi predmeti s simbolno vsebino pa zasluži še posebno pozornost na naslovnici kataloga upodobljeno kovinsko sonce s plamenastimi žarki kiparja Tomaža Kolariča. Posamezne žarke so ponesli v svet kot spomin na strokovno srečanje ob osamosvojitvi Slovenije strokovni kolegi, in tudi »botri« pričajoče zbirke ulitkov!

Ob predaji besede drugim lahko le še zaželim, da bi zbirka doseglja svoj namen tako med študenti fakultete kot tudi krepitvi skupne samozavesti v livaški stroki, ki se že ponaša z bogato tradicijo.

## POZDRAVNI NAGOVAR

PROF.DR.REINHARD DÖPP  
– TEHNIČNA UNIVERZA CLAUSTHAL

Ob otvoritvi galerije »Zbirka umetniških ulitkov profesorja Milana Trbižana« prisrčno čestita Tehnična univerza v Clausthalu. Prisotno je pomembno število predstavnikov TU Clausthal ob 50 letnici kooperacije med partnerskima univerzama v Ljubljani in Clausthalu, med njimi so prisotni bivši rektor prof. dr. Georg Müller pod vodstvom nove podpredsednice dr.-inž. Ines Schwarz, prof. dr.-inž. Günter Borchardt, prof. dr.-inž. Günter Brenner, prof. dr. rer. nat. Dieter Kaufmann, prof. dr. rer. nat. Wolfgang Schade.

Veselimo se nad lepo zbirko umetniških ulitkov, za kar gre zahvala profesorju M. Trbižanu. Pri razstavljenih ulitkih gre za umetniške eksponate, ki nimajo samo zahtevne in lepe oblike, temveč imajo tudi posebno povezavo z donatorjem zbirke in Ljubljano. V našem primeru je povezava med Ljubljano in Clausthalom podana z ulitkom sv. Barbare iz litega železa kot vez med železarji in livarji v Ljubljani in Clausthalom, ki ni samo tradicionalna, temveč tudi izredno živahna. Pri tem mislim na prof. Rekarja iz Ljubljane, ki je prof. Oelsnu v Clausthalu podaril bogato okrašen kovan lestenec, ki se nahaja v avli Inštituta za metalurgijo. Nadalje mislim na prof. Cirila Pelhana in prof. Eberharda Schürmanna iz Clausthalia. Prof. Milan Trbižan se je pojavit v nemški literaturi že v letu 1972, kasneje je kolega Trbižan večkrat predaval na Clausthalskih livaških kolokvijih. Nasprotno sva s kolegom Schürmannom imela mnoga leta priložnost poročati na posvetovanjih v Portorožu o raziskovalnih dosežkih v Clausthalu. Moja želja je, da bi tudi naslednje generacije iz Ljubljane in Clausthala obdržale prijateljsko izmenjavo in jo nadgrajevale. V zahvalo za dolgoletne strokovne in osebne stike podarjam dragoceno knjigo avtorjev R. Nemetz in D. Thiersen: »Sv. Barbara: Pot svetnice skozi čas« v založbi Glückauf Verlag Essen. Za konec še moje osebne 4 verze za vse in posebej za Milana Trbižana:

*Wir wünschen Glück und Gottes Segen,  
Gesundheit, Vertrauen auf allen Wegen!  
Für Ihren und Deinen weiteren Lebenslauf  
mit Dank der Gruss und Wunsch: Glückauf!*

Vaš in Tvoj Reinhard Döpp

## SLOVENSKA AKADEMIJA ZNANOSTI IN UMETNOSTI

AKADEMIK PROF.DR. BOŠTJAN ŽEKŠ,  
PREDSEDNIK SAZU

V veliko čast in v veliko zadovoljstvo mi je, da lahko sodelujem na odprtju te zbirke in da vas pozdravim v imenu Slovenske akademije znanosti in umetnosti. Razlogov, da sem vesel, da lahko sodelujem pri tem odprtju, je več, pa bi naštel samo tri.

Eden je to, da prihajam iz Slovenske akademije znanosti in umetnosti in včasih ljudje sprašujejo, kako pa to paše skupaj. Paše skupaj tako: ta zbirka predstavlja umetnost in znanost, umetnost in tehnologijo in posega v tisto, kar je najboljšega v človeku: da zna nekaj narediti in da ve, kako narediti nekaj lepega. Prevečkrat pozabljamo, da vse te stvari, znanost in umetnost, izvirajo iz iste osnovne obrtniške želje človeka, da bi nekaj naredil in te stvari so se razvile na žalost preveč vsaka po svoje in take zbirke prispevajo k temu, da nas spomnijo, da smo celota.

Druga stvar, zaradi katere me veseli, da sem tukaj, je to, da ta zbirka ni posvečena samo umetnosti, ampak deloma tudi zgodovini na področju tehnologije. Večkrat si mislimo, da smo preživelci kot narod in na koncu dobili svojo državo samo zaradi kulture, samo zaradi jezika, samo zaradi literature, seveda tudi zaradi tega, ampak tudi zaradi velikega tehnološkega znanja, obrtniškega znanja, ki nas je postavilo na isti nivo kot so ga imeli ostali narodi, ki so imeli svoje države. Zato se bomo lahko ob tej zbirki vedno spomnili, da smo tudi na tem tehničnem področju pomembno prispevali svetu in da moramo še naprej pomembno prispevati svetu, da ne

bomo živeli samo od umetnosti, da bomo živeli tudi od kruha.

Tretja stvar, ki bi jo rad omenil ob tej priliki pa je to, da je ta zbirka donacija, kar je pri nas še malo nenavadno. Mi nismo v obdobju, ko bi ljudje kaj dajali, donirali. Enkrat lani sem bil na sestanku v Nemčiji, ko so nam predstavljali vse donacije, fundacije, privatne, državne, milijone stvari, pa sem jaz začudeno na glas vprašal, zakaj pa pri nas tega ni. Pa so Nemci rekli, saj pri nas do 25 let po vojni tudi ni bilo ničesar, ko se stvari spremenijo, ko iz revščine prehajamo v bogastvo, ljudje neradi kaj dajo. In če zdaj računamo, da bo pri nas tudi trajalo 25 let, 15 smo jih že preživelici, ugotavljam, da profesor Trbižan za 10 let prehiteva ostale in mu zato čestitam. Mislim, da je to lepa gesta, prepričan sem, da boste bolj uživali v tej zbirki, ko jo boste prišli včasih pogledat in videli, da jo študentje gledajo, kot bi jo imeli doma zaprto v omarah.

Razstava ulitkov profesorja Trbižana je odprta, želim ji lepo, dolgo in mirno življenje kot tudi fakulteti.

## AVTOR ZBIRKE

PROF.DR. MILAN TRBIŽAN

Zeleno luč za postavitev Zbirke je dal Oddelek za materiale in metalurgijo ter dekan prof. dr. Rado Turk, ki so takoj in enoglasno podprli predlog o donaciji. Priprave za razstavo, katalog, zloženko in spletno stran je več mesecev vodila Katarina Trbižan, ki je tudi skrbela, da se delo med mojo boleznjijo ni ustavilo. Moj naslednik, doc. dr. Primož Mrvar, je zaslužen za ureditev prostora in pomoč pri organizaciji.

Seveda pa moram poseči tudi desetletja nazaj, ko sta na mojo tovrstno usmeritev vplivala dva prijatelja: umetnostni zgodovinar prof. dr. Mirko Juteršek, ki mi je nenehno odpiral umetniški svet in dr.-inž. Karl-Heinz Caspers iz Nürnbergga, ki je ob vsakem obisku prinesel ne samo nove ulitke, ki jih je ulival, temveč tudi obilo navdušenja. Mnoge od njih vidimo v zbirki.

Težišče mojega mednarodnega delovanja je bilo 5 držav, od koder je v zbirki tudi največ eksponatov: Nemčija, Češka, Avstrija, Hrvaška in Poljska, zato posebej pozdravljam delegacije iz teh držav, ki so se udeležile današnjega odprtja, ravno tako pa tudi njeno ekselenco češko veleposlanico Ivano Hlavsovo in podpredsednico TU Clausthal dr.-inž. Ines Schwarz.

Veliko je tudi eksponatov slovenskih podjetij, pomemben je prispevek kiparjev iz Slovenije, ki so se radi odzvali na pobude Katedre za livarstvo, za oblikovanje in izdelavo priznanj ob raznih priložnostih. To so Tomaž Kolarič, docent mag. Jure Smole, Nataša Prestor in Miha Kač.

Zahvaljujem se tudi vsem, ki so danes nastopali: Andreji Humar in Maticu Smolnikarju za glasbeni uvod, dekanu prof. dr. Radu Turku za uvodne besede, umetnostnemu kritiku prof. dr. Mirku Juteršku za prikaz razstave, kolegu prof. dr.-inž Reinhardu Döppu iz TU Clausthal za prijateljske besede, posebej pa predsedniku SAZU akademiku prof. dr. Boštjanu Žekšu, da je bil pripravljen razstavo otvoriti.



Slika 4. Gotski krožnik, 20 cm, siva litina

Figure 4. Gothic plate, 20 cm, grey iron



Slika 5. Krožnik z ornamentiko, 23 cm, bron

Figure 5. Plate with ornamental, 23 cm, bronze



**Slika 6.** Krožnik z morskimi bogovi, 22 cm, siva litina

**Figure 6.** Plate with sea Gods, 22 cm, grey iron



**Slika 7.** Schinkel krožnik, 27 cm, siva litina

**Figure 7.** Schinkel plate, 27 cm, grey iron



**Slika 8.** Svečnik s kariatido, 26 cm, siva litina

**Figure 8.** Candlestick with caryatid, 26 cm, grey iron



**Slika 9.** Sveta Barbara, zaščitnica montanistov, 43 cm, bron

**Figure 9.** Saint Barbara, patroness of miners and metallurgists, 43 cm, bronze



**Slika 10.** Bronasta skleda z idrijsko čipko, 24 cm, bron

**Figure 10.** Bronze bowl with impression of Idrija's bobbin lace, 24 cm, bronze



**Slika 11.** Bronasta skleda z idrijsko čipko, 17 cm, bron

**Figure 11.** Bronze bowl with impression of Idrija's bobbin lace, 17 cm, bronze



**Slika 12.** Sonce, 23 cm, bron

**Figure 12.** The sun, 23 cm, bronze

Vstop in ogled razstave je brezplačen in je mogoč vsak delovni dan med 8. in 17. uro, vodenje skupin ali posameznikov je možno po dogovoru z Milanom Trbižanom (GSM: 031 605 566), ki daje tudi informacije o kataloških podatkih in drugem.

## POVZETEK

V prostorih Oddelka za materiale in metallurgijo Naravoslovnotehniške fakultete je od 21. junija 2006 razstavljena zbirka umetniških ulitkov, ki jo je doniral prof. dr. Milan Trbižan. Vsi eksponati so opisani v katalogu, ki ga je pripravila Katarina Trbižan, univ. dipl.inž. Razstava želi opozoriti na delež slovenskega prostora pri velikem razcvetu umetniškega litja, ki je tedaj vladalo v tedanji Nemčiji in v deželah Avstroogrsko monarhije. Tedanji dosežki, posebno na področju litega želeta, so do danes nepresegjeni. V drugem delu zbirke so eksponati domačih kiparjev, ki so na pobudo avtorja pripravili nekaj zelo uspešnih stvaritev, kot so sonce ob osamosvojitvi, slovenska sv. Barbara in v bron ulit odtis idrijske čipke.

## SUMMARY

### Casting collection of professor Milan Trbižan

At Department for Materials and Metallurgy, Faculty of Natural Sciences and Engineering was on 21st June 2006 exhibited collection of art castings, donated by Prof. Dr. Milan Trbižan. All exhibits are described in catalogue, which was prepared by Dipl. Eng. Katarina Trbižan. Exhibition wants to warn on part of Slovenian region by great bloom

of art casting, which at that time ruled in Germany and countries of Austrian-Hungary monarchy. Those achievements, specially in the field of grey iron, are still not exceeded. In second part of collection are exhibits of Slovenian sculptors, who prepared on the initiative of author some very successful creations, such as the sun by the Slovenian independence, Slovenian St. Barbara and in bronze casted impression of Idrija's bobbin lace.

## REFERENCE

- [<sup>1</sup>] K. TRBIŽAN: Razstavni katalog »Zbirka ulitkov profesorja M. Trbižana«, Naravoslovnotehniška fakulteta, 2006, 138 strani
- [<sup>2</sup>] Spletna stran [www.isc.si](http://www.isc.si)
- [<sup>3</sup>] Spletna stran [www.omm.ntf.uni-lj.si](http://www.omm.ntf.uni-lj.si)
- [<sup>4</sup>] Zloženka »Zbirka ulitkov profesorja M. Trbižana«

## Autor's Index, Vol. 53, No. 2

Anžel I.	ivan.anzel@uni-mb.si	193
Bizjak M.	milan.bizjak@ntf.uni-lj.si	193
Cvahté Peter	peter.cvahte@impol.si	163
Čadež Jurij	jurij.cadez@geoportal.si	203
Dervarič Evgen	evgen.dervaric@rlv.si	203
Dolenec Matej	matej.dolenec@s5.net	229
Döpp Reinhard	giessereitechnik@tu-clausthal.de	261
Dozet Stevo	stevo.dozet@geo-zs.si	229
Durgutović Anes	anes.durgutovic@oikos.si	221
Fajfar Peter	peter.fajfar@ntf.uni-lj.si	163
Fazarinc Matevž		175
Jeromel Gregor	gregor.jeromel@rlv.si	203
Juteršek Mirko	mjutersek@volja.net	261
Katayama Iwao		155
Kneissl A. C.	kneissl@unileoben.ac.at	193
Kosec B.	borut.kose@ntf.uni-lj.si	193
Kosec L.	ladislav.kosec@ntf.uni-lj.si	193
Kugler Goran	goran.kugler@ntf.uni-lj.si	163, 193
Likar Jakob	jakob.likar@ntf.uni-lj.si	203
Lojen Sonja	sonja.lojen@ijs.si	229
Manasijević Dragan		155
Medved Jožef	jozef.medved@ntf.uni-lj.si	193
Medved Milan	milan.medved@hse.si	203
Mrvar Primož	primož.mrvvar@ntf.uni-lj.si	175
Šuler M.	marko.suler@gmail.com	193
Terčelj Milan	milan.tercelj@ntf.uni-lj.si	163, 175
Trbižan Katarina	institut.isc@t-2.net	261
Trbižan Milan	milan.trbican@ntf.uni-lj.si	261
Turk Radomir	rado.turk@ntf.uni-lj.si	163, 261
Vulić Milivoj	milivoj.vulic@ntf.uni-lj.si	221
Yamashita Hiromi		155
Yilmaz Levent	lyilmaz@itu.edu.tr	247
Žekš Boštjan	sazu@sazu.si	261
Živković Dragana	dzhivkovic@tf.bor.ac.yu	155
Živković Živan		155

## (NEW) INSTRUCTIONS TO AUTHORS (from Sep. 2003)

**RMZ-MATERIALS & GEOENVIRONMENT** (RMZ- Materiali in geokolje) is a periodical publication with four issues per year (established 1952 and renamed to RMZ-M&G in 1998). The main topics of contents are Mining and Geotechnology, Metallurgy and Materials, Geology and Geoenvironment.

**RMZ-M&G** publishes original Scientific articles, Review papers, Technical and Expert contributions (also as short papers or letters) **in English**. In addition, evaluations of other publications (books, monographs, ...), short letters and comments are welcome. A short summary of the contents in Slovene will be included at the end of each paper. It can be included by the author(s) or will be provided by the referee or the Editorial Office.

\* **Additional information and remarks for Slovenian authors:**

*English version with extended "Povzetek", and additional roles (in Template for Slovenian authors) can be written. Only exceptionally the articles in the Slovenian language with summary in English will be published. The contributions in English will be considered with priority over those in the Slovenian language in the review process.*

**Authorship and originality** of the contributions. Authors are responsible for originality of presented data, ideas and conclusions as well as for correct citation of data adopted from other sources. The publication in RMZ-M&G obligate authors that the article will not be published anywhere else in the same form.

### Specification of Contributions

*Optimal number of pages of full papers is 7 to 15, longer articles should be discussed with Editor, but 20 pages is limit.*

**Scientific papers** represent unpublished results of original research.

**Review papers** summarize previously published scientific, research and/or expertise articles on the new scientific level and can contain also other cited sources, which are not mainly result of author(s).

**Technical and Expert papers** are the result of technological research achievements, application research results and information about achievements in practice and industry.

**Short papers (Letters)** are the contributions that contain mostly very new short reports of advanced investigation. They should be approximately 2 pages long but should not exceed 4 pages.

**Evaluations or critics** contain author's opinion on new published books, monographs, textbooks, exhibitions ... (up to 2 pages, figure of cover page is expected).

**In memoriam** (up to 2 pages, a photo is expected).

**Professional remarks (Comments)** cannot exceed 1 page, and only professional disagreements can be discussed. Normally the source author(s) reply the remarks in the same issue.

**Supervision and review of manuscripts.** All manuscripts will be supervised. The referees evaluate manuscripts and can ask authors to change particular segments, and propose to the Editor the acceptability of submitted articles. Authors can suggest the referee but Editor has a right to choose another. **The name of the referee remains anonymous.** The technical corrections will be done too and authors can be asked to correct missing items. The final decision whether the manuscript will be published is made by the Editor in Chief.

### The Form of the Manuscript

The manuscript should be submitted as a complete hard copy including figures and tables. The figures should also be enclosed separately, both charts and photos in the original version. In addition, all material should also be provided in electronic form on a diskette or a CD. The necessary information can conveniently also be delivered by E-mail.

## Composition of manuscript is defined in the attached Template

The original file of Template is temporarily available on E-mail addresses:

joze.pezdic@ntfgeo.uni-lj.si, joze.pezdic@guest.arnes.si

barbara.bohar@ntf.uni-lj.si

**References** – can be arranged in two ways:

- first possibility: alphabetic arrangement of first authors – in text: (Borgne, 1955),

or

- second possibility: <sup>[1]</sup> numerated in the same order as cited in the text: example<sup>[1]</sup>

Format of papers in journals:

Le Borgne, E. (1955): Susceptibilite magnetic anomale du sol superficiel. *Annales de Geophysique*, 11, pp. 399-419.

Format of books:

Roberts, J. L. (1989): Geological structures, *MacMillan, London*, 250 p.

**Text** on the hard print copy can be prepared with any text-processor. The electronic version on the diskette, CD or E-mail transfer should be in MS Word or ASCII format.

**Captions of figures and tables** should be enclosed separately. **Figures (graphs and photos)** and tables should be original and sent separately in addition to text. They can be prepared on paper or computer designed (MSExcel, Corel, Acad)

**Format.** Electronic figures are recommended to be in CDR, AI, EPS, TIF or JPG formats. Resolution of bitmap graphics (TIF, JPG) should be at least 300 dpi. Text in vector graphics (CDR, AI, EPS) must be in MSWord Times typography or converted in curves.

**Color prints.** Authors will be charged for color prints of figures and photos.

**Labeling** of the additionally provided material for the manuscript should be very clear and must contain at least the lead author's name, address, the beginning of the title and the date of delivery of the manuscript. In case of an E-mail transfer the exact message with above asked data must accompany the attachment with the file containing the manuscript.

**Information about RMZ-M&G:**

Editor in Chief prof. dr. Jože Pezdič (tel. ++386 1 4704-633) or

Secretary Barbara Bohar Bobnar, un. dipl. ing. geol. (++386 1 4704-630),  
Aškerčeva 12, Ljubljana, Slovenia

or at E-mail addresses:

joze.pezdic@ntfgeo.uni-lj.si, joze.pezdic@guest.arnes.si

barbara.bohar@ntf.uni-lj.si

**Sending of manuscripts.** Manuscripts can be sent by mail to the **Editorial Office** address:

- RMZ-Materials & Geoenvironment

Aškerčeva 12,

1001 Ljubljana, Slovenia

or delivered to:

- **Reception** of the Faculty of Natural Sciences and Engineering (for RMZ-M&G)

Aškerčeva 12, Ljubljana

- E-mail – addresses of Editor and Secretary

- You can also contact them on their phone numbers.

*These instructions are valid from September 2003*

## **TEMPLATE**

**The title of the manuscript should be written in bold letters  
(Times New Roman, 14, Center)**

NAME SURNAME<sup>1</sup>, ...., & NAME SURNAME<sup>X</sup> (TIMES NEW ROMAN, 12, CENTER)

<sup>x</sup>Faculty of ... , University of ... , Address..., Country, e-mail: ... (Times New Roman, 12, Center)

THE LENGTH OF FULL PAPER SHOULD NOT EXCEED TWENTY (20, INCLUDING FIGURES AND TABLES) PAGES (OPTIMAL 7 TO 15), SHORT PAPER FOUR (4) AND OTHER TWO (2) WITHOUT TEXT FLOWING BY GRAPHICS AND TABLES.

**Abstract**(Times New Roman, Bold/Normal, 11): The text of the abstract is placed here. The abstract should be concise and should present the aim of the work, essential results and conclusion. It should be typed in font size 11, single-spaced. Except for the first line, the text should be indented from the left margin by 10 mm. The length should not exceed fifteen (15) lines (10 are recommended).

**Key words:** a list of up to 5 key words (3 to 5) that will be useful for indexing or searching.  
Use the same styling as for abstract.

### **INTRODUCTION (TIMES NEW ROMAN, BOLD, 12)**

Two lines below the keywords begin the introduction. Use Times New Roman, font size 12, Justify alignment.

There are two (2) admissible methods of citing references:

1. by stating the first author and the year of publication of the reference in the parenthesis at the appropriate place in the text and arranging the reference list in the alphabetic order of first authors; e.g.:  
“Detailed information about geohistorical development of this zone can be found in: Antonijević (1957), Grubić (1962), ...”  
“... the method was described previously (Hoefs, 1996)”
2. by consecutive Arabic numerals in square brackets, superscripted at the appropriate place in the text and arranging the reference list at the end of the text in the like manner; e.g.:  
“... while the portal was made in Zope<sup>[3]</sup> environment.”

## **RESULTS AND DISCUSSION (TIMES NEW ROMAN, BOLD, 12)**

Tables, figures, pictures, and schemes should be incorporated (inserted, not pasted) in the text at the appropriate place and should fit on one page. Break larger schemes and tables into smaller parts to prevent extending over more than one page.

## **CONCLUSIONS (TIMES NEW ROMAN, BOLD, 12)**

This paragraph summarizes the results and draws conclusions.

### **Acknowledgements (Times New Roman, Bold, 12, Center - optional)**

This work was supported by the \*\*\*\*.

## **REFERENCES (TIMES NEW ROMAN, BOLD, 12)**

Regardless of the method used, in the reference list, the styling, punctuation and capitalization should conform to the following:

### **FIRST OPTION – in alphabetical order**

- Casati, P., Jadoul, F., Nicora, A., Marinelli, M., Fantini-Sestini, N. & Fois, E. (1981): Geologia della Valle dell'Anisici e dei gruppi M. Popera – Tre Cime di Lavaredo (Dolomiti Orientali). *Riv. Ital. Paleont.*; Vol. 87, No. 3, pp. 391-400, Milano.  
Folk, R. L. (1959): Practical petrographic classification of limestones. *Amer. Ass. Petrol. Geol. Bull.*; Vol. 43, No. 1, pp. 1-38, Tulsa.

### **SECOND OPTION – in numerical order**

- [<sup>1</sup>]Trček, B. (2001): *Solute transport monitoring in the unsaturated zone of the karst aquifer by natural tracers*. Ph.D. Thesis. Ljubljana: University of Ljubljana 2001; 125 p.  
[<sup>2</sup>]Higashitani, K., Iseri, H., Okuhara, K., Hatade, S. (1995): Magnetic Effects on Zeta Potential and Diffusivity of Nonmagnetic Particles. *Journal of Colloid and Interface Science* 172, pp. 383-388.

### **Citing the Internet site:**

CASREACT-Chemical reactions database [online]. Chemical Abstracts Service, 2000, updated 2.2.2000 [cited 3.2.2000]. Accessible on Internet:<<http://www.cas.org/CASFILES/casreact.html>>.

## **POVZETEK (TIMES NEW ROMAN, 12)**

A short summary of the contents in Slovene (up to 400 characters) can be written by the author(s) or will be provided by the referee or by the Editorial Board.

## TEMPLATE for Slovenian Authors

**The title of the manuscript should be written in bold letters  
(Times New Roman, 14, Center)**

### **Naslov članka (Times New Roman, 14, Center)**

NAME SURNAME<sup>1</sup>, ...., & NAME SURNAME<sup>X</sup> (TIMES NEW ROMAN, 12, CENTER)  
IME PRIIMEK<sup>1</sup>, ..., IME PRIIMEK<sup>X</sup> (TIMES NEW ROMAN, 12, CENTER)

<sup>x</sup>Faculty of ..., University of ..., Address..., Country; e-mail: ... (Times New Roman, 12, Center)

<sup>x</sup>Fakulteta..., Univerza..., Naslov..., Država; e-mail: ... (Times New Roman, 12, Center)

THE LENGTH OF ORIGINAL SCIENTIFIC PAPER SHOULD NOT EXCEED TWENTY (20, INCLUDING FIGURES AND TABLES) PAGES (OPTIMAL 7 TO 15), SHORT PAPER FOUR (4) AND OTHER TWO (2) WITHOUT TEXT FLOWING BY GRAPHICS AND TABLES.

DOLŽINA IZVIRNEGA ZNANSTVENEGA ČLANKA NE SME PRESEGATI DVAJSET (20, VKLJUČNO S SLIKAMI IN TABELAMI), STROKOVNEGA ČLANKA ŠTIRI (4) IN OSTALIH PRISPEVKOV DVE (2) STRANI.

**Abstract** (Times New Roman, Bold/Normal, 11): The text of the abstract is placed here. The abstract should be concise and should present the aim of the work, essential results and conclusion. It should be typed in font size 11, single-spaced. Except for the first line, the text should be indented from the left margin by 10 mm. The length should not exceed fifteen (15) lines (10 are recommended).

**Izvleček (TNR, B/N, 11):** Kratek izvleček namena članka ter ključnih rezultatov in ugotovitev. Razen prve vrstice naj bo tekst zamaknjen z levega roba za 10 mm. Dolžina naj ne presega petnajst (15) vrstic (10 je priporočeno).

**Key words:** a list of up to 5 key words (3 to 5) that will be useful for indexing or searching.  
Use the same styling as for abstract.

**Ključne besede:** seznam največ 5 ključnih besed (3-5) za pomoč pri indeksiranju ali iskanju.  
Uporabite enako obliko kot za izvleček.

### **INTRODUCTION – UVOD (TIMES NEW ROMAN, BOLD, 12)**

Two lines below the keywords begin the introduction. Use Times New Roman, font size 12, Justify alignment. All captions of text and tables as well as the text in graphics must be prepared in English and Slovenian language.

Dve vrstici pod ključnimi besedami se začne Uvod. Uporabite pisavo Times New Roman, velikost črk 12, z obojestransko poravnavo. Naslovi slik in tabel (vključno z besedilom v slikah) morajo biti pripravljeni v slovenskem in angleškem jeziku.

There are two (2) admissible methods of citing references – obstajata dve sprejemljivi metodi navajanja referenc:

1. by stating the first author and the year of publication of the reference in the parenthesis at the appropriate place in the text and arranging the reference list in the alphabetic order of first authors; e.g.:
1. z navedbo prvega avtorja in letnice objave reference v oklepaju na ustreznem mestu v tekstu in z ureditvijo seznama referenc po abecednem zaporedju prvih avtorjev; npr.: “Detailed information about geohistorical development of this zone can be found in: Antonijević (1957), Grubić (1962), ...”  
“... the method was described previously (Hoefs, 1996)”
2. by consecutive Arabic numerals in square brackets, superscripted at the appropriate place in the text and arranging the reference list at the end of the text in the like manner; e.g.:
2. z zaporednimi arabskimi številkami v oglatih oklepajih na ustreznem mestu v tekstu in z ureditvijo seznama referenc v številčnem zaporedju navajanja; npr.;  
“... while the portal was made in Zope<sup>[3]</sup> environment.”

## **RESULTS AND DISCUSSION – REZULTATI IN RAZPRAVA (TIMES NEW ROMAN, BOLD, 12)**

Tables, figures, pictures, and schemes should be incorporated (inserted, not pasted) in the text at the appropriate place and should fit on one page. Break larger schemes and tables into smaller parts to prevent extending over more than one page.

Tabele, sheme in slike je potrebno vnesti (z ukazom Insert, ne Paste) v tekst na ustreznem mestu. Večje sheme in tabele je potrebno ločiti na manjše dele, da ne presegajo ene strani.

## **CONCLUSIONS – SKLEPI (TIMES NEW ROMAN, BOLD, 12)**

This paragraph summarizes the results and draws conclusions.  
Povzetek rezultatov in zaključki.

## **Acknowledgements – Zahvale (Times New Roman, Bold, 12, Center - optional)**

This work was supported by the \*\*\*\*.

## REFERENCES - VIRI (TIMES NEW ROMAN, BOLD, 12)

Regardless of the method used, in the reference list, the styling, punctuation and capitalization should conform to the following:

Ne glede na uporabljeno metodo pri seznamu citiranih referenc upoštevajte naslednjo obliko:

### FIRST OPTION – in alphabetical order (v abecednem zaporedju)

Casati, P., Jadoul, F., Nicora, A., Marinelli, M., Fantini-Sestini, N. & Fois, E. (1981): Geologia della Valle dell'Anisici e dei gruppi M. Popera – Tre Cime di Lavaredo (Dolomiti Orientali). *Riv. Ital. Paleont.*; Vol. 87, No. 3, pp. 391-400, Milano.

Folk, R. L. (1959): Practical petrographic classification of limestones. *Amer. Ass. Petrol. Geol. Bull.*; Vol. 43, No. 1, pp. 1-38, Tulsa.

### SECOND OPTION – in numerical order (v numeričnem zaporedju)

[<sup>1</sup>]Trček, B. (2001): *Solute transport monitoring in the unsaturated zone of the karst aquifer by natural tracers*. Ph.D. Thesis. Ljubljana: University of Ljubljana 2001; 125 p.

[<sup>2</sup>]Higashitani, K., Iseri, H., Okuhara, K., Hatade, S. (1995): Magnetic Effects on Zeta Potential and Diffusivity of Nonmagnetic Particles. *Journal of Colloid and Interface Science* 172, pp. 383-388.

### Citing the Internet site:

CASREACT-Chemical reactions database [online]. Chemical Abstracts Service, 2000, updated 2.2.2000 [cited 3.2.2000]. Accessible on Internet:<<http://www.cas.org/CASFILES/casreact.html>>.

### Citiranje internetne strani:

CASREACT-Chemical reactions database [online]. Chemical Abstracts Service, 2000, obnovljeno 2.2.2000 [citirano 3.2.2000]. Dostopno na svetovnem spletu: <<http://www.cas.org/CASFILES/casreact.html>>.

## POVZETEK – SUMMARY (TIMES NEW ROMAN, 12)

An extended summary of the contents in Slovene (from one page to approximately 1/3 of the original article length).

Razširjeni povzetek vsebine prispevka v Angleščini (od ene strani do približno 1/3 dolžine izvirnega članka).

**Citation and indexing of RMZ-Materials and geoenvironment  
 (Število citatov in indeksiranja člankov RMZ-M&G)**  
 (prepared by Pezdič, J. - from search done by Šercelj, M., CTK Ljubljana)

**Citation index according to Web of Science 1970 –2006:**

**110 papers have 165 citations (4x before 1998, max. 49x in 2004)**

(110 člankov je bilo citirano 165 krat – 4x pred 1998; največ 49x v letu 2004))

**No. of indexing of RMZ- M&G in singular Databases  
 (Število indeksiranih člankov iz RMZ- M&G v posameznih bazah)**

Database Name	Total	before 1998
1: Civil Engineering Abstracts	773	770
2: CA SEARCH® - Chemical Abstracts® (1967- present)	760	475
3: Inside Conferences	313	237
4: Materials Business File	253	253
5: METADEX®	164	38
6: ANTE: Abstracts in New Technologies and Engineering	158	158
7: GeoRef	154	30
8: Aluminium Industry Abstracts	36	9
9: PASCAL	30	30
10: Energy Science and Technology	27	27
11: TEME - Technology and Management	27	27
12: Ei Compendex®	13	13
13: CSA Aerospace & High Technology Database	12	12
14: Computer and Information Systems	10	10
15: Mechanical & Transportation Engineering Abstracts	8	7
16: Engineered Materials Abstracts®	3	3
17: Corrosion Abstracts	3	3
18: Analytical Abstracts	1	1
19: FLUIDEX	1	1
20: Solid State and Superconductivity Abstracts	1	1
21: Electronics and Communications Abstracts	1	1
	<b>2748</b>	<b>2004</b>
		<b>744</b>

- Total No. of Databases (število vseh baz): 21
- No. of new bases in RMZ-M&G after 1998 (število novih baz v RMZ-M&G po 1998): 7
- Total No. of indexing (število indeksov skupaj): 2748
- No. of indexing after 1998 (število indeksov po 1998): 2004
- No. of indexing between 1970-1998 (število indeksov med 1970-1998): 744

# RMZ - Materials and Geoenvironment

---

RMZ-M&G, Vol. 53, No. 2

pp. 155-283 (2006)

---

## Contents

Investigation of the Thermodynamic Model and Ternary Interaction Parameter Influence for Sn-Ag-Bi Liquid Alloys ŽIVKOVIĆ, D., KATAYAMA, I., YAMASHITA, H., MANASIKEVIĆ, D., ŽIVKOVIĆ, Ž.	155
Measured temperatures on die bearing surface in aluminium hot extrusion TERČELJ, M., TURK, R., KUGLER, G., FAJFAR, P., CVAHTE, P.	163
Characterization of solidification and hot workability of MgAl <sub>6</sub> Mn foundry alloy MRVAR, P., TERČELJ, M., KUGLER, G., FAZARINC, M., MEDVED, J.	175
Sinteza in analiza hitro strjenih trakov iz bakrovih zlitin ŠULER, M., BIZJAK, M., KOSEC, L., KOSEC, B., KNEISSL, A. C., ANŽEL, I.	193
Some methods of analysing caving processes in sublevel coal mining LIKAR, J., DERVARIČ, E., MEDVED, M., ČADEŽ, J., JEROMEL, G.	203
Calculation of volume with the use of "NTF" method VULIĆ, M., DURGUTOVIĆ, A.	221
Permsko-triasna meja ter zgornjepermski in spodnjeskitski skladi na jugovzhodnem obrobju Ljubljanskega Barja, osrednja Slovenija DOLENEC, M., DOZET, S., LOJEN, S.	229
Some Considerations on the Series Solution of Differential Equations and its Engineering Applications YILMAZ, L.	247
Zbirka ulitkov profesorja Milana Trbižana TRBIŽAN, K., TURK, R., JUTERŠEK, M., DÖPP, R., ŽEKŠ, B., TRBIŽAN, M.	261
Autor's Index, Vol. 53, No. 2	275
Instructions to Authors	276
Template	278
Number of paper indexing in different bases	283